

MSc  
2.º CICLO  
FCUP  
2017



Study of descending noradrenergic pain modulation in a model of neuropathic pain induced by chemotherapy

Joana Gomes Ribeiro

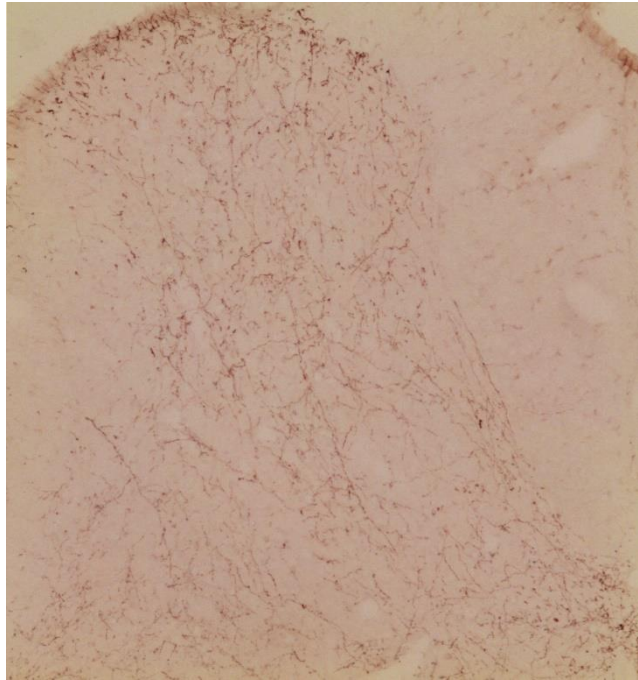


# Study of descending noradrenergic pain modulation in a model of neuropathic pain induced by chemotherapy

Joana Gomes Ribeiro  
Dissertação de Mestrado apresentada à  
Faculdade de Ciências da Universidade do Porto em  
Biologia Celular e Molecular  
2017







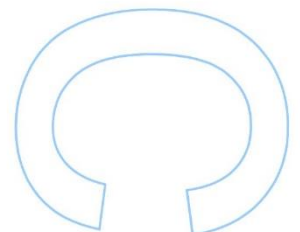
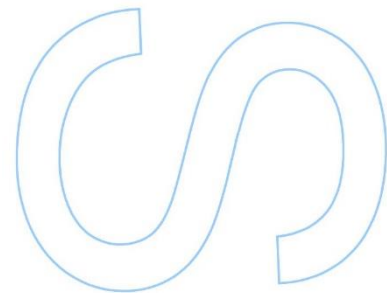
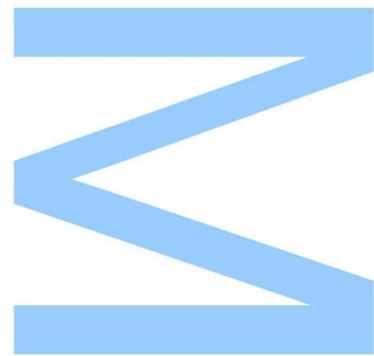
# Study of descending noradrenergic pain modulation in a model of neuropathic pain induced by chemotherapy

Joana Gomes Ribeiro

Biologia Celular e Molecular  
Departamento de Biologia  
2017

## Orientador

Isabel Martins, Professora Auxiliar, Faculdade de Medicina da Universidade do Porto



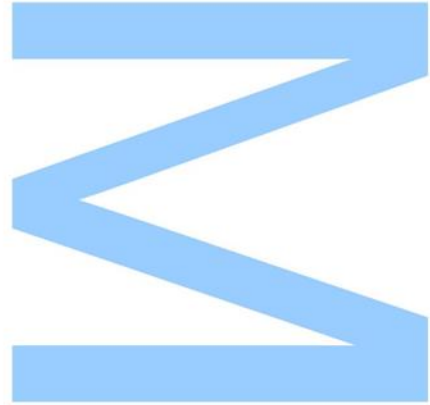




Todas as correções determinadas pelo júri, e só essas, foram efetuadas.

O Presidente do Júri,

Porto, \_\_\_\_/\_\_\_\_/\_\_\_\_

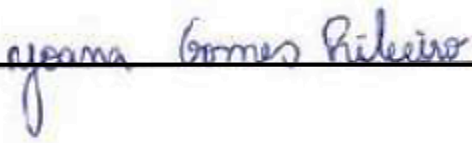




## **Declaração de autoria**

Eu, Joana Gomes Ribeiro, aluna com o número 201502149 do mestrado em Biologia Celular e Molecular da edição de 2016/2017, declaro por minha honra que sou a autora da totalidade do texto apresentado, não apresento texto plagiado, e tomei conhecimento das consequências de uma situação de plágio.

Porto, 28 de setembro de 2017

  
\_\_\_\_\_





# Acknowledgments

---

The completion of the present dissertation would not have been possible without the hard work, collaboration and support of several important people, to whom I express my deepest gratitude.

To my supervisor, Professor Doctor Isabel Martins, the person who inspired me the most for her scientific drive and knowledge, perseverance, positive thinking and who always took the time to care for my scientific and personal well-being along the way, I express you my most heartfelt gratitude. Your support, patience, dedication and organizational skills were also crucial throughout the writing process of this dissertation.

To Professor Doctor Isaura Tavares for accepting me in your investigation group and for allowing me to autonomously develop the research work in your laboratory facilities.

To José Tiago Pereira for being one of the most thoughtful, erudite, kind and joyful people I have come to know. Thank you for always guiding me whenever I had trouble during any of the experimental procedures and for the nice occasional discussions which contributed to expand my critical and creative scientific thinking.

To Ana Rita Costa for being one of the most supportive, friendly and funny people I ever had the pleasure to meet and work with. Your toughness, hard work and teaching skills have always delighted and inspired me to become a better student.

To Rita Oliveira for the amazing companionship right from the start of this journey, for the bond we created and for helping to boost my confidence in times of need. Your intelligence and strong spirit have always enlightened me.

To Elisa and Sr. Fernando for their amiability and availability anytime I solicited your help.

To my parents for all their love, hard work and wise advising along the way which inspired me to get up every day and go fight for what I believe and want in life. And to my brother Francisco, I express you my gratitude for being the greatest brother I could have ever asked for, for your maturity so early in your life and for inspiring me to open myself up to the world.

Lastly, to my best friends Carla Rodrigues, Diana Martins, Sónia Rocha and Marta Brandão for your love, encouragement, selflessness, strong friendship and even madness. If we keep dreaming it, we will accomplish it.

## Abstract

---

Chemotherapeutic drugs are widely used for the treatment of cancer but their debilitating side effects often lead to alterations in dose regimens and the premature cessation of treatment, which ultimately impacts on patient's survival. Chemotherapy-induced neuropathy (CIN) is one of the most common side effects of chemotherapeutic drugs. CIN results from the damaging action of cytostatic drugs on peripheral nerves. Paclitaxel is a commonly prescribed cytostatic known to damage sensory nerves and to produce neuropathic pain characterized by mechanical and thermal hypersensitivity. The molecular mechanisms underlying the onset of CIN by paclitaxel have been mainly investigated at the level of the peripheral nervous system but the effects of paclitaxel at the central nervous system level are still understudied. Here we studied the effects of the cytostatic paclitaxel at the spinal cord, the first relay site in the transmission of nociceptive information from the periphery to the brain. Three studies were included in the present thesis which aimed at: *i*) determining the onset and maintenance of nociceptive and aversive behaviors; *ii*) assessing basal and noxious-evoked activation of spinal dorsal horn neurons and *iii*) studying the descending inhibitory noradrenergic modulatory system.

Adult male Wistar rats were intraperitoneally injected with paclitaxel (Taxol®, 2.0 mg/kg) or the vehicle solution Dimethyl Sulfoxide (DMSO) or saline on four alternate days. Nociceptive and aversive behaviors were assessed by the von Frey and the Conditioned Place Aversion (CPA) tests, respectively. The von Frey test, which allows to evaluate mechanical sensitivity, was performed at baseline (i.e. before paclitaxel injection) and from day 3 after the first injection onwards for a period of two months. The CPA test is an established rodent paradigm to detect aversiveness to a drug. The test was used to determine if the animals developed aversiveness towards paclitaxel. Basal and noxious-evoked activation of spinal dorsal neurons was assessed at one month after induction of the model by evaluating the expression of pCREB and c-Fos, respectively, by immunohistochemistry. The expression of c-Fos was evaluated after subjecting the animals to noxious cold at 0°C. To study the descending noradrenergic pain modulatory system, we assessed the expression of dopamine- $\beta$ -hydroxylase (DBH), a noradrenaline biosynthetic enzyme expressed in noradrenergic fibers at the spinal dorsal horn. The expression of DBH was evaluated by immunohistochemistry at one and two months after CIN induction. We also studied the expression and function of the  $\alpha_2$ -adrenergic receptor,

whose activation induces antinociceptive actions. The expression of the receptor was assessed by western blotting and immunofluorescence at one month after CIN induction. The function of the receptor was assessed by evaluating the effect of intrathecally administered clonidine, an  $\alpha_2$ -adrenergic receptor agonist, on pain behaviors. Clonidine was administered at 1 and 10  $\mu\text{g}$  and its effects were evaluated on the von Frey and cold plate tests at one month after CIN induction.

Our results showed that paclitaxel treatment induced mechanical allodynia early after initiation of the treatment and this behavior was maintained until the last time point tested at two months after CIN induction. Animals also showed aversiveness towards paclitaxel which remained until one week (last time point tested) after the last injection of paclitaxel. These results indicate that paclitaxel affects the sensorial component of pain, but also likely engages the affective/emotional component of pain as detected by the aversiveness induced by paclitaxel, leading to the development and maintenance of neuropathic like-behaviors. Our results also showed that while the expression of pCREB at basal levels was unaltered in comparison to DMSO-treated animals, c-Fos expression was increased upon noxious cold stimulation in paclitaxel-treated animals. The increased c-Fos expression is indicative of hypersensitivity of spinal dorsal horn neurons and is likely an indirect evidence of central sensitization. Our results further showed that DBH expression was increased at one month after initiation of the treatment, but not at two months. The expression of the  $\alpha_2$ -adrenergic receptor was unaltered. Clonidine induced antinociception with more pronounced effects in paclitaxel-treated animals. It remains to ascertain if DHB upregulation results in increased spinal noradrenaline levels, but the increase of  $\alpha_2$ -adrenergic receptor antinociceptive potency in paclitaxel-treated animals suggests the recruitment of descending noradrenergic inhibition probably to compensate for the increased spinal sensitization.

Considering the scarce knowledge about how paclitaxel, through a peripheral action, engages the affective/emotional dimension of pain in non-verbal animals, future work should be developed to fully establish how paclitaxel affects this component/dimension of pain. It would also be interesting to continue studying the alterations in the descending noradrenergic modulatory system namely in what concerns the mechanisms underlying the phenomenon of potentiation of the  $\alpha_2$ -AR as this phenomenon reinforces the spinal noradrenergic antinociceptive activity.

**Keywords:** Chemotherapy-induced neuropathy, paclitaxel, neuropathic pain, descending noradrenergic modulation, spinal sensitization,  $\alpha_2$ -adrenergic receptors

## Resumo

---

As drogas quimioterápicas são amplamente usadas no tratamento de cancro, mas os seus efeitos secundários debilitantes levam frequentemente a alterações na dosagem prescrita e à conclusão prematura do ciclo de tratamento, o que, em última análise, afeta a sobrevivência dos pacientes. A neuropatia induzida por quimioterapia (NiQ) é um dos efeitos secundários mais comuns do uso de drogas quimioterápicas. A NiQ resulta da ação adversa das drogas citostáticas nos nervos periféricos. O paclitaxel é um citostático comumente prescrito e conhecido pela sua ação danosa nos nervos sensoriais e por produzir dor neuropática caracterizada por hipersensibilidade mecânica e térmica. Os mecanismos moleculares responsáveis pelo desenvolvimento de NiQ pelo paclitaxel têm sido maioritariamente investigados ao nível do sistema nervoso periférico, mas os efeitos no sistema nervoso central ainda estão pouco estudados. Neste trabalho, estudou-se os efeitos do citostático paclitaxel ao nível da medulla espinhal, o primeiro local de transmissão de informação nociceptiva desde a periferia até ao cérebro. Três estudos foram incluídos na presente tese, cujos objetivos foram: i) determinar o início e a manutenção de comportamentos nociceptivos e aversivos; ii) avaliar a ativação basal e evocada por estímulo nócico de neurónios do corno dorsal da medula espinhal; iii) estudar o sistema de modulação descendente noradrenérgico.

Ratos Wistar machos adultos receberam injeções intraperitoneais de paclitaxel (Taxol®, 2.0 mg/kg) ou da solução veículo sulfóxido de dimetilo (DMSO) ou solução salina em quatro dias alternados. Os comportamentos nociceptivos e aversivos foram avaliados através dos testes de von Frey e de aversão condicionada de lugar (*Conditioned Place Aversion – CPA*), respetivamente. O teste de von Frey, que permite avaliar sensibilidade mecânica, foi realizado basalmente (isto é, antes das injeções de paclitaxel) e a partir do dia 3 após a primeira injeção até ao fim de dois meses. O teste de *CPA* é um estabelecido paradigma em animais roedores para detetar aversão a determinada droga. Este teste foi usado para determinar se os animais desenvolviam aversão ao paclitaxel. A avaliação da ativação basal e evocada por estímulo nócico de neurónios espinhais do corno dorsal foi realizada um mês após indução do modelo de NiQ através da análise da expressão de pCREB e c-Fos, respetivamente, por imunohistoquímica. A expressão de c-Fos foi avaliada após sujeição dos animais a frio nócico a 0°C. Para estudar o sistema de modulação descendente noradrenérgico, avaliou-se a expressão da dopamina-β-hidroxilase (DBH), uma enzima biosintética de síntese de noradrenalina expressa em fibras noradrenérgicas no corno dorsal da medula

espinhal. A expressão de DBH foi avaliada por imunohistoquímica, um e dois meses após a indução de NiQ. A expressão e função do recetor  $\alpha_2$ -adrenérgico na medula espinhal, cuja ativação induz antinocicepção, também foram estudadas. A expressão do recetor foi determinada por técnicas de *western blotting* e imunofluorescência, um mês após indução de NiQ. A função do recetor foi avaliada através da análise do efeito da administração intratecal de clonidina, um agonista dos recetores  $\alpha_2$ -adrenérgicos, em comportamentos nociceptivos. A clonidina foi administrada nas doses de 1 e 10  $\mu\text{g}$  e os seus efeitos foram avaliados nos testes de von Frey e de placa fria, um mês após indução de NiQ.

Os resultados mostraram que a administração de paclitaxel induziu alodínia mecânica logo após o início do tratamento e este comportamento foi mantido até ao último intervalo de tempo testado, isto é, dois meses após indução de NiQ. Os animais também mostraram aversão ao paclitaxel, um comportamento que se manteve até ao último intervalo de tempo testado, isto é, uma semana após a última injeção de paclitaxel. Estes resultados indicam que o paclitaxel afeta a componente sensorial da dor, mas provavelmente também a componente afetiva/emocional da dor, tal como detetado pela aversão induzida pelo paclitaxel, o que em última análise conduz ao desenvolvimento e manutenção de comportamentos de dor neuropática. Os resultados também demonstraram que, enquanto a expressão basal de pCREB pareceu inalterada em comparação com os animais tratados com DMSO, a expressão de c-Fos aumentou após estimulação fria nóxica em animais tratados com paclitaxel. O aumento da expressão de c-Fos é indicativo de hipersensibilidade dos neurónios espinhais do corno dorsal e é possivelmente uma evidência indireta de sensibilização central. Os resultados mostraram, ainda, que a expressão de DBH surgiu aumentada, um mês após o início do tratamento, mas não aos dois meses. A expressão do recetor  $\alpha_2$ -adrenérgico não surgiu alterada. A clonidina induziu antinocicepção com efeitos mais pronunciados nos animais tratados com paclitaxel. Permanece por determinar se o aumento da expressão de DBH resulta num aumento dos níveis espinhais de noradrenalina, mas o aumento da potência antinociceptiva dos recetores  $\alpha_2$ -adrenérgicos em animais tratados com paclitaxel sugere o recrutamento de inibição descendente noradrenérgica provavelmente em compensação do aumento da sensibilização espinhal.

Considerando o escasso conhecimento sobre como o paclitaxel, através de uma ação periférica, é capaz de afetar a dimensão afetiva/emocional da dor em animais não-verbais, trabalho futuro deve ser desenvolvido para inteiramente estabelecer como o paclitaxel afeta esta componente da dor. Seria igualmente interessante dar continuidade ao estudo sobre as alterações no sistema de modulação descendente noradrenérgico, nomeadamente no que respeita aos mecanismos inerentes ao fenómeno de

potenciação dos recetores  $\alpha_2$ -adrenérgicos, uma vez que este fenómeno reforça a atividade espinhal antinociceptiva noradrenérgica.

**Palavras-chave:** Neuropatia induzida por quimioterapia, paclitaxel, dor neuropática, modulação descendente noradrenérgica, sensibilização espinhal, recetores  $\alpha_2$ -adrenérgicos

# Table of contents

---

|   |    |
|---|----|
| <b>Acknowledgments</b> .....  | 1  |
| <b>Abstract</b> .....   | 2  |
| <b>Resumo</b> .....   | 4  |
| <b>Table of contents</b> .....  | 7  |
| <b>List of figures</b> .....  | 9  |
| <b>List of schemes</b> .....  | 10 |
| <b>Abbreviations</b> .....  | 11 |
| <b>Introduction</b> .....   | 12 |
| 1. Pain .....   | 12 |
| 1.1. Pain definition .....  | 12 |
| 1.2. Pain transmission.....   | 12 |
| 1.3. Pain modulation .....  | 15 |
| 1.3.1.The endogenous pain control system .....                                | 15 |
| 1.3.2.Descending noradrenergic modulation .....                               | 16 |
| 1.4. Affective dimension of pain .....  | 17 |
| 2. Types of pain .....  | 20 |
| 2.1. Nociceptive pain.....  | 20 |
| 2.2. Inflammatory pain.....   | 20 |
| 2.3. Neuropathic pain.....  | 21 |
| 2.3.1.Peripheral neuropathic pain.....  | 21 |
| 2.3.2.Central neuropathic pain .....  | 22 |
| 3. Chemotherapy-induced peripheral neuropathic pain .....                     | 23 |
| 3.1. Epidemiology, symptoms and treatments.....                               | 23 |
| 3.2. Pathophysiology of paclitaxel-induced neuropathic pain .....             | 25 |
| <b>Aims and methodologies</b> .....   | 28 |
| <b>Materials and Methods</b> .....  | 30 |
| 1. Animals.....   | 30 |
| 2. Induction of chemotherapy-induced neuropathy and experimental design ..... | 30 |
| 3. Intrathecal surgery .....  | 33 |
| 4. Behavioral evaluation.....   | 34 |
| 4.1. Nociceptive behavior.....  | 34 |
| 4.2. Aversive behavior.....   | 36 |
| 5. Vascular perfusion and material processing for immunohistochemistry.....   | 39 |

|   |    |
|---|----|
| 6. Immunohistochemical studies .....  | 40 |
| 6.1. Immunohistochemical detection and analysis of dopamine- $\beta$ -hydroxylase (DBH) expression..... | 40 |
| 6.1.1.Immunohistochemical detection .....   | 40 |
| 6.1.2.Optimization of the methodology to analyze DBH expression.....                                    | 41 |
| A. Selection of the method for image analysis.....  | 41 |
| B. Delineation of the region of analysis .....  | 41 |
| 6.1.3.Analysis of DBH expression .....  | 42 |
| 6.2. Immunohistochemical detection and analysis of pCREB expression.....                                | 43 |
| 6.3. Immunohistochemical detection and analysis of c-Fos expression.....                                | 44 |
| 6.4. Immunohistochemical detection and analysis of $\alpha_{2A}$ -AR expression.....                    | 44 |
| 7. Western blotting analysis of $\alpha_{2A}$ -AR expression.....                                       | 45 |
| 8. Statistical analysis.....  | 47 |
| <b>Results</b> .....  | 48 |
| 1. Behavioral characterization of paclitaxel-induced neuropathy .....                                   | 48 |
| 1.1. Nociceptive behavior .....   | 48 |
| 1.2. Aversive behavior.....   | 49 |
| 2. Effects of paclitaxel on spinal neuronal activation .....  | 50 |
| 2.1. Expression of pCREB .....  | 50 |
| 2.2. Cold-induced c-Fos expression.....   | 51 |
| 3. Study of descending noradrenergic modulation in the paclitaxel-induced model of neuropathy.....      | 53 |
| 3.1. Analysis of DBH expression .....   | 53 |
| 3.1.1.Optimization of the methodology to analyze DBH expression.....                                    | 53 |
| A. Selection of the method of image analysis .....  | 53 |
| B. Delineation of the region of analysis .....  | 53 |
| 3.1.2.Effects of paclitaxel on DBH expression .....   | 55 |
| 3.2. Analysis of $\alpha_{2A}$ -AR expression.....  | 58 |
| 3.3. Analysis of $\alpha_{2A}$ -AR function .....   | 60 |
| <b>Discussion</b> .....   | 63 |
| 1. Behavioral alterations during CIN .....  | 63 |
| 2. Central sensitization .....  | 64 |
| 3. Engagement of descending noradrenergic modulation.....   | 66 |
| 4. Conclusions and future perspectives.....   | 69 |
| <b>References</b> .....   | 71 |
| <b>Appendix A: Composition of solutions</b> .....   | 78 |
| <b>Appendix B: Publication and oral communication</b> .....   | 79 |



## List of figures

---

|  |    |
|--|----|
| Figure 1. Nociceptive pathways from the periphery to the brain .....   | 13 |
| Figure 2. Spinal projections of primary sensory neurons.....   | 14 |
| Figure 3. Pathways and brain regions involved in the transmission and modulation of pain signals.....  | 16 |
| Figure 4. Corticolimbic circuit involved in the encoding of the sensory-discriminative and affective/emotional aspects of pain .....                             | 18 |
| Figure 5. Chemotherapy toxicity in the peripheral nervous system.....  | 25 |
| Figure 6. Catheter implantation into the intrathecal space of the lumbar enlargement of the spinal cord .....  | 34 |
| Figure 7. Nociceptive behavior testing apparatuses.....  | 35 |
| Figure 8. CPA testing apparatus .....  | 37 |
| Figure 9. Thresholding analysis for determination of the percentage of DBH positive pixels inside a 228 x 112 $\mu\text{m}$ rectangle using ImageJ software..... | 42 |
| Figure 10. Time course effects of systemic paclitaxel administration on mechanical sensitivity assessed by the von Frey test .....                               | 49 |
| Figure 11. Conditioned place aversion evaluated by the CPA test .....  | 50 |
| Figure 12. Expression of pCREB in the spinal dorsal horn at one month after CIN induction .....  | 51 |
| Figure 13. Expression of c-Fos after noxious-cold stimulation in the spinal dorsal horn at one month after CIN induction.....                                    | 52 |
| Figure 14. Optimization of the methodology to quantify DBH expression .....  | 54 |
| Figure 15. Optimization of the area for analysis of DBH expression.....  | 54 |
| Figure 16. Expression of DBH in the spinal dorsal horn at one month after CIN induction .....  | 56 |
| Figure 17. Expression of DBH in the spinal dorsal horn at two months after CIN induction .....   | 57 |
| Figure 18. Expression of $\alpha_{2A}$ -AR at the spinal dorsal horn at one month after CIN induction. ....  | 59 |
| Figure 19. Expression of $\alpha_{2A}$ -AR in the dorsal portion of the lumbar spinal cord (L4-L5) at one month after CIN induction.....                         | 60 |
| Figure 20. Effects of intrathecal administration of clonidine in the von Frey and the cold plate tests. ....   | 62 |

## List of schemes

---

|  |    |
|--|----|
| Scheme 1. Schematic diagram of the experimental groups.....  | 32 |
| Scheme 2. Diagram depicting the timing of the experimental procedures performed in group 1 on and von Frey test .....      | 35 |
| Scheme 3. Evaluation of the aversive effects of paclitaxel following a conditioning period of four days with the drug..... | 38 |

## Abbreviations

---

|   |  |
|---|--|
| $\alpha_2$ -AR – $\alpha_2$ -adrenergic receptor    | IR – Immunoreactive  |
| ABC – Avidin-biotin complex                         | I.t. – Intrathecal   |
| ACC – Anterior Cingulate Cortex                     | LC – Locus coeruleus   |
| BSA – Bovine serum albumin                          | NAc – Nucleus accumbens                                      |
| cAMP – Cyclic adenosine monophosphate               | NGS – Normal goat serum                                      |
| C-fos – Transcription factor of the Fos family      | NHS – Normal horse serum                                     |
| CGRP – Calcitonin-gene related peptide              | NPY – Neuropeptide Y   |
| CIN – Chemotherapy-induced Neuropathy               | NSS – Normal swine serum                                     |
| CPA – Conditioned Place Aversion                    | OFC – Orbitofrontal cortex                                   |
| CPP – Conditioned Place Preference                  | PAG – Periaqueductal gray                                    |
| CPSP – Central poststroke pain                      | PBS – Phosphate Buffered Saline                              |
| DAB – 3,3'-diaminobenzidine                         | PBS-T – Phosphate Buffered Saline with Triton                |
| DBH – Dopamine $\beta$ -hydroxylase                 | pCREB – phosphorylated cAMP response element-binding protein |
| DMSO – Dimethyl sulfoxide                           | PFA – Paraformaldehyde                                       |
| DRG – Dorsal Root Ganglion                          | PFC – Prefrontal cortex                                      |
| DRT – Dorsal reticular nucleus                      | ROI – Region of interest                                     |
| DTT – Dithiothreitol                                | RVM – Rostroventral medulla                                  |
| F-CPA – Formalin-induced Conditioned Place Aversion | S.c. – Subcutaneous  |
| GABA – Gamma aminobutyric acid                      | SCI – Spinal cord injury                                     |
| GAPDH – Glyceraldehyde 3-phosphate dehydrogenase    | SP – Substance P   |
| GAT-1 – GABA transporter 1                          | TNF- $\alpha$ – Tumor necrosis factor $\alpha$               |
| GPCR – G protein coupled receptor                   | TRPV1 – Transient receptor potential vanilloid subtype 1     |
| IL-1 $\beta$ – Interleukin-1 $\beta$                | VTA – Ventral tegmental area                                 |
| IL-6 – Interleukin-6                                | WDR – Wide dynamic range                                     |
| I.p. – Intraperitoneal                              |  |

# Introduction

---

## 1. Pain

### 1.1. Pain definition

According to the International Association for the Study of Pain (IASP), pain is defined as an unpleasant sensory and emotional experience associated with actual or potential tissue damage or described in terms of such damage [1]. Nociception is the process of detection of noxious stimuli and the subsequent transmission of encoded information to the brain, which will then produce pain as a sensation [2]. Acute pain serves a protective role as it works to motivate individuals to react to a tissue-damaging stimulus, preventing further damage. It also motivates us to protect the damaged area and seek treatment [3, 4]. In some cases, pain may persist beyond the necessary time for tissue healing, rendering it no longer beneficial for the individual. On that note, pain is considered chronic if it persists longer than three months and its maintenance is due to changes that occurred to the nervous system in consequence of the tissue damage or it can also occur for no apparent pathophysiological reason (as in fibromyalgia) [5]. Risk factors such as genetic predisposition, age, gender and previous pain experience also likely play a part in the transition from acute to chronic pain [6].

### 1.2. Pain transmission

In normal physiological conditions, the pain process begins after specialized peripheral sensory neurons called nociceptors detect high threshold physical (pressure and temperature) and noxious chemical stimuli extreme enough to potentially cause tissue injury and convert them into electrochemical signals [4]. Nociceptors, whose cell bodies are located in the dorsal root ganglia (DRG), ramify in the skin, muscle, connective tissue and internal environment of the organism such as the abdominal, pelvic and thoracic viscera. They initiate the transmission process of action potentials to the central nervous system, for which they are known as first order neurons [7]. There are two classes of first order nociceptive neurons, the myelinated A $\delta$ - and unmyelinated C-fibers (Figure 1), and they differ on their diameter and conduction velocities. Although they are both slow conducting fibers, the fact that the A $\delta$ -fibers are lightly myelinated and

have a larger diameter renders them faster than the C-fibers [8]. Because A $\delta$ -fibers transmit nociceptive impulses quicker, they initiate the response to tissue injury and are responsible for sharp and localized pain. The unmyelinated C-fibers transmit the impulses more slowly and are, therefore, responsible for dull, aching and poor localized pain [9].

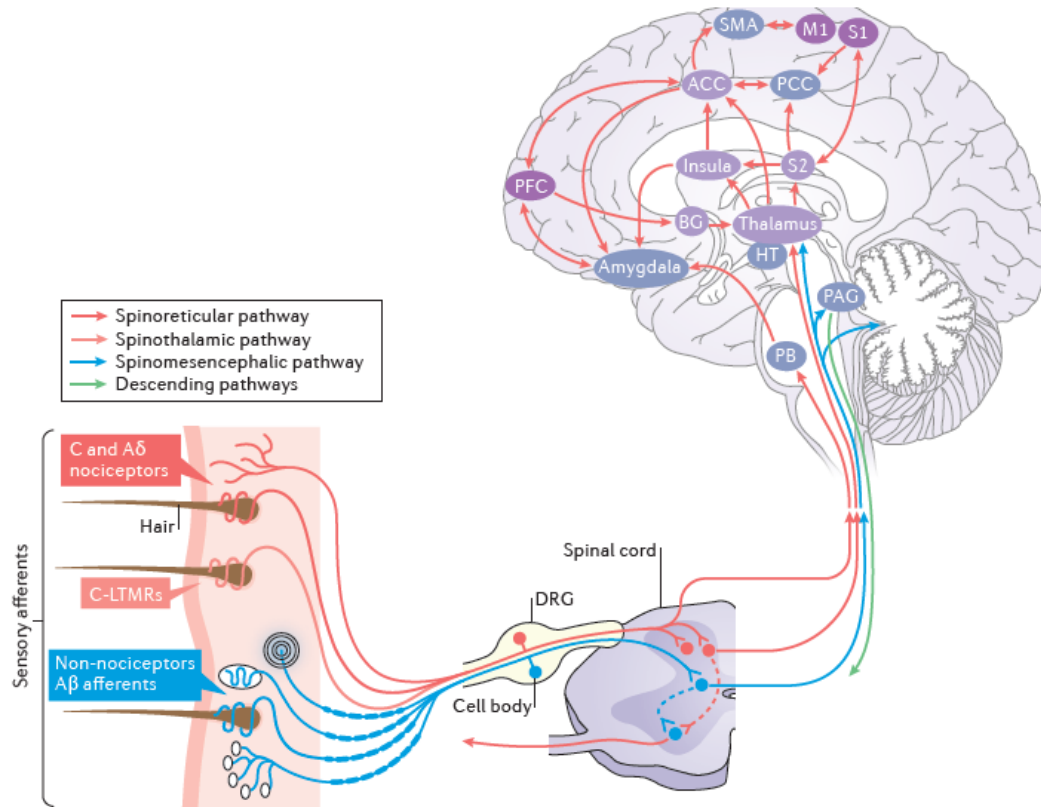


Figure 1. Nociceptive pathways from the periphery to the brain. High threshold thinly myelinated A $\delta$  and unmyelinated C nociceptor fibers (red box), whose cell bodies are localized in the DRG, detect, transduce and transmit information about noxious stimuli from peripheral tissues to the spinal dorsal horn, the first relay site in the transmission of nociceptive information. From the spinal cord, ascending neurons continue to transmit nociceptive signals, via the spinoreticular, spinothalamic and spinomesencephalic pathways (red and pink lines), to the several cortical and subcortical structures in the brain, in charge of further signal processing culminating in pain perception. Abbreviations: ACC, anterior cingulate cortex; BG, basal ganglia; C-LTMRs, C-type low-threshold mechanoreceptors; HT, hypothalamus; M1, primary motor cortex; PAG, periaqueductal grey; PB, parabrachial nucleus; PCC, posterior cingulate cortex; PFC, prefrontal cortex; S1, primary somatosensory cortex; SMA, supplementary motor area [10].

Adequate intensity of noxious stimulation or the release of chemicals at the site of an injury excite the nerve endings of first order primary afferent neurons and nociceptive information is then transmitted to second order neurons primarily located in the superficial laminae I and II and lamina V of the spinal dorsal horn [4] (Figure 2). The spinal dorsal horn neurons within laminae I and II are responsive to noxious stimulation via A $\delta$ - and C-fibers (high-threshold neurons), and neurons in laminae V receive both noxious and nonnoxious input via direct (monosynaptic) A $\delta$ - and A $\beta$ -fiber inputs,

respectively, and indirect (polysynaptic) C-fiber inputs. These neurons are called wide dynamic range (WDR) neurons since they respond to a broad range of stimuli intensities. Neurons in laminae III and IV are primarily responsive to innocuous stimulation via A $\beta$ -fibers (Figure 2) [11, 12]. The central projections of first order neurons can also synapse with inhibitory or excitatory interneurons that work to modulate nociceptive information before being further transmitted to the brain by second order neurons [7] (Figure 2).

The axons of second order neurons ascend to the brain, via the spinothalamic tract, to the thalamus (an important supraspinal pain processing center), or via the spinothalamic tract to the brainstem reticular formation before the nociceptive information is transmitted to the thalamus (Figure 1). At the thalamus, the nociceptive information is sent to the somatosensory (involved in the memory of sensory input) and prefrontal cortices, via third order neurons, for encoding and perception of the pain experience [13] (Figure 1). The reticular formation sends fibers transmitting nociceptive input not only to the thalamus but also to the hypothalamus, which is involved in the autonomic and reflex responses, and the limbic system, which encodes the emotional component of nociception (Figure 1).

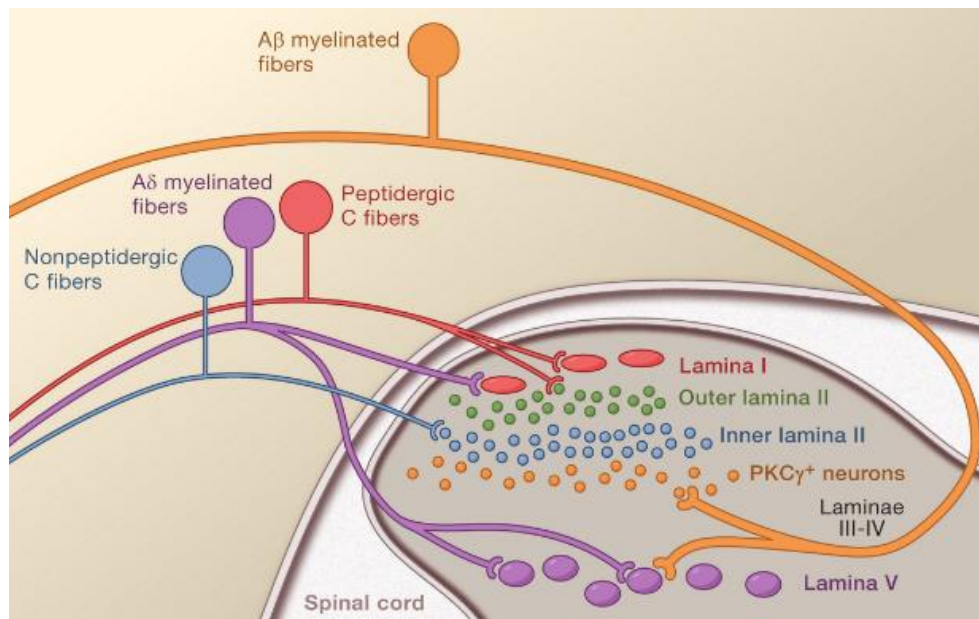


Figure 2. Spinal projections of primary sensory neurons. Unmyelinated peptidergic C-fibers, which release substance P, and calcitonin-gene related peptide (CGRP), and myelinated A $\delta$ -fibers terminate mainly at the superficial dorsal horn where they synapse with high-threshold projection neurons in lamina I (red) and interneurons in lamina II (green). A $\delta$ -fibers also converge on projection neurons of the wide dynamic range type in lamina V (purple). Large myelinated A $\beta$ -fibers, which carry innocuous input, terminate on lamina III [11].

### 1.3. Pain modulation

#### 1.3.1. The endogenous pain control system

The transmission of pain signals at the spinal cord can be altered by a complex process known as endogenous pain modulation. About 85% of the ascending axons of second order neurons in the spinal cord project to the brainstem reticular formation (via the spinoreticular tract), which includes areas in charge of pain modulation, such as the dorsal reticular nucleus (DRt), the rostral ventromedial medulla (RVM), the noradrenergic locus coeruleus (LC) and the periaqueductal gray region (PAG) [7, 14] (Figure 3). Descending axonal projections from these pain modulatory centers to the spinal cord modulate the spinal nociceptive transmission [15, 16] (Figure 3). This modulatory process, also known as descending pain modulation, works to inhibit or facilitate spinal nociceptive processing which ultimately controls the experience of pain. Descending modulation serves an evolutionary purpose important for survival and its activation depends on the emotional and cognitive states and level of arousal [17]. During stressful or threatening situations, descending inhibitory control of pain is activated to allow escape and protection. In such situations, the PAG, which receives projections from regions associated with the processing of emotions (including the hypothalamus, amygdala, and prefrontal cortex), forms excitatory synapses with the serotonin-releasing neurons of the raphe nucleus magnus and the nucleus gigantocellularis localized in the RVM, which ultimately project to the spinal dorsal horn [14]. The RVM mediates a bidirectional control of nociception by its resident on-cells, off-cells, or neutral-cells. Activation of the on-cells enhances firing as well as the intensity of the nociceptive response to noxious stimulation. Activity of the off-cells exerts antinociception. Activity of neutral-cells was found not to correlate with nociceptive stimuli. These cells are not serotonergic but they can modulate serotonergic neurons of the raphe nucleus magnus and the nucleus gigantocellularis. Once serotonin is released in the spinal dorsal horn, it plays inhibitory or facilitatory actions depending on the receptor subtype activated [14]. The PAG and RVM also project to noradrenergic areas (Figure 3) which in turn send projections to the spinal dorsal horn where they exert antinociception [18].

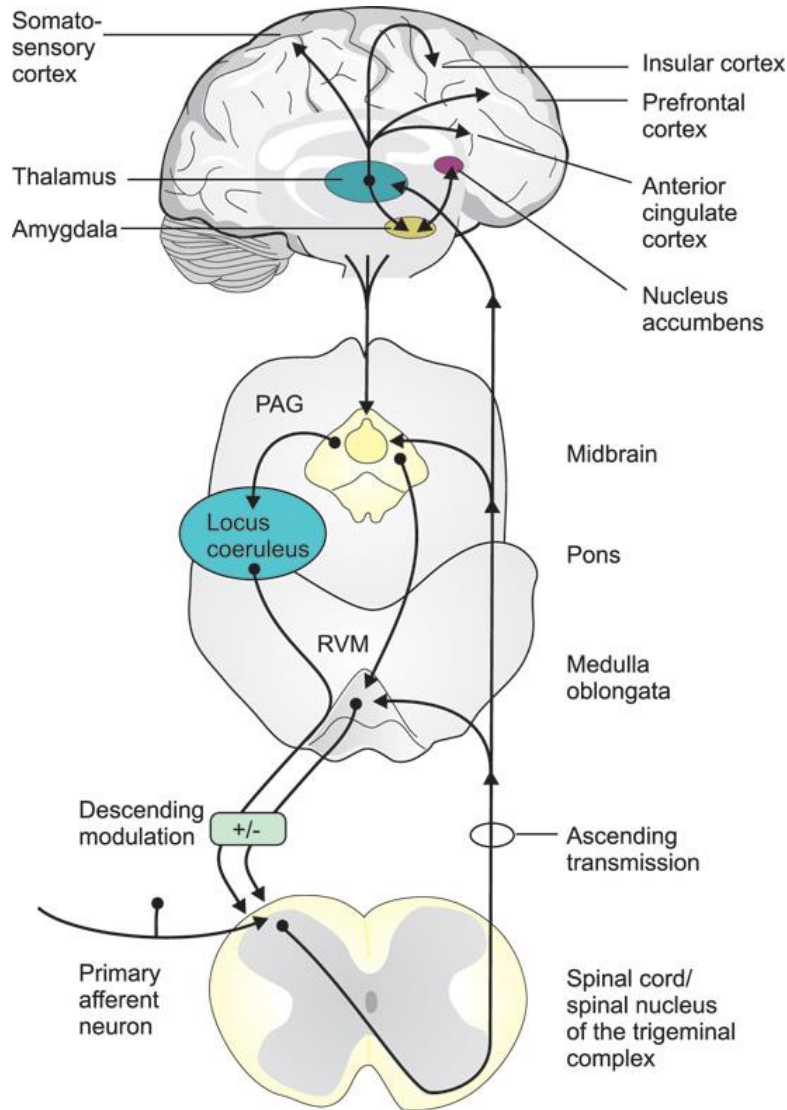


Figure 3. Pathways and brain regions involved in the transmission and modulation of pain signals. Nociceptive information ascending from the spinal cord is transmitted to the thalamus and to brainstem structures (medulla oblongata, pons and mid brain), including the rostral ventral medulla (RVM) and the periaqueductal grey (PAG). The thalamus projects to cortical (somatosensory, anterior cingulate, insular and prefrontal cortices) and subcortical (amygdala, nucleus accumbens) areas, which are involved in the processing of nociceptive information into a sensation. These brain regions project to the PAG, which in turn projects to the serotonergic raphe nuclei of the RVM and noradrenergic locus coeruleus. Descending pain modulatory projections from these sites to the first synapses in the spinal cord modulate nociceptive transmission [16].

### 1.3.2. Descending noradrenergic pain modulation

Three brainstem noradrenergic cell groups, the locus coeruleus (or A6 noradrenergic cell group), the A5 and A7 noradrenergic cell groups, are the main sources of noradrenergic projection to the spinal cord [19]. Descending noradrenergic fibers release noradrenaline at the spinal cord where it mainly exerts an inhibitory action at the



level of the afferent nociceptive terminals or spinal dorsal horn neurons (pre- and postsynaptic inhibition, respectively) via activation of  $\alpha_2$ -adrenergic receptors ( $\alpha_2$ -AR) [20].

Alpha-adrenergic receptors are pharmacologically subdivided into  $\alpha_1$  (further subdivided into  $\alpha_{1A}$ ,  $\alpha_{1B}$  and  $\alpha_{1D}$  subtypes) and  $\alpha_2$  (further subdivided into  $\alpha_{2A}$ ,  $\alpha_{2B}$  and  $\alpha_{2C}$  subtypes) adrenergic receptors belonging to the group A rhodopsin-like G protein-coupled receptor class [21]. Located in the dorsal root ganglion and in the spinal dorsal horn,  $\alpha_1$ -AR are coupled to phospholipase C through Gq and its activation by noradrenaline increases spinal and presynaptic neuronal excitability hence facilitation of nociceptive transmission [22]. The  $\alpha_2$ -AR are located on terminals of noradrenergic descending fibers (autoreceptors), on local spinal neurons, on central terminals of primary afferent nociceptors and on dorsal root ganglia [20]. They are negatively coupled to adenylate cyclase through Gi proteins and when activated, they exert an inhibitory action on neurotransmitter release by reducing the formation of cyclic AMP and calcium influx during an action potential. When noradrenaline is released from descending fibers, it suppresses pain by acting on the different subtypes of spinal  $\alpha_2$ -AR. The  $\alpha_{2A}$ -AR subtype is markedly expressed in noradrenergic descending fibers and its activation inhibits noradrenaline release to spinal neurons [21]. They are also expressed on central terminals of primary afferent neurons containing the excitatory neurotransmitters substance P and glutamate and upon activation of  $\alpha_{2A}$ -AR, the presynaptic inhibition of the release of these substances promotes antinociception [23]. The  $\alpha_{2C}$ -AR are located presynaptically on DRG terminals and postsynaptically on terminals of spinal excitatory interneurons which innervate second order neurons. Activation of postsynaptic  $\alpha_{2C}$ -AR inhibits transmission of nociceptive input to ascending neurons projecting to the supraspinal pain processing areas [24]. The  $\alpha_{2B}$ -AR appears to be the least expressed  $\alpha_2$  subtype in the spinal cord and primary afferent neurons of postnatal animals.

#### 1.4. Affective dimension of pain

Composed of both sensorial and affective dimensions, pain is considered a negative affective (unpleasant) state that works not only to motivate animals to maintain homeostasis by escaping/avoiding harmful situations (e.g. injuries, noxious stimuli) or to seek relief but also to promote learning about the outcome of those situations that might present again in the future [25]. Several corticolimbic regions integrate the brain circuit involved in encoding nociceptive signal valuation, pain-motivated decision-making and learning (Figure 4). One such area is the dopaminergic nucleus accumbens (NAc), which signals affective value and saliency of noxious stimuli [26]. The NAc receives projections from dopaminergic neurons in the ventral tegmental area (VTA). Natural rewards such

as pain relief activates these mesolimbic neurons and elicit dopamine release in the NAc. VTA dopaminergic inputs to the NAc signal saliency, as well as the value of pain or relief. Reward-related information is also encoded in frontal lobe areas, specifically in the anterior cingulate cortex (ACC), lateral orbitofrontal cortex (OFC), and ventromedial and anterior prefrontal cortices (PFC). The connections between these prefrontal, orbitofrontal and anterior cingulate cortices and the mesolimbic dopaminergic neurons contribute to affective, emotional and cognitive control of pain perception and are involved in motivational decision-making [25]. Chronic pain states are characterized by anatomical and functional reorganization of the corticolimbic circuit.

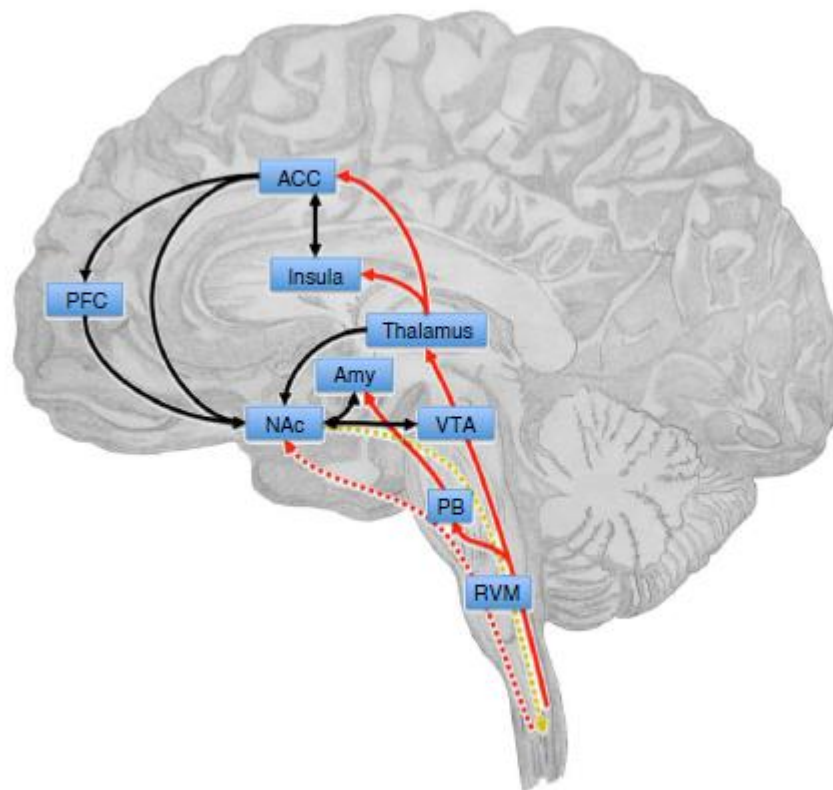


Figure 4. Corticolimbic circuit involved in the encoding of the sensory-discriminative and affective/emotional aspects of pain. The dopaminergic NAc plays a role in reward-motivated behavior by encoding quantitative reward prediction error, which is important for learning and decision-making in relation to noxious stimuli. Reward-related information is also encoded in the ACC, OFC and PFC. These structures contribute to affective, emotional and cognitive control of pain perception and are involved in motivational decision-making [25].

In chronic pain states, both nociceptive signaling and associated affective/emotional and cognitive functions are altered. This emotional component of pain does not receive much attention in animal studies of chronic pain, more so because of the lack of experimental tools for these types of studies. One such tool that has been gaining attention is the conditioned place aversion (CPA) paradigm. The CPA paradigm

is an operant model used to assess escape/avoidance behaviors under the principle that animals, once taught how to associate an environment to the feeling of unpleasantness derived from a painful situation, will exhibit an escape response towards an alternative environment that they learned not to be associated with pain [27, 28]. In that case, it is possible to study the affective component of pain originating from noxious stimulation (thermal, mechanical or chemical) or from spontaneous neuronal discharge (chronic ongoing pain). The formalin test (a noxious chemical stimulus) in the context of the conditioning-place paradigm is very commonly used to distinguish pain emotion from pain sensation in rats [29]. More than eliciting nociceptive behavior, such as lifting responses, subcutaneous injection of dilute formalin produces CPA (F-CPA), which means that animals learn about its aversiveness similarly as humans learn about the outcome of a noxious stimuli [30]. One of the best-known brain areas to be involved in processing information related to pain-derived unpleasantness is the ACC. Neurons in the ACC were found to be necessary for the acquisition of CPA elicited by nociceptive stimulus such as formalin injection, seen as lesions of the rostral ACC reportedly reduced F-CPA by reducing the aversiveness or perceived unpleasantness of the stimulus, without reducing formalin-induced nociceptive behaviors [30]. In a model of chronic inflammatory pain, repeated activation of ACC neurons resulting from persistent peripheral nociceptive input has been shown to serve as an aversive teaching signal, leading animals to display generalized increased aversive responses to noxious stimuli [31]. Imaging and neurophysiologic studies revealed increased activity in the ACC in patients and animal models of neuropathic pain. One such study found enhanced affective pain ratings in response to noxious heat in diabetes patients with neuropathic pain consistent with augmented cerebral activity in the ACC [32]. In chemotherapy-induced neuropathic pain, which is the main subject of this thesis, little is known about the affective component of pain in animals, but in humans the painful symptoms are often accompanied by mood disorders such as depression [33].

## 2. Types of pain

### 2.1. Nociceptive pain

Nociceptive pain is a fundamental type of pain and overall an important physiological process for homeostasis. It serves as a warning sign for animals to withdraw from noxious peripheral stimulation and pay special care to an injured site in the body, at the same time serving as a teaching signal about the outcome of similar harmful situations in the future [25]. Information about the nature, intensity and duration of peripheral noxious stimulation travels from peripheral nerve endings of A $\delta$ - and C-fibers which upon noxious stimulation release neurotransmitters like the excitatory amino acids glutamate and aspartate, calcitonin gene-related peptide (CGRP), substance P (SP) and neuropeptide Y (NPY) at the spinal dorsal horn. Second order neurons in the spinal cord then continue the transmission process through ascending projections to the brain, which in turn will interpret the nociceptive signals and produce the pain experience [34]. The benefits of nociception cease the moment it becomes permanent as a result of disease processes directly or indirectly affecting the nerves [35].

### 2.2. Inflammatory pain

Inflammatory pain occurs following activation of the inflammatory process upon tissue damage. The underlying release of sensitizing inflammatory mediators, including bradykinin, prostaglandins, H<sup>+</sup>, ATP, nerve growth factors, pro-inflammatory cytokines and interleukins by infiltrating immune cells such as macrophages, T-cells, mast cells and neutrophils leads to activation of receptors in the nociceptors innervating the damaged tissue [36]. As a consequence of increased ambient inflammatory mediators, there is a reduction in the activation threshold of the A $\delta$ - and C-fibers upon noxious stimulation [37]. One of the features of inflammatory pain states is that normally innocuous stimuli produce pain because low-threshold A $\beta$ -fibers, that normally only conduct innocuous tactile stimuli, are sensitized by these inflammatory mediators as well [38]. The peripheral sensitization process during inflammation is important for optimal healing, because it motivates protection behaviors of the injured area as well as prevention from contact or movement to reduce further damage and pain [37]. Spinal cord neurons are also more excitable and amplify ascending inputs to the brain. The changes in neuronal sensitivity following inflammation are generally reversible and sensitivity will most likely be restored when the inflammation has disappeared. However, repetitive nociceptive stimulation, whether being inflicted in previously inflamed

peripheral tissues or new ones, may result in a prolonged inflammatory process through activation of lymphocytes and release of tumor necrosis factor (TNF- $\alpha$ ) and interleukins IL1, IL6, and IL1 $\beta$ , which eventually leads to chronic inflammatory pain and subsequent aggravation of neuronal sensitization [39].

### **2.3. Neuropathic pain**

Neuropathic pain is defined as pain resulting from abnormal activity of neuronal tissues, either of the peripheral and central nervous systems, due to disease, injury or dysfunction, which can lead to a persistent pain state [5]. Abnormal signals may arise directly from injured axons and/or from the intact nociceptors that share their innervation territory [40]. Peripheral and central sensitization mechanisms are at the basis of altered neuronal activity. This type of pain is distinct from the inflammatory pain as the latter arises from intact nociceptive signaling pathways [37]. There is neuronal sensitization occurring during inflammatory pain, but it is for securing optimal healing conditions, while in neuropathic pain there is no benefit in neurons being sensitized. Inflammation is a component process seen in neuropathic pain, but it is one of the many sources of increased neuronal excitability in neuropathic pain.

There are two types of neuropathic pain: peripheral and central neuropathic pain and they differ on the location of the nerve lesion.

#### **2.3.1. Peripheral neuropathic pain**

A peripheral neuropathy is described as a painful and debilitating condition caused by disease or direct damage inflicted on peripheral nerves. The leading causes of nerve damage include disease processes such as diabetes, traumatic nerve injuries and exposure to neurotoxic compounds, such as chemotherapeutic drugs [41]. Diabetic neuropathy manifests due to complex metabolic modifications in the organism that lead to neuronal impairment [42]. Traumatic events like vehicle accidents, sports injuries and surgical procedures can cause nerve injury by compression or severing and such physical damage may ultimately result in loss of nerve function and cause neuropathy [41]. Chemotherapeutic drugs, which are administered to patients with cancer for their ability to disrupt the division and growth processes of cancer cells, often cause damage to peripheral nerves.

In any presentation of peripheral neuropathy, symptoms develop according to the type of nerve that has been damaged. Patients with neuropathy can experience positive and negative sensory symptoms, motor symptoms and/or autonomic symptoms. Positive sensory symptoms range from numbness and tingling to neuropathic pain manifested as

intense pain episodes without any seeming provocation (spontaneous pain), pain to tactile and thermal stimuli that would not otherwise be felt (allodynia) and enhanced pain sensation after a painful stimulus (hyperalgesia) [4]. The negative sensory symptoms include an overall loss of stimuli perception (e.g. tactile and thermal). Motor symptoms include muscle weakness and wasting [43]. And the autonomic symptoms are mainly related to cardiovascular (blood pressure oscillations), gastrointestinal (constipation) and urological (urinary retention) abnormalities [44].

The painful symptoms of peripheral neuropathy develop due to peripheral and central sensitization mechanisms. In peripheral sensitization, nociceptors become hypersensitive due to several molecular changes following damage, such as formation of new channels and altered gene expression culminating in altered receptor protein expression and activity. Notably, expression of voltage-gated sodium channels, which form clusters that accumulate at the site of injury and proximally within the intact dorsal root ganglion, lead to ectopic firing and lowering of the action-potential threshold [45]. Damage to peripheral nerves also induces upregulation of receptor proteins such as the Transient receptor potential vanilloid 1 (TRPV1) in A- and C-fibers, which contributes to enhanced responses to noxious heat (heat hyperalgesia) [46]. There is also release of proinflammatory cytokines, chemokines and neurotrophic factors from immune cells. All of these alterations contribute to hyperexcitability of A- and C-fibers [47]. The amplified pain signals from the periphery alter the sensitivity of spinal dorsal horn neurons, leading to central sensitization. Central sensitization corresponds to an enhancement in the activity of neurons and circuits in nociceptive pathways caused by increases in membrane excitability, synaptic efficacy and reduced inhibition [48]. Due to central sensitization, nonpainful peripheral stimuli are interpreted as painful and peripheral noxious stimuli are interpreted as overly painful.

### **2.3.2. Central neuropathic pain**

Central neuropathic pain occurs due to insult to the spinal cord, brain or brainstem. The main sources of injury include ischemic or hemorrhagic strokes, infections, demyelinating multiple sclerosis, traumatic spinal cord or brain injury, and cancer [49]. Central neuropathic pain stems from impairment within somatosensory pathways. Indeed, dysfunction of spino-thalamic-cortical pathways results in impaired pain in response to pinprick and temperature sensation in a neurologically affected painful limb [50]. Regarding pathophysiology of central neuropathic pain, intact spinothalamic tract neurons become hyperexcited and chronically activated at the level of the spinal cord injury (SCI) site, directly via microglial activation and/or via disruption of descending inhibition. Disinhibition is also associated with lesions of the thalamus, for

which there is disruption of GABAergic neurons and increased sensory input to cortical regions resulting in painful sensation [51]. Spontaneous activity has also been reported in deafferented thalamic regions during central poststroke pain (CPSP) and in the intact thalamus following SCI [52, 53].

### **3. Chemotherapy-induced peripheral neuropathic pain**

#### **3.1. Epidemiology, symptoms and treatments**

In the current century, the estimate of individuals that successfully underwent chemotherapy for treatment of hematological and solid tumors is, as of 2013, over 25 million worldwide [54]. The incessant effort to improve the effectiveness of chemotherapeutic drugs while reducing their inherent side-effects explains the observed survivorship rates. However, there is much concern about the adverse effects at the whole-body level. One of the most problematic side-effects of chemotherapeutic treatment is the onset of peripheral neuropathy, which may begin early on or long after treatment [55] and estimates show that 30 to 40 percent of cancer patients develop this chemotherapy-related complication that limits both drug dose and duration of treatment [41].

Chemotherapy-induced neuropathy (CIN) is a condition that develops from damage to peripheral nerves inflicted by chemotherapeutic drugs and that interferes with the active treatment of cancer by forcing dosage reduction, treatment delay or premature cessation. More than hindering the battle against cancer, CIN produces a set of symptoms with variable levels of severity that reduce the quality of life of cancer patients [56]. Anticancer drugs can harm any of the peripheral nerves (sensory, motor and autonomic), especially sensory and autonomic nerves given their anatomical location outside the blood-brain barrier. The reason is that capillaries with fenestrated and leaky walls supply these neurons allowing for the passage of exogenous toxic substances from the circulation (in contrast to what happens in the brain and spinal cord) and making them very susceptible to damage [57]. The way these neurotoxic drugs interfere with peripheral nerve function may be through perturbation of metabolic processes inside neuronal cell bodies, impairment of axonal transport by microtubule disruption and activation of apoptosis pathways in consequence of DNA damage [58].

CIN symptoms may present at any time after initiation of the treatment or even weeks to several months after its completion, depending on the extent of damage [59]. Particularly, sensory symptoms are generally the most prominent, with pain, tingling, numbness and loss of sensibility being often present in the lower and upper limbs [60].

Motor symptoms are not very common and it is not well known why motor nerves are less affected [61], but in some cases, muscle cramps in the forearm and hands may be experienced and in the worst cases (which are rare), they can progress to paralysis. Unlike the sensory symptoms, autonomic symptoms are infrequently seen in CIN, though both types of nerves are vulnerable to damage given their location outside the blood-brain barrier. The reason for this is that it takes only a small loss of sensory neurons or axons to produce the typical associated symptoms than to disrupt organ function [62].

The severity and duration of CIN symptoms vary among patients and depend on factors such as the drug dose per cycle of treatment, the cumulative dose in the body over time, the frequency of its administration, the nature of the drug and predisposing factors such as a history of pathology in the nerves [62, 63]. Before initiating chemotherapy, the treatment is established based on the type of cancer and its stage of development and also based on the response rate to a particular chemotherapeutic drug or combination of drugs [64]. When it comes to drug dosage, a high dose of the drug may be prescribed for cancers in advanced stages in order to increase chances of survival. However, studies on patients with ovarian cancer, for example, show that increasing dose intensity per cycle shows no benefit in survival when compared to a low dose per cycle regimen [65] and leads to a more severe neuropathy, that often starts in a few days after initiation of the treatment [66]. On the other hand, when patients receive a low dose per cycle, they usually show longer overall survival and present mild neuropathic symptoms. Nevertheless, receiving a low dose per cycle means receiving it on a weekly basis and such frequency increases neurotoxicity and the risk of developing neuropathy due to higher cumulative doses in the body [59]. When it comes to choosing which drug to use in the treatment, special attention is paid to the information on the cancer and response rates as well as the nature of the drug and how severe its neurotoxic effects can be.

The cytostatic agents known to induce CIN are the platinum agents (cisplatin, carboplatin and oxaliplatin), anti-tubulin (paclitaxel, docetaxel and vincristine) and the proteasome inhibitor bortezomib. Given their individual structural properties, these agents promote different pathological processes on peripheral nerves, causing a dissimilar degree of damage which subsequently influences the severity of CIN symptoms [63] (Figure 5).



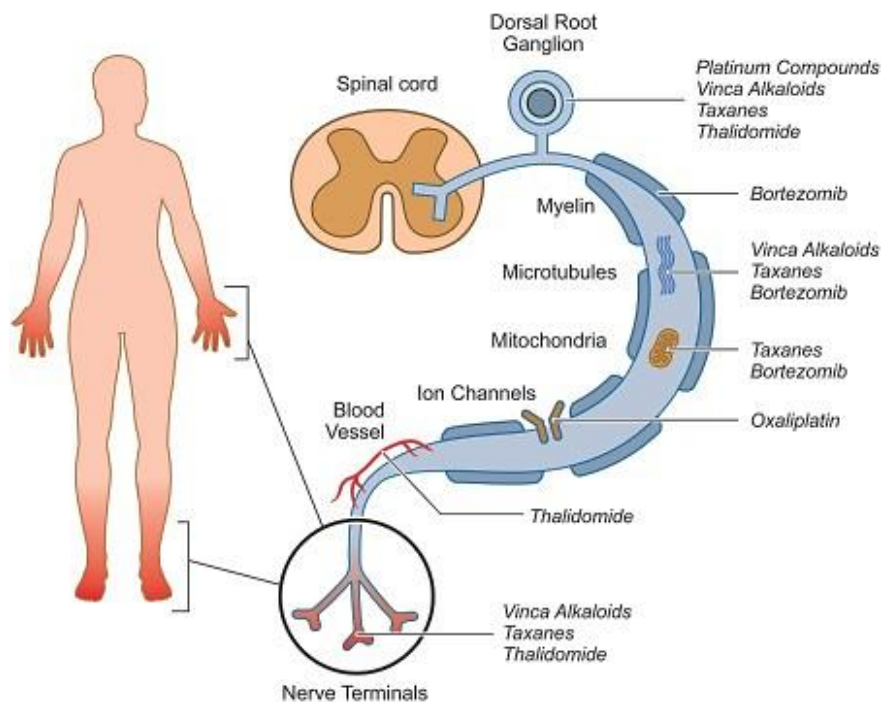


Figure 5. Chemotherapy toxicity in the peripheral nervous system. Several chemotherapeutic drugs have been shown to affect the distal nerve terminals, axons and its components (myelin, microtubules, mitochondria, ion channels and vascular network) and dorsal root ganglia, all of which lead to peripheral sensitization and painful neuropathy [55].

### 3.2. Pathophysiology of paclitaxel-induced neuropathic pain

Paclitaxel is a taxane-derived chemotherapeutic agent that was first isolated from *Taxus brevifolia* and is now extensively used for the treatment of breast, ovarian and non-small cell lung carcinomas. The drug exerts its antineoplastic effects by binding to  $\beta$ -tubulin of microtubules in cancer cells, preventing depolymerization, blocking the progression of the cell cycle and inducing apoptosis [67]. The best-known side-effects of paclitaxel arise from damage to peripheral sensory nerves which ultimately leads to the development of peripheral neuropathy.

Several studies have been conducted to investigate the pathological processes initiated by paclitaxel within the pain modulatory system, some of which have used animal models treated with different regimens of paclitaxel to mimic the paclitaxel-induced neuropathic pain condition in humans. *In vitro* studies have demonstrated that paclitaxel causes microtubule dysfunction in cultured sensory neurons by promoting microtubule stabilization, condensation and reorientation [68, 69], which in turn causes disruption of axoplasmic organelle transport, abnormal neurite outgrowth, demyelination and neuronal death [66]. *In vivo* studies using rodent models have demonstrated that paclitaxel causes degeneration of peripheral terminal arbors of sensory neurons in the

hind paw skin of rats, which originates spontaneous discharge and mechanical and thermal hypersensitivity [70]. Paclitaxel is also known to promote axonal mitochondrial swelling through a calcium efflux mechanism [71], contributing to hyperexcitability of nociceptors which results in mechano-allodynia and mechano-hyperalgesia. The drug also increases the expression and activity of the Transient receptor potential vanilloid subtype 1 (TRPV1) ion channel in rat and human DRGs, leading to increased pain signaling that ultimately results in thermal hyperalgesia [72]. At last, paclitaxel promotes the release of proinflammatory cytokines upon astrocyte activation in the spinal cord and macrophage activation in the DRG, which lead to nociceptor sensitization [68]. Differences in the severity of pathological, electrophysiological and behavioral abnormalities produced by paclitaxel have been reported among regimens and animal models used. Paclitaxel administration in rats at high dosing regimens of 16 mg/kg once a week for 5 weeks or 2 doses of 12-18 mg/kg 3 days apart produced mitochondrial swelling, axonal loss and slow conduction velocities in sensory and motor nerves that persisted for 4 months with no abnormalities to thermal sensation [73]. Lower doses given to rats intraperitoneally (0,5-2,0 mg/kg) every other day for a total of 4 injections produced no impairment in motor function and degeneration of sensory and motor axons, but resulted in heat-hyperalgesia, mechano-allodynia, mechano-hyperalgesia and cold allodynia which resolved in a few weeks [74, 75]. Other studies using mouse models have reported a dependence of the neuropathic phenotype on the genetic background of the mice since the same dose of paclitaxel was shown to produce different effects and did not result in any neuropathic behavior in some mice strains [75].

The majority of these studies have looked at the pathophysiological processes induced by paclitaxel occurring in the peripheral nervous system. But even though paclitaxel does not seem to cross the blood-spinal cord barrier, it likely causes peripherally-mediated alterations in the spinal cord by enhancing the nociceptive input from the functionally-impaired and hypersensitive nociceptors into second-order neurons and/or interneurons and by promoting the activation of glial cells, as described in other neuropathic pain models [10]. Namely, there is an activity-dependent increase in the density of synaptic spines in dendrites of spinal neurons that leads to hypersensitivity (structural plasticity) [76]; also, the increased incoming afferent activity can deregulate spinal interneurons causing a disturbed balance between spinal excitation and inhibition of pain signals (functional plasticity). Additionally, in a peripheral nerve transection model, damage to first-order neurons was shown to initiate central immune signaling first by activation of microglia and then astrocytes, both of which release proinflammatory cytokines such as interleukin-1 $\beta$  (IL-1 $\beta$ ), interleukin-6 (IL-6) and tumor necrosis factor- $\alpha$  (TNF- $\alpha$ ) that diffuse and bind to receptors on presynaptic and postsynaptic terminals in

the spinal dorsal horn to control excitatory and inhibitory synaptic transmission [13, 77]. These and other glia-derived mediators have been shown: i) to increase excitatory synaptic transmission at central terminals by enhancing glutamate release, which contributes to the development of central sensitization and pain behaviors; and ii) to reduce the activity of inhibitory interneurons or inhibitory descending projections, causing nociceptive hypersensitivity [10, 13].

In the paclitaxel model, recent studies using the rat model of paclitaxel-induced neuropathy have reported signaling alterations in the spinal cord, namely an increase in TRPV1 expression on spinal terminals of primary afferent neurons in animals with thermal hypersensitivity [72] and decreased expression of glutamate transporters in spinal astrocytes, which fails to clear excitatory glutamate from synapses and induces spontaneous nociceptive behaviors and hypersensitivity [78]. However, little is still known about the mechanisms of neuronal plasticity and glial cell functioning during neuropathy at the level of the spinal cord.

## Aims and methodologies

---

The pathophysiological mechanisms at the central nervous system leading to the development of neuropathic pain during and after chemotherapeutic treatment with paclitaxel are still understudied. The main purpose of this thesis was to study the alterations that the chemotherapeutic agent paclitaxel produces in the descending noradrenergic modulatory system. For that, we used a rat model replicating CIN induced by paclitaxel. The research work conducted for this thesis was comprised of three parts: i) behavioral characterization of paclitaxel-induced neuropathic pain; ii) study of the activation patterns of superficial and deep spinal dorsal horn neurons induced by paclitaxel treatment; and iii) study of the descending noradrenergic modulatory system in paclitaxel-treated rats, the main focus of the thesis.

First, we studied the effects of paclitaxel in mechanical sensitivity and in the affective/emotional component of pain. For that, CIN was induced by administering four intraperitoneal injections of paclitaxel at 2.0 mg/kg on four alternating days [74]. To determine the onset and maintenance of mechanical sensitivity in paclitaxel-treated animals, we used the von Frey test which was performed prior to initiation of the treatment and several days after initiating the treatment, for two months. To study the affective/emotional component of pain, we aimed at assessing if animals developed escape or avoidance behaviors towards receiving paclitaxel as they were conditioned in an environment with specific cues that allowed them to associate the physical space to the feeling of receiving the drug. For that, we used a variation of the Conditioned Place Preference (CPP) test, an established rodent paradigm of drug reward, which was the Conditioned Place Aversion (CPA) test. The tests differ only on the feeling that the drug under study triggers on animals. In our case, we aimed at determining whether paclitaxel induced aversive-like behaviors.

The second goal of the present thesis was to evaluate the activation patterns of spinal dorsal horn neurons in paclitaxel-treated rats by studying the expression of two markers of neuronal activation: pCREB and c-Fos. The spinal expression of pCREB has been reported to be activated after nerve injury in several neuropathic pain models and is known to be driven by ongoing abnormal afferent input, rendering it important for maintaining central sensitization [79]. C-fos is a proto-oncogene whose protein product, c-Fos, is used as a marker for the activation of nociceptive neurons in the superficial and deep spinal dorsal horn of rats following depolarization after a noxious stimulus [80]. In

normal conditions, there is a direct correlation between the levels of c-Fos expression and the intensity of the noxious stimulation. In pathological conditions, a low-intensity innocuous stimulus is sufficient to elicit neuronal activation [81]. We aimed at assessing the basal expression of pCREB in the dorsal horn of the spinal lumbar L4 segment by immunohistochemistry, at one month after CIN induction. We aimed at determining the expression of c-Fos after noxious cold stimulation, in the dorsal horn of the spinal lumbar L4 segment by immunohistochemistry at one month after CIN induction. We selected the one-month time point for this analysis because it is reported in the literature as the peak of pain severity in this animal model [71].

The third goal of this thesis was to study the descending inhibitory noradrenergic pain modulation during CIN induced by paclitaxel treatment. Based on animal studies of other types of peripheral nerve injury, it is thought that one of the underlying mechanisms for the development of the typical painful symptoms in neuropathic pain (ongoing or spontaneous pain, allodynia and hyperalgesia) is loss of inhibition of nociceptive transmission, either by physical loss of inhibitory neurons or changes in the activity of pain inhibitory pathways [10]. In normal conditions, the activation of the presynaptic  $\alpha_2$ -adrenergic receptors (ARs) on central terminals of primary afferent nociceptors in the spinal cord by noradrenaline inhibits the presynaptic release of excitatory neurotransmitters responsible for transmission of pain signals [20]. In neuropathic conditions, this inhibitory mechanism is presumably lost which may account for the manifestation of the painful symptoms [82]. Here we aimed at evaluating the noradrenergic innervation in the spinal dorsal horn and then the expression and function of the presynaptic  $\alpha_{2A}$ -AR subtype. The noradrenergic innervation was evaluated at the spinal dorsal horn of L4 and L5 segments by immunohistochemical detection and quantification of the noradrenaline biosynthetic enzyme dopamine- $\beta$ -hydroxylase (DBH), at one and two months after initiation of paclitaxel treatment. DBH is a highly-used marker of pontospinal noradrenergic innervation [83, 84]. The  $\alpha_{2A}$ -AR expression was assessed by western blotting and immunofluorescence in the same lumbar segments of the spinal cord at one month after CIN induction. The function of  $\alpha_{2A}$ -AR was assessed by studying behavioral nociceptive responses of the rats after intrathecal administration of two doses of the  $\alpha_2$ -AR agonist clonidine which mimics the effects of spinally released noradrenaline. The effects of clonidine were evaluated on evoked pain by the von Frey and Cold Plate tests which assess mechanical and cold allodynia, respectively.

# Materials and Methods

---

## 1. Animals

Adult male Wistar rats (Charles River, France) were used in this study. The animals were pair-housed in plastic cages at  $22 \pm 2^\circ\text{C}$  and  $55 \pm 5\%$  humidity in a 12/12h light/dark cycle. The animals had unrestricted access to food and water. Upon arrival, rats were allowed one week of acclimation before any procedure.

All experiments were conducted following the ethical guidelines of the European Community Council Directive 2010/63/EU and of the International Association for the Study of Pain in conscious animals [85].

## 2. Induction of chemotherapy-induced neuropathy and experimental design

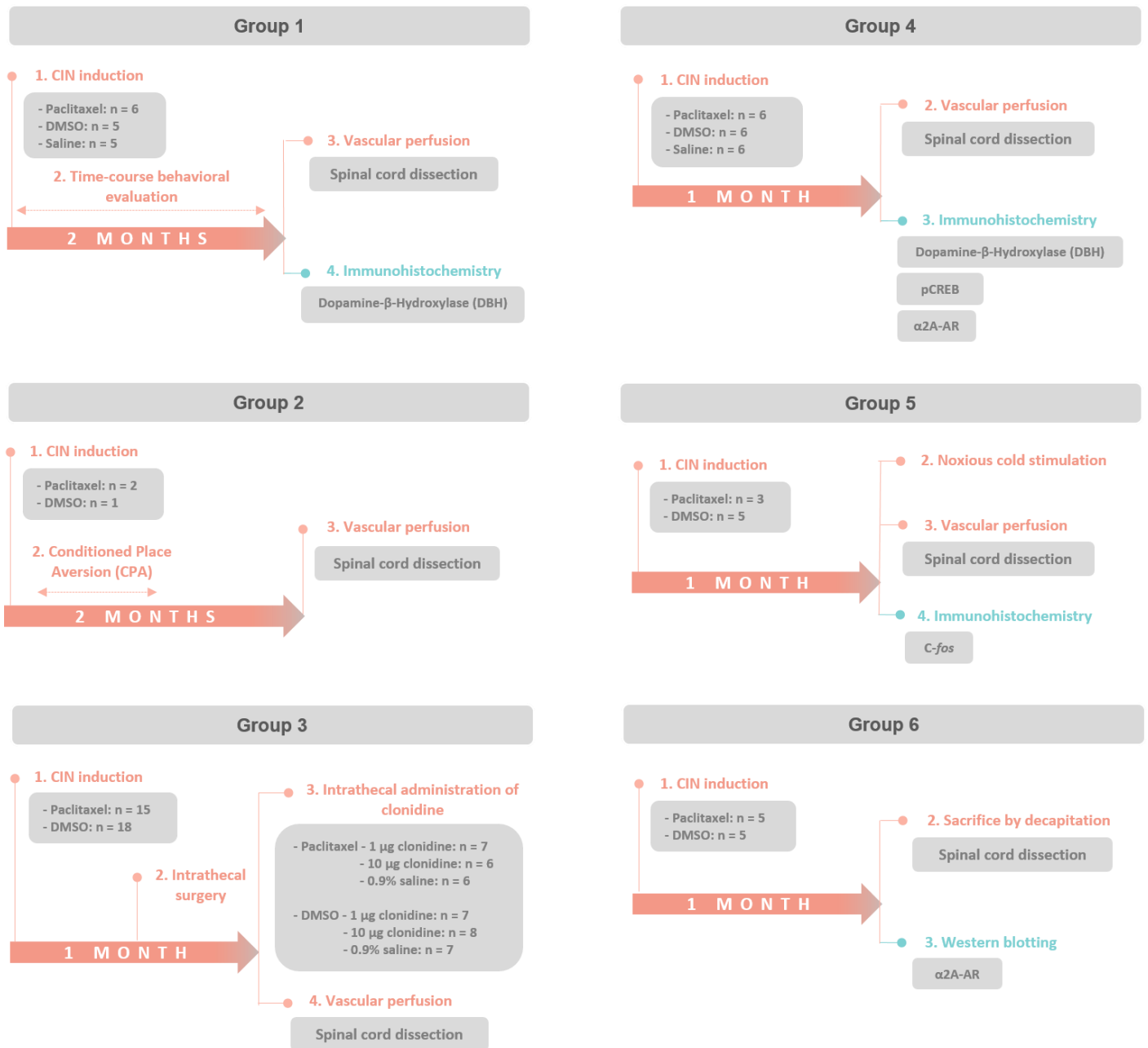
Chemotherapy-induced neuropathy (CIN) was induced in animals weighing 175-190 g by four intraperitoneal (i.p.) injections of paclitaxel (Taxol®, Tocris Bioscience, United Kingdom) at a dose of 2.0 mg/kg in four alternating days (1, 3, 5 and 7) as previously described by Polomano et al. (2001) [74]. Stock solutions of paclitaxel were prepared according to supplier's standard recommendations by dissolving 50 mg of paclitaxel in 1 ml dimethyl sulfoxide (DMSO, Sigma-Aldrich®, USA) with gentle agitation at  $37^\circ\text{C}$ . The stock solutions were aliquoted and stored at  $-20^\circ\text{C}$ . Before administration of paclitaxel, the aliquots were thawed and diluted in saline solution (NaCl 0,9%) at  $37^\circ\text{C}$  with gentle agitation to a final concentration of 2.0 mg/ml of paclitaxel and 4% DMSO. Control animals were either treated with the vehicle solution 4% DMSO (DMSO group) or 0.9% NaCl (saline group).

CIN was induced in six different experimental groups in order to perform behavioral, immunohistochemical and western blotting analysis (scheme 1). The behavioral studies aimed at evaluating nociceptive and aversive behaviors. The experimental group 1 (paclitaxel n = 6, DMSO n = 5, saline n = 5) was used to evaluate mechanical sensitivity for a period of two months following CIN induction (scheme 1). The experimental group 2 (paclitaxel n = 2, DMSO n = 1) was used to assess aversive behaviors (scheme 1).

The experimental group 3 was used to study the effects of spinal  $\alpha_{2A}$  adrenergic receptor ( $\alpha_{2A}$ -AR) activation on nociceptive behaviors, at one month after CIN induction. For this, we used paclitaxel- (n = 19) and DMSO-treated (n = 22) animals, submitted to an intrathecal surgery for implantation of a catheter in the lumbar segment of the spinal cord through which the  $\alpha_2$ -AR agonist clonidine was administered (scheme 1).

Immunohistochemical analyses were performed to analyze the expression of DBH, pCREB,  $\alpha_{2A}$ -AR and c-Fos at the spinal dorsal horn. These analyses were performed upon vascular perfusion and spinal cord dissection (scheme 1). The expression of DBH was analyzed at two different time points, one and two months after CIN induction. The experimental group 1 was used to analyze DBH expression at the two-month time point (scheme 1). The experimental group 4 (paclitaxel n = 6, DMSO n = 6, saline n = 6) was used to analyze the one-month time point (scheme 1). The experimental group 4 was also used to analyze the expression of pCREB and  $\alpha_{2A}$ -AR. The experimental group 5 (paclitaxel n = 3, DMSO n = 4), which was submitted to noxious cold stimulation prior to vascular perfusion, was used to analyze the expression of c-Fos (scheme 1).

The expression of the  $\alpha_{2A}$ -AR at the spinal dorsal horn was also evaluated by western blotting analysis. The experimental group 6 (paclitaxel n = 5, DMSO n = 5) was used for this purpose (scheme 1).



**Scheme 1:** Schematic diagram of the experimental groups. Timelines display the timing at which each experience was performed.



### 3. Intrathecal surgery

Intrathecal surgeries were performed in the third experimental group, three weeks after the first paclitaxel or DMSO injection (group 3; scheme 1) in animals weighing 290-300 g deeply anesthetized with a mixture of ketamine hydrochloride (0.06 g/kg) and medetomidine (0.25 g/kg) delivered via i.p. injections. After confirming total sedation, rats were trichotomized with a battery-operated shaver from the area of the ribs to the skull and placed in ventral recumbency on top of a styrofoam plate. A midline skin incision was made with a scalpel at the level of the T8 vertebra to allow exposure of the bone. Muscle and fatty tissue were detached using round tipped scissors. The T8 thoracic vertebra region was chosen because this vertebra is the most isolated of all vertebrae and therefore the easiest to locate and use as reference. The vertebra bone was cut with a fine-tipped rongeur to expose the *dura mater* which was then carefully perforated with an 18-gauge needle parallel to the spinal cord. At this point, a sterilized polyurethane catheter (VWR®, France) with a 2.5 cm length was inserted into the intrathecal space and moved without resistance towards the lumbar enlargement of the spinal cord using fine-tipped forceps (Figure 6-A). This length of the catheter allowed its caudal tip to stand proximally to the end of the L3 lumbar segment and beginning of the L4 lumbar segment. At the rostral edge of the catheter, a small portion was glued to the intact vertebrae with quick glue gel and the muscle around it was sutured. The remaining portion was passed subcutaneously to the region of the scapulae. The opened skin around the vertebrae was then sutured with surgical staples and the tip of the catheter was externalized in the region of the scapulae to prevent the animals from reaching it (Figure 6-B). The catheter was filled with 0.9% saline solution and sealed with quick glue gel to prevent cerebrospinal fluid leakage. The suture was disinfected with povidone-iodine (Betadine®) and the anesthesia was reverted with a subcutaneous injection (s.c.) of atipamezole hydrochloride (Revertor® - 0.5 g/kg). The animals were then individually housed and monitored daily for body weight and any signs of motor deficit.

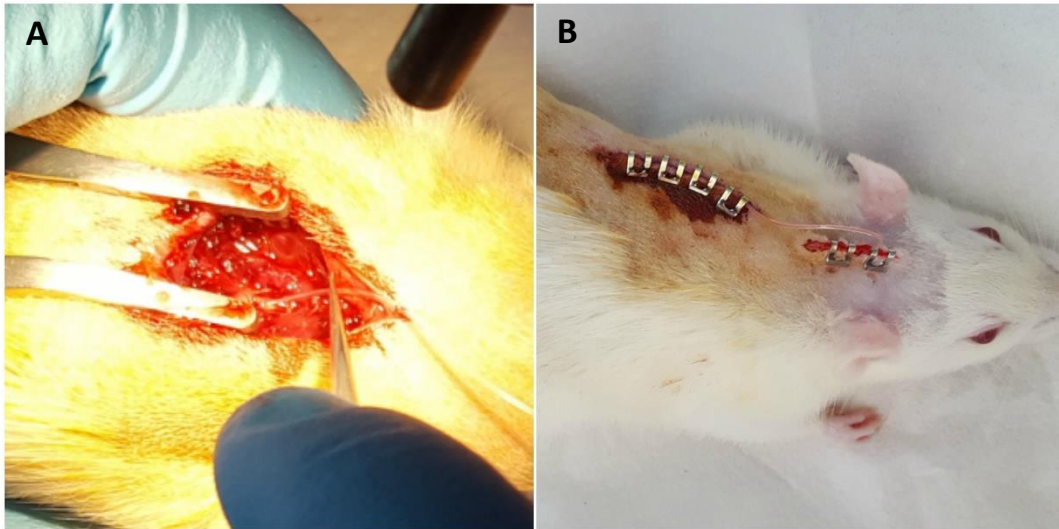


Figure 6. Catheter implantation into the intrathecal space of the lumbar enlargement of the spinal cord (between L3 and L4 lumbar segments). (A) The catheter was inserted at the level of the T8 thoracic vertebra and moved towards the lumbar spinal cord. (B) The animals were sutured and the catheter was externalized and sealed at its rostral tip.

## 4. Behavioral evaluation

### 4.1. Nociceptive behavior

Nociceptive behavior was assessed using the von Frey and cold plate tests which allow to evaluate mechanical and thermal sensitivity, respectively. The tests were performed after a period of habituation of one week, during which the animals were handled by the experimenter in the test room for 30 minutes and placed in the testing apparatus for another 20 minutes every day. The criteria for adequate habituation were that animals did not freeze or defecate when placed in the testing apparatus.

To perform the von Frey test, the animals were placed in elevated transparent Plexiglas cages with metallic mesh floor (Figure 7-A) and allowed to acclimate to the environment for 15-20 minutes before testing. The von Frey test was performed by the “up and down” method which consisted on the application of monofilaments, with forces ranging from 0.6 g to 60.0 g (Stoelting®, USA), starting with the monofilament 2 g. Each filament was consecutively applied to the mid-plantar region of the animal’s paws until it bent, for 2-3 seconds. In the absence of a paw withdrawal to a filament, the next higher force was delivered whereas in the presence of paw withdrawal, the next lower force was delivered. A brisk withdrawal and/or hind paw elevation was recognized as a positive response. Two trials were performed for both the left and right hind paws (group 1;

scheme 1) or for the left hind paw (group 3; scheme 1) and each value obtained was transformed in logarithm and averaged for each paw.

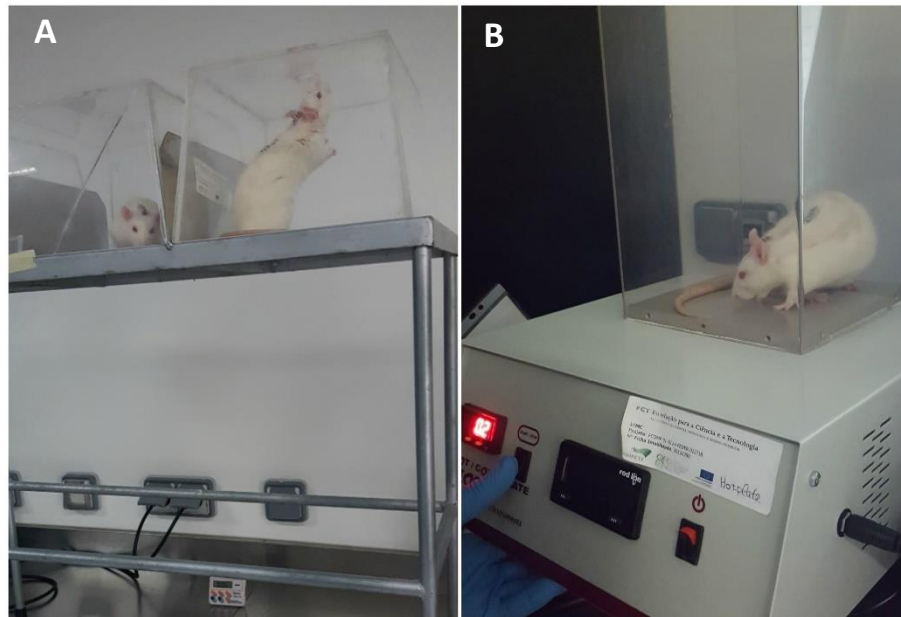
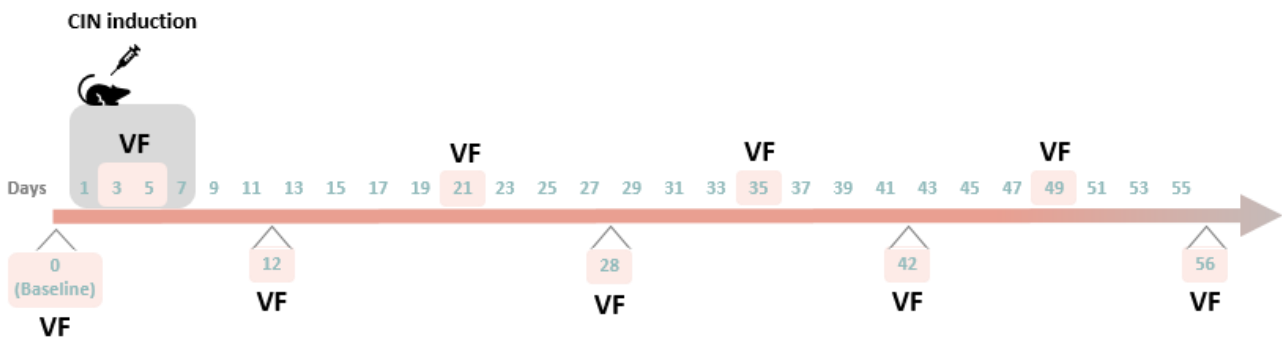


Figure 7. Nociceptive behavior testing apparatuses. (A) Mechanical sensitivity was tested in animals placed in elevated Plexiglas cages with metallic mesh floor for application of von Frey monofilaments to the mid-plantar region of the hind paws. (B) Thermal sensitivity was tested in animals placed on a cold plate maintained at 0°C.

The von Frey test was used to evaluate the time-course effects of paclitaxel over a period of two months (group 1: paclitaxel n = 6; DMSO and saline n = 5 each; scheme 1) at the following days: before paclitaxel injection (baseline testing) and at 3, 5, 12, 21, 28, 35, 42, 49 and 56 days after the first injection of paclitaxel (scheme 2).



Scheme 2. Diagram depicting the timing of the experimental procedures performed in group 1 on and von Frey test. CIN induction was performed by i.p. injections of paclitaxel (n = 6), DMSO (n = 5) or saline (n = 5) at days 1, 3, 5 and 7 (grey box). Von Frey testing was performed at days 0 (baseline), 3, 5, 12, 21, 28, 35, 42, 49 and 56 (VF, orange boxes).

The cold plate test was adapted from Jasmin et al. (1998) [86]. During the habituation sessions, the animals were placed on the surface of a plate (BIO-CHP Hot/Cold Plate Test, Bioseb®, USA/Canada) maintained at 35°C for 20 minutes. On testing days, animals were placed on the surface of the plate that was maintained at 0°C (Figure 7-B) with a cut-off period of 60 s to avoid tissue damage. The time animals spent on the cold surface before reacting to the stimulus was recorded and expressed as the paw withdrawal latency. A brisk lift or licking of the hind paw was considered a positive response.

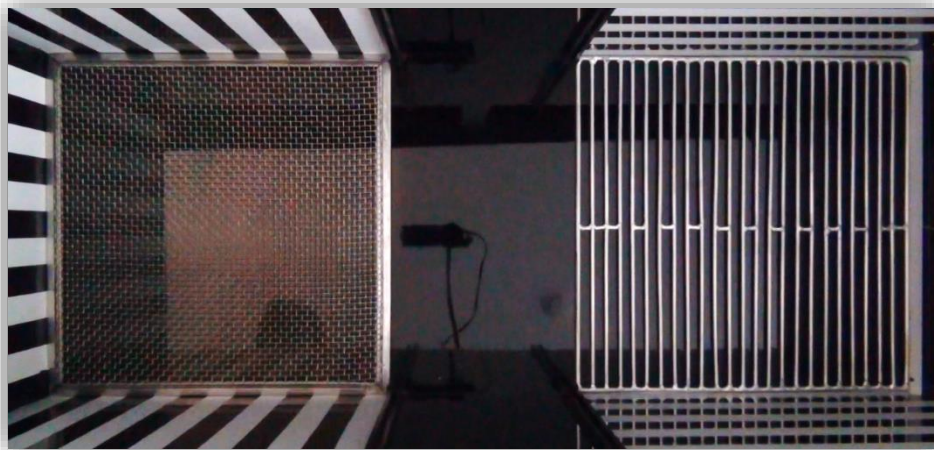
The von Frey and cold plate tests were used to study the effects of spinal  $\alpha_{2A}$ -AR activation by the agonist clonidine (group 3; scheme 1). One week after the intrathecal surgery, the animals were injected a volume of 10  $\mu$ l of either clonidine (Sigma-Aldrich®, USA) at 1  $\mu$ g (paclitaxel n = 7; DMSO n = 7), clonidine at 10  $\mu$ g (paclitaxel n = 6; DMSO n = 8) or 0.9% saline (paclitaxel n = 6; DMSO n = 7) through the intrathecal catheter using a 50  $\mu$ l syringe with a 28-gauge needle (Hamilton®, USA). To minimize reflux, the same volume of 0.9% saline was immediately injected following clonidine or saline injection. The tests were performed before (i.e. baseline) and 15 to 20 minutes after clonidine or saline administration. Baseline values of the von Frey test were acquired immediately before the injection of clonidine or saline. Baseline values of the cold plate test were acquired on the previous day to avoid skin sensitization due to repeated exposure to cold. The effects of clonidine were tested at 15 to 20 minutes, which is the timing of maximum effect of intrathecal clonidine [87]. After clonidine or saline injection, the animals were first tested for mechanical and then cold sensitivity given the noxious nature of the cold stimulus which could have biased the response to mechanical stimulation [88].

#### 4.2. Aversive behavior

The Conditioned Place Preference test is a standard behavioral test used to study the rewarding and aversive effects of drugs. This paradigm has been increasingly used to investigate the affective (aversive) aspects of pain [89] and it is now admitted that this operant paradigm allows the detection of spontaneous (i.e., non-evoked) pain that is otherwise difficult to assess in nonverbal animals. The test involves the association of a particular environment with a drug treatment through visual and tactile cues (**conditioning phase**). Following the conditioning phase there is a **post-conditioning phase**, during which the animals associate a different environment with the effect of the drug but in the absence of the drug. A common variation of this design consists of a **three-compartment chamber with two different conditioning**

**compartments/contexts**, distinguished by visual and sensory cues to which the animal is exposed once or several times, that are connected by a **neutral compartment**, with no special characteristics and that is not paired with a drug. Before the conditioning phase (i.e. during the **pre-conditioning phase**), the animal should not present a previous preference for any chamber/context.

In this study, we aimed to determine whether paclitaxel induced conditioned-place aversion (CPA) by pairing this drug to a compartment with specific environmental cues. These cues helped the animals associate the compartment where the drug was administered to the emotion it elicited when visiting that compartment [27, 28]. The second experimental group was used for CPA testing (paclitaxel  $n = 2$ ; DMSO  $n = 1$ ; scheme 1). The CPA testing apparatus consisted of a 100 x 40 x 40 cm Plexiglas chamber divided in three compartments: two 40 x 40 x 40 cm conditioning compartments that contained visual and tactile cues and one middle/neutral 20 x 40 x 40 cm compartment with no visual or tactile cues. One of the conditioning compartments had a floor constituted by 0.5 cm diameter metal rods spaced 2 cm and walls with alternating 3 cm wide black and white horizontal stripes. The second conditioning compartment had a mesh wire floor and walls with alternating 3 cm wide black and white vertical stripes. The central/neutral compartment had black Plexiglas walls and floor (Figure 8). Each

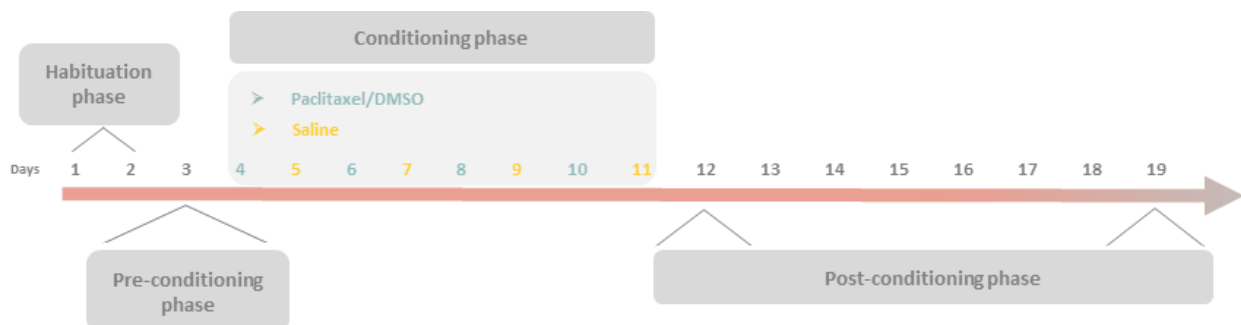


compartment was separated by removable doors.

Figure 8. CPA testing apparatus (top view). The chamber has two conditioning compartments with distinct visual and tactile cues and one neutral compartment with no cues. The cues help animals associate a compartment to the emotion elicited by a drug.

The CPA protocol was adapted from Li et al. (2009) [28] and Noda et al. (2014) [27], and was conducted as follows. Rats were placed in the neutral chamber, one at a time, with full access to all chambers for 15 minutes for 3 consecutive days. **Days 1** and

2 were used for habituation purposes and on **Day 3 (pre-conditioning phase;** Scheme 3), rat's behavior was video-recorded for 15 minutes and the time spent in each chamber was analyzed on EthoLog 2.2. Rats spending less than 20% or more than 80% of the entire time in one of the chambers were excluded. Each rat was then randomly assigned to a treatment group and a conditioning chamber/environment in a counterbalanced fashion. From **Days 4 to 11 (conditioning phase;** Scheme 3), the animals were allowed 4 conditioning sessions with paclitaxel (paclitaxel-treated animals  $n = 2$ ) or DMSO (control group;  $n = 1$ ) on the alternate days **4-6-8-10**, during which the animals received an i.p. injection of paclitaxel (2.0 mg/kg) or 4% DMSO and were immediately placed into their respective assigned conditioning compartment (doors closed) for 1 hour. On days **5-7-9-11**, the animals received an i.p. injection of 0.9% saline and were immediately placed into the second/opposite conditioning compartment (doors closed) for 1 hour. We performed **two post-conditioning sessions** (scheme 3), the first on **day 12** (the day after the last conditioning session), and the second on **day 19** (one week after the last conditioning session). During both post-conditioning sessions, the rats were placed in the neutral chamber in a drug-free state, with access to all chambers, their behavior was recorded for 15 minutes and the time spent in each chamber was analyzed on EthoLog 2.2. The difference between post- and pre-conditioning time spent in each chamber was calculated to determine the place preference/aversion score.



**Scheme 3.** Evaluation of the aversive effects of paclitaxel following a conditioning period of four days with the drug. Days 1 and 2 were used for habituation to the apparatus; day 3 was a pre-conditioning day in which the animals' behavior was filmed. Days 4, 6, 8 and 10 were used for paclitaxel or DMSO administration and days 5, 7, 9 and 11 were used for saline administration. Days 12 and 19 were used for evaluation of the place preference/aversion score.

## 5. Vascular perfusion and material processing for immunohistochemistry

All animals, except animals from the experimental group 6, were sacrificed by vascular perfusion (scheme 1). Animals from groups 1, 2 and 3 were perfused upon completion of behavioral assays. Animals from group 5, upon completing one month after CIN induction, were placed on the cold plate surface, which was set at 0°C, three times for 50 seconds each, at an interval of 5 minutes. Then, 2 hours after the first cold stimulation, the animals were perfused. The 2-hour interval was required to ensure maximal expression of the proto-oncogene c-fos in the spinal dorsal horn after noxious stimulation [90, 91]. The vascular perfusion was performed in animals deeply anesthetized with 65 mg/kg sodium pentobarbital (Eutasil®) via i.p. injection as follows. After confirming sedation by pinching the tail or a hind paw, the animals were placed in the supine position and their thorax was opened with scissors to allow access to the heart. To prevent blood coagulation, the heart was injected with 0,2 ml of heparin into the left ventricle. Then, a nick was inflicted on the left ventricle to allow the insertion of a catheter on the way to the ascending aorta for perfusion with 200 ml of calcium-free Tyrode's solution followed by 800 ml of fixative solution of 4% paraformaldehyde (PFA) in 0,1 M phosphate buffer (pH = 7.2).

The spinal cords of the animals from the experimental group 3 (implanted with a catheter in the intrathecal space) were carefully exposed for verification of the position of the catheter. No further processing of the spinal cord was carried out. Only animals whose catheter terminated at the spinal L4 segment were included in the analysis. The spinal cord of the animals from the experimental groups 1, 2, 4 and 5 were carefully exposed, dissected out and immersed in 4% PFA for 4 hours and then cryopreserved, at least for 24 hours, in 30% sucrose solution. The spinal L4 and L5 segments were then transversally sliced into 3 sets of 30 µm thick sections in a freezing microtome (Leica CM1325 microtome, Leica Biosystems® with a Huber Ministat 240 thermostat, Huber®) and preserved in a cryoprotectant solution at -20°C. The spinal lumbar sections from groups 1 and 4 were used for immunohistochemical analysis of DBH expression. The L4 and L5 sections from group 4 were further used for immunohistochemical analysis of  $\alpha_{2A}$ -AR expression and only the L4 sections for immunohistochemical analysis of pCREB. The L4 sections from group 5 were used for immunohistochemical analysis of c-Fos expression.

## 6. Immunohistochemical studies

### 6.1. Immunohistochemical detection and analysis of dopamine- $\beta$ -hydroxylase (DBH) expression

#### 6.1.1. Immunohistochemical detection

Immunodetection of DBH was performed using one set of spinal L4 and L5 sections from the experimental groups 1 (paclitaxel n = 6; DMSO n = 5; saline n = 5) and 4 (paclitaxel n = 6; DMSO n = 6; saline n = 6), as follows. All transverse sections were processed under identical experimental conditions. Free-floating sections were first washed with 0.1 M phosphate-buffered saline (PBS) to remove any traces of cryoprotectant (four times, 10 minutes each). Then, they were incubated for 15 minutes with a 30% hydrogen peroxide solution to block endogenous peroxidase activity, followed by a 10-minute permeabilizing step using 0.3% Triton X-100 diluted in PBS (PBS-T). Sections were then incubated for 2 hours with a blocking solution of glycine and 10% normal horse serum (NHS) diluted in PBS-T to prevent nonspecific binding of the antibodies, followed by incubation for one overnight with a mouse-raised anti-DBH primary antibody (Millipore®) diluted at 1:5000 in PBS-T and 2% NHS at 4°C. After further washing with PBS-T, the sections were incubated for 1 hour with a horse biotinylated anti-mouse secondary antibody (Dako, Agilent Technologies, Denmark) diluted at 1:200 in PBS-T and 2% NHS at room temperature. Sections were washed before incubation for 1 hour with the Avidin-Biotin Complex (ABC) solution (Vector Laboratories). The detection step took place upon incubation with 3,3'-diamino-benzidine (DAB, Sigma-Aldrich®, USA). The sections were mounted on gelatine-coated slides, cleared in xylol and coverslipped with mounting medium (Eukitt®, Fluka Analytical, Germany).

Photomicrographs were taken from the left and right sides of the spinal dorsal horn of each animal. A total of five non-contiguous random sections were acquired under the same exposure and lighting settings from a light microscope (Axioskop 40 model, Zeiss®, Switzerland) coupled to a high-resolution digital camera (Leica EC3 model) and the LAS 4.6.0. software (Leica Microsystems®).

The quantification of DBH labelling was performed on the ImageJ® software (U. S. National Institutes of Health, USA). Before proceeding to the actual quantitative analysis, we first optimized the methodology as explained in the next section.



### 6.1.2. Optimization of the methodology to analyze DBH expression

The optimization procedures described in this section were performed using photomicrographs of five L4 sections per animal from the experimental group 1 (scheme 1).

#### A. Selection of the method for image analysis

In the first step of optimization we aimed at establishing and validating in the lab a new method of quantification of immunolabelling in fibers, which is the thresholding method [83]. For that, we compared the results yielded by this new method with the results obtained by the densitometric analysis of pixels, which has been classically used in the lab for the quantification of the expression of proteins both at the cell bodies and fibers [92].

The densitometric analysis was performed on the superficial spinal dorsal laminae (I-II) and the total dorsal laminae (I-VI), which were delimited by using the freehand selection tool on ImageJ. The mean intensity of pixels inside each area was then measured as follows. Two regions of background staining were selected for measuring pixel intensity, one including an area of the dorsal horn without visible fibers (A) and the other from the glass of the slide (B). The DBH fiber density within laminae I-II and I-VI was determined by subtracting the mean intensity of pixels in background A to the mean intensity of pixels in the total area and by normalizing it with the corresponding value for background B.

The thresholding analysis was performed by selecting a small random area of background staining using the freehand selection tool on ImageJ and measuring its intensity statistics. Mean and standard deviation (SD) values of the background staining were obtained. Images were then converted to an 8-bit grayscale. The threshold level for DBH positive pixels was determined by setting a value of 5 SDs above the mean light background level, as follows: Threshold level (rounded to units) = mean background value – (5 x SD). The regions of interest (ROI) for this analysis, which comprised the superficial (laminae I-II) and the total (laminae I to VI) regions of the dorsal horn, were delimited manually for each image using the freehand selection tool and saved in the ROI Manager tool. The percentage of DBH positive pixels inside the ROIs was automatically calculated by the ImageJ software.

#### B. Delineation of the region of analysis

In the second step of optimization, we aimed at determining whether a fixed area, measuring 228 x 112  $\mu\text{m}$  and positioned along the spinal dorsal horn at the same location

in each section encompassing a portion of laminae I, II, III, IV and V (Figure 9), could be a representative sampling of the spinal dorsal horn labelling. For that, we compared the results obtained by this method of delineation with the density of DBH labelling in the total area of laminae I-VI manually delimited with the freehand tool. We performed this analysis using the thresholding method, which was selected from the first step of optimization, to measure the percentage of DBH positive pixels inside the ROIs, as explained above.

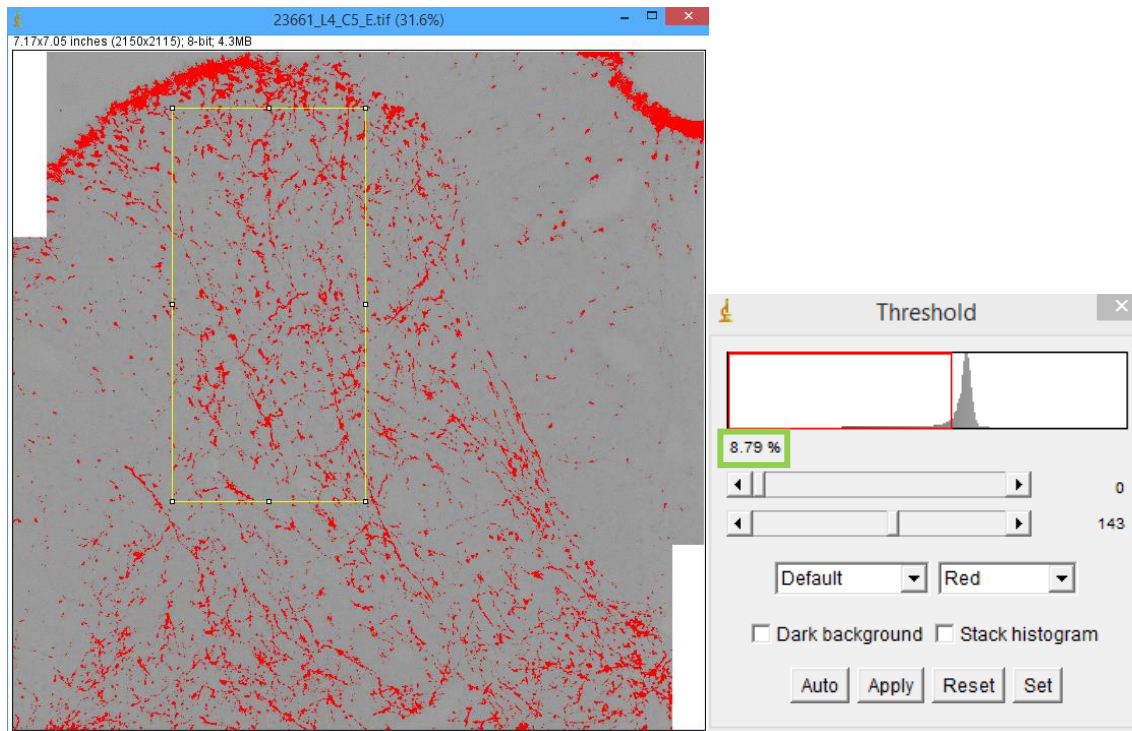


Figure 9. Thresholding analysis for determination of the percentage of DBH positive pixels inside a  $228 \times 112 \mu\text{m}$  rectangle using ImageJ software. The ROI (yellow rectangle) was positioned along the spinal dorsal horn encompassing a portion of laminae I, II, III, IV and V. The percentage of DBH positive pixels inside this ROI was automatically calculated by ImageJ software (green box).

### 6.1.3. Analysis of DBH expression

The thresholding method was selected for image analysis and the density of DBH labelling was quantified by using the  $228 \times 112 \mu\text{m}$  fixed rectangle as the ROI. The ROI was thoroughly positioned in the same region of the dorsal horn of each section to minimize variance. DBH labelling was analyzed in five random non-contiguous L4 and five random non-contiguous L5 sections per animal from the experimental groups 1 and 4 (scheme 1).

## 6.2. Immunohistochemical detection and analysis of pCREB expression

The analysis of pCREB expression was performed using one set of spinal L4 and L5 sections from the experimental group 4 (paclitaxel n = 6; DMSO n = 6; saline n = 6; scheme 1), immunoreacted as follows. All transverse sections were processed under identical experimental conditions. Free-floating sections were first washed with 0.1 M PBS to remove any traces of cryoprotectant (four times for 10 minutes). Then, they were incubated for 15 minutes with a 30% hydrogen peroxide solution to block endogenous peroxidase activity, followed by a 10-minute permeabilizing step using PBS-T. Sections were then incubated for 2 hours with a blocking solution of glycine and 10% normal goat serum (NGS) diluted in PBS-T to prevent nonspecific binding of the antibodies, followed by incubation for two overnights with a rabbit-raised anti-pCREB primary antibody (Millipore®) diluted at 1:5000 in PBS-T and 2% NGS at 4°C. After further washing with PBS-T, the sections were incubated for 1 hour with a swine biotinylated anti-rabbit secondary antibody (Dako, Agilent Technologies, Denmark) diluted at 1:200 in PBS-T and 2% NGS at room temperature. Sections were washed before incubation for 1 hour with the Avidin-Biotin Complex (ABC) solution (Vector Laboratories). The detection step took place upon incubation with 3,3'-diamino-benzidine (DAB, Sigma-Aldrich®, USA). The sections were mounted on gelatine-coated slides, cleared in xylol and coverslipped with mounting medium (Eukitt®, Fluka Analytical, Germany).

Photomicrographs were taken from the left and right sides of the spinal dorsal horn of each animal. A total of six random non-contiguous L4 and six random non-contiguous L5 sections were acquired under the same exposure and lighting settings from a light microscope (Axioskop 40 model, Zeiss®, Switzerland) coupled to a high-resolution digital camera (Leica EC3 model) and the LAS 4.6.0. software (Leica Microsystems®).

The quantification of pCREB-immunoreactive (IR) nuclei was performed on the ImageJ® software (U. S. National Institutes of Health, USA) using an adaptation of the thresholding analysis, as follows. Images were first converted to an 8-bit grayscale and the threshold level for pCREB-IR positive pixels was automatically determined by ImageJ. Images were then converted into binary images and labelling appeared as black particles. The particles were segmented using the Watershed tool to separate overlapping particles. The number of particles was then calculated by ImageJ on four different ROIs: the superficial laminae I-II, lamina III, IV and V of the spinal dorsal horn, carefully delimited by superimposing a digital diagram of the L4 segment taken from the atlas of the rat's brain by Paxinos & Watson [93] on each section of the spinal cord.

### 6.3. Immunohistochemical detection and analysis of c-Fos expression

The analysis of c-Fos expression was performed using one set of spinal L4 sections from the experimental group 5 (paclitaxel n = 3; DMSO n = 4; scheme 1). We only immunoreacted the L4 segment as this is the main spinal segment receiving noxious sensory inputs from the hind paws [94]. The sections were immunoreacted as follows. All transverse sections were processed under identical experimental conditions. Free-floating sections were first washed with 0.1 M PBS to remove any traces of cryoprotectant (four times for 10 minutes). Then, they were incubated for 20 minutes with a 30% hydrogen peroxide solution to block endogenous peroxidase activity, followed by a 10-minute permeabilizing step using PBS-T. Sections were then incubated for 2 hours with a blocking solution of glycine and 10% normal swine serum (NSS) diluted in PBS-T to prevent nonspecific binding of the antibodies, followed by incubation for two overnights with a rabbit-raised anti-c-Fos primary antibody (Oncogene®) diluted at 1:2500 in PBS-T and 2% NSS at 4°C. After further washing with PBS-T, the sections were incubated for 1 hour with a swine biotinylated anti-rabbit secondary antibody (Dako, Denmark) diluted at 1:200 in PBS-T and 2% NSS at room temperature. Sections were again washed before incubation for 1 hour with the Avidin-Biotin Complex (ABC) solution (Vector Laboratories). The detection step took place upon incubation with 3,3'-diamino-benzidine (DAB, Sigma-Aldrich®, USA). The sections were mounted on gelatine-coated slides, cleared in xylol and coverslipped with mounting medium (Eukitt®, Fluka Analytical, Germany).

Photomicrographs were taken from the left and right sides of the spinal dorsal horn of each animal. A total of seven random non-contiguous L4 sections were acquired under the same exposure and lighting settings from a light microscope (Axioskop 40 model, Zeiss®, Switzerland) coupled to a high-resolution digital camera (Leica EC3 model) and the LAS 4.6.0. software (Leica Microsystems®).

The quantification of c-Fos-IR nuclei was performed on the ImageJ® software (U. S. National Institutes of Health, USA). The Cell Counter tool was used to manually count the number of c-Fos-IR nuclei on lamina I-II, lamina III, lamina IV and lamina V of the spinal dorsal horn. The spinal laminae were carefully delimited by superimposing a digital diagram of the L4 segment taken from the atlas of the rat's brain by Paxinos & Watson [93] on each section of the spinal cord.

### 6.4. Immunohistochemical detection and analysis of $\alpha_{2A}$ -AR expression

The analysis of  $\alpha_{2A}$ -AR expression was performed using one set of spinal L4 and L5 sections from the experimental group 4 (paclitaxel n = 6; DMSO n = 6; saline n = 6;

scheme 1), immunoreacted as follows. All transverse sections were processed under identical experimental conditions. Free-floating sections were washed with 0.1 M PBS to remove any traces of cryoprotectant (four times for 10 minutes). Then, they were incubated for 30 minutes with a 1% sodium borohydride solution to reduce the tissue autofluorescence, followed by a 10-minute permeabilizing step using PBS-T. Sections were then incubated for 2 hours with blocking solution of glycine and 10% normal horse serum (NHS) diluted in PBS-T to prevent nonspecific binding of the antibodies, followed by incubation for two overnights with a rabbit-raised anti- $\alpha_{2A}$  primary antibody (Neuromics®) diluted at 1:500 in PBS-T and 2% NHS at 4°C. After further washing with PBS-T, the sections were incubated for 1 hour with a donkey anti-rabbit Alexa 488 (Molecular Probes®) diluted at 1:1000 in PBS-T. The sections were mounted on gelatine-coated slides, coverslipped with glycerol-phosphate buffer 0.4 M (3:1).

Photomicrographs were taken from the left and right sides of the spinal dorsal horn of each animal. A total of five random non-contiguous L4 and five random non-contiguous L5 sections were acquired under the same time exposure and laser light wavelength (488 nm) on an ApoTome Slider (Zeiss®) fluorescence microscope coupled to the AxioVision Rel. 4.8. software (Zeiss®).

The quantification of  $\alpha_{2A}$ -AR was performed on the ImageJ® software (U. S. National Institutes of Health, USA) using a thresholding analysis as explained above, but with small alterations as the method was now applied to fluorescence staining. Mean and SD values of background staining were obtained. Images already in the 16-bit grayscale format were thresholded. The threshold level for  $\alpha_{2A}$ -AR positive pixels was determined by setting a value of 5 SDs above the mean dark background level on the threshold tool, as follows: Threshold level (rounded to units) = mean background value + (5 x SD). The  $\alpha_{2A}$ -AR labelling appeared as white in a dark background, which explains why we added the value of 5 standard deviations to the mean background staining instead of subtracting it as in DBH expression analysis. The ROI was the superficial laminae I-II which was manually drawn for each image using the freehand selection tool. The percentage of  $\alpha_{2A}$ -AR positive pixels inside the ROI was automatically calculated by the ImageJ software.

## 7. Western blotting analysis of $\alpha_{2A}$ -AR expression

Western blotting analysis of  $\alpha_{2A}$ -AR expression was performed using lumbar spinal cord sections of experimental group 6 (paclitaxel n = 5; DMSO n = 5; scheme 1), harvested at one month after CIN induction, as follows. Animals were deeply

anesthetized with an overdose of 65 mg/kg sodium pentobarbital via i.p. injection and sacrificed by decapitation. A portion of the lumbar spinal cord containing the L4 and L5 segments was harvested and the left and right spinal cord were separated. Each hemisection was further dissected to separate the dorsal and ventral horn and the biological material was immediately stored at -80°C.

The expression of  $\alpha_{2A}$ -AR was studied in the dorsal portion of the L4 and L5 segments. For that, the tissues were homogenized in lysis buffer (TBS-T: 20 mM Tris HCl pH 7.4; 150 mM NaCl; 0.1% Triton X-100) containing phosphatase inhibitor cocktail 2 (sodium orthovanadate, sodium molybdate, sodium tartrate and imidazole) and 3 (cantharidin, (-)-*p*-bromolevamisole oxalate and calyculin A; Sigma-Aldrich®, USA) and protease inhibitor ([4-(2-aminoethyl) benzenesulfonyl fluoride hydrochloride], aprotinin, bestatin hydrochloride, -[N-(trans-epoxysuccinyl)-L-leucine 4-guanidinobutylamide], leupeptin, hemisulfate salt and pepstatin A; Sigma-Aldrich®, USA) using a MagNA Lyser® (Roche, Switzerland). The total protein concentration was quantified by the Bradford method using Bovine Serum Albumin (BSA) protein as a standard. A total of 20  $\mu$ g of protein was denatured at 60°C for 10 minutes and centrifuged at 14800 rpm for 2 minutes in the 1x GLB (1.875 M Tris pH8.8; 15% glycerol; 6% SDS; 0.1% - 0.05% Bromophenol Blue) containing 100 mM Dithiothreitol (DTT). Samples were loaded and electrophoresed on 12% SDS-PAGE at 200 V and 32 mA. Pre-stained molecular weight marker (NZY Colour Protein Marker II®, NZYTech, Portugal) was simultaneously loaded to monitor electrophoresis and identify molecular weights. The proteins were then electroblotted onto nitrocellulose membranes by Trans-Blot® Turbo™ (BioRad, USA). After several washes with TBS-T, the membrane was blocked with 5% of Blotting-Grade Blocker (Bio-Rad, USA) in TBS-T for 1 hour at room temperature and then incubated with the primary antibodies, rabbit anti- $\alpha_{2A}$ ARs (1:1000, Neuromics, USA) in TBS-T containing 5% of Blotting-Grade Blocker (Bio-Rad, USA) for 24 hours at 4°C. Membranes were then washed and incubated in anti-rabbit secondary antibodies conjugated to horseradish peroxidase (HRP, 1:10000, Jackson ImmunoResearch Europe, UK) in TBS-T with 5% of Blotting-Grade Blocker for 1 hour. After 2 washes in TBS-T, the membranes were incubated with Clarity Western ECL Substrate (Bio-Rad, USA), a chemiluminescence reagent, for 5 minutes and immunoreactive bands were detected by Chemidoc system (Bio-Rad, USA). Semi-quantification of bands was performed using Image Lab software (Bio-Rad, USA) and expressed in arbitrary units.

Glyceraldehyde 3-phosphate dehydrogenase (GAPDH) was used as loading protein internal control, with the membranes being incubated with mouse anti-GAPDH (1:10000, Abcam, UK) followed by incubation in anti-mouse secondary antibody

conjugated to HRP (1:10000, Jackson ImmunoResearch Europe, UK). Detection and quantification of GAPDH immunoreactive bands were performed as described above. The results of the quantification of  $\alpha_{2A}$ -AR expression were presented as normalized for GAPDH.

## 8. Statistical analysis

The behavioral data obtained in the von Frey and cold plate tests were analyzed by two-way repeated measures ANOVA followed by Tukey's post-hoc test for multiple comparisons when applied. The behavioral data collected in the CPA test was not statistically analyzed because only three (two paclitaxel-treated and one control/DMSO-treated) animals were used and this was a preliminary study. Data obtained in the histochemical analysis of pCREB and c-Fos was analyzed by two-way ANOVA followed by Tukey's test for multiple comparisons when applied. Data obtained in the histochemical analysis of DBH and  $\alpha_{2A}$ -AR expression was analyzed by one-way ANOVA followed by Tukey's test for multiple comparisons when appropriate. Data obtained in the western blot analysis of  $\alpha_{2A}$ -AR expression was compared by unpaired student t-test. Statistical analysis was performed by GraphPad Prism version 6.00 (GraphPad Software, USA). Significance level was set at 0.05.

# Results

---

## 1. Behavioral characterization of paclitaxel-induced neuropathy

### 1.1. Nociceptive behavior

The effects of paclitaxel on pain behavior were assessed by the von Frey test prior to and at 3, 5, 12, 21, 28, 35, 42, 49 and 56 days following the first paclitaxel injection (scheme 2). Paw withdrawal thresholds from each animal at each time tested were determined both from the left and right hind paws. No significant differences were found between the left and right paw withdrawals ( $F_{1,10} = 0.328$ ;  $p = 0.579$ ). Paw withdrawal thresholds from each animal of this experimental group were then determined as the average of the left and right hind paws (Figure 10).

Overall, the analysis of the data revealed a significant effect of the treatment ( $F_{2,13} = 63.36$ ,  $p < 0.0001$ ), time ( $F_{9,117} = 3.747$ ,  $p = 0.0004$ ) and interaction (treatment x time):  $F_{18,117} = 4.869$ ,  $p < 0.0001$ . Paclitaxel-treated animals differed significantly from both DMSO- ( $p < 0.0001$ ) and saline-treated ( $p < 0.0001$ ) animals. DMSO- and saline-treated animals were not significantly different ( $p > 0.9999$ ). The time course analysis revealed that at baseline (i.e. before the first injection of paclitaxel), no significant differences were observed between the groups. Paclitaxel-treated animals showed significant lower paw withdrawal thresholds compared to baseline at days 5, 12, 21, 42, 49 and 56 and also compared both to DMSO- and saline-treated animals from D5 to D56 (Figure 10).



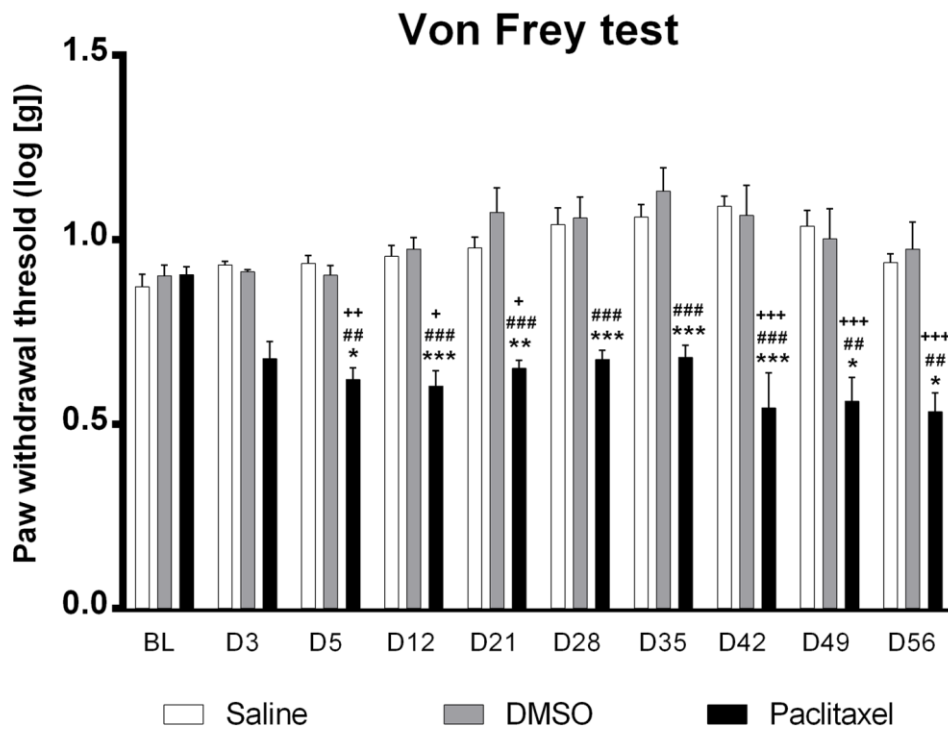


Figure 10. Time course effects of systemic paclitaxel administration on mechanical sensitivity assessed by the von Frey test. The test was performed before i.e. at baseline (BL) and several days (D) after the first injection of paclitaxel. Data are presented as mean  $\pm$  SEM (paclitaxel n = 6; DMSO and saline n = 5 each group). +p < 0.05; ++p < 0.01; +++p < 0.001 vs baseline; #p < 0.05; ##p < 0.01; ###p < 0.001 vs saline; \*p < 0.05; \*\*p < 0.01; \*\*\*p < 0.001 vs DMSO.

## 1.2. Aversive behavior

The aversive behavior was studied using the CPA test. The animals were conditioned with either paclitaxel and saline (n = 2) or DMSO and saline (n = 1). Two post-conditioning sessions were conducted, the first which took place the day after the last conditioning session (post-conditioning 1) and the second which took place a week after the last conditioning session (post-conditioning 2). Paclitaxel-treated animals spent less time in the compartment paired with paclitaxel compared to pre-conditioning either at the first (difference score:  $-211,34 \pm 75,185$  s; Figure 11-A) and second (difference score:  $-284,015 \pm 97,15$  s; Figure 11-A) post-conditioning sessions. The animals spent almost the same amount of time in the compartment paired with saline compared to pre-conditioning either at the first ( $15,945 \pm 197,365$  s; Figure 11-A) and second (difference score:  $60,875 \pm 211,645$  s; Figure 11-A) post-conditioning sessions. The control animal (DMSO-treated) also spent less time in the DMSO-paired compartment at the first (difference score:  $-236,23$  s; Figure 11-B) and second (difference score:  $-171,64$  s) post-conditioning sessions. The DMSO-conditioned rat spent more time in the saline-paired compartment at the first (difference score:  $203,915$  s; Figure 11-B) and second (difference score:  $231,145$  s; Figure 11-B) post-conditioning sessions.

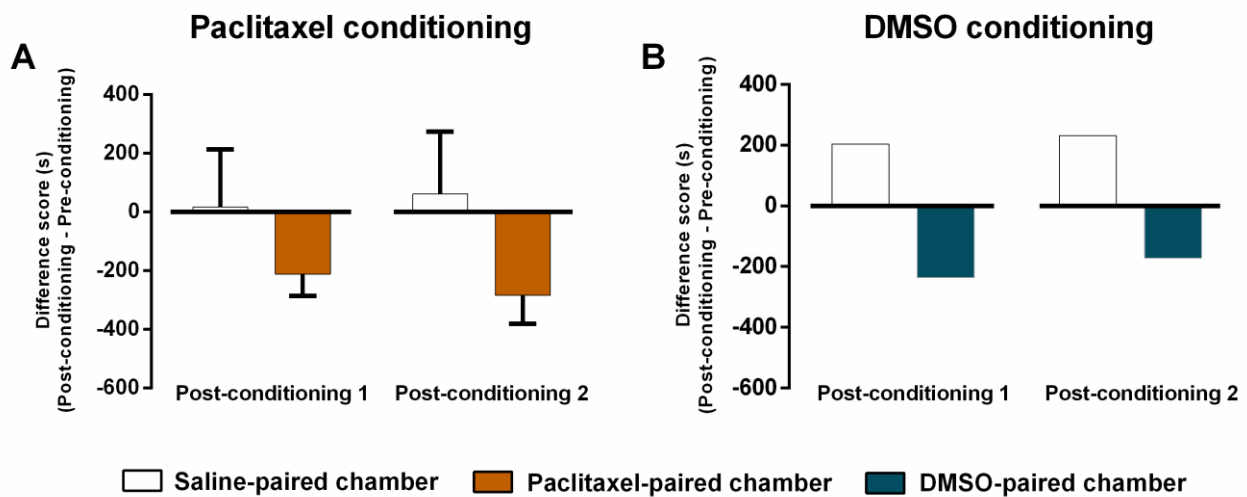


Figure 11. Conditioned place aversion evaluated by the CPA test. The animals were conditioned in two different compartments with paclitaxel and saline (A), respectively, or DMSO and saline (B), respectively. The time spent in each compartment was evaluated before (pre-conditioning) and after (post-conditioning) the conditioning sessions and the difference between the two sessions was determined. Two post-conditioning sessions were conducted: one following the last conditioning session (post-conditioning 1), and the second, a week after the last conditioning session (post-conditioning 2). Data are presented as mean of the difference  $\pm$  SEM (paclitaxel/saline  $n = 2$ ; DMSO/saline  $n = 1$ ).

## 2. Effects of paclitaxel on spinal neuronal activation

### 2.1. Expression of pCREB

The expression of pCREB was studied at the spinal lumbar L4 dorsal horn of saline- ( $n = 6$ , Figure 12-A), DMSO- ( $n = 6$ ; Figure 12-B) and paclitaxel-treated ( $n = 6$ ; Figure 12-C) animals at one month after CIN induction without any further manipulation before vascular perfusion. The overall analysis revealed a main effect of treatment ( $F_{2, 60} = 11.57$ ,  $p < 0.0001$ ) and a main effect of dorsal horn laminae ( $F_{3, 60} = 78.70$ ,  $p < 0.0001$ ), but no interaction (treatment  $\times$  dorsal horn laminae:  $F_{6, 60} = 0.05809$ ,  $p = 0.9992$ ). Overall, regardless of the dorsal horn laminae, saline-treated animals presented a higher number of pCREB-IR nuclei compared to DMSO- ( $p = 0.0002$ ; Figure 12-D) and paclitaxel-treated ( $p = 0.0005$ ; Figure 12-D) animals. No differences were found between DMSO- and paclitaxel-treated animals ( $p = 0.9499$ ; Figure 12-D). Regardless of the treatment, the total number of pCREB-IR nuclei was significantly higher in laminae I-II compared to lamina III, lamina IV and lamina V ( $p < 0.0001$  for each comparison; Figure 12-D).

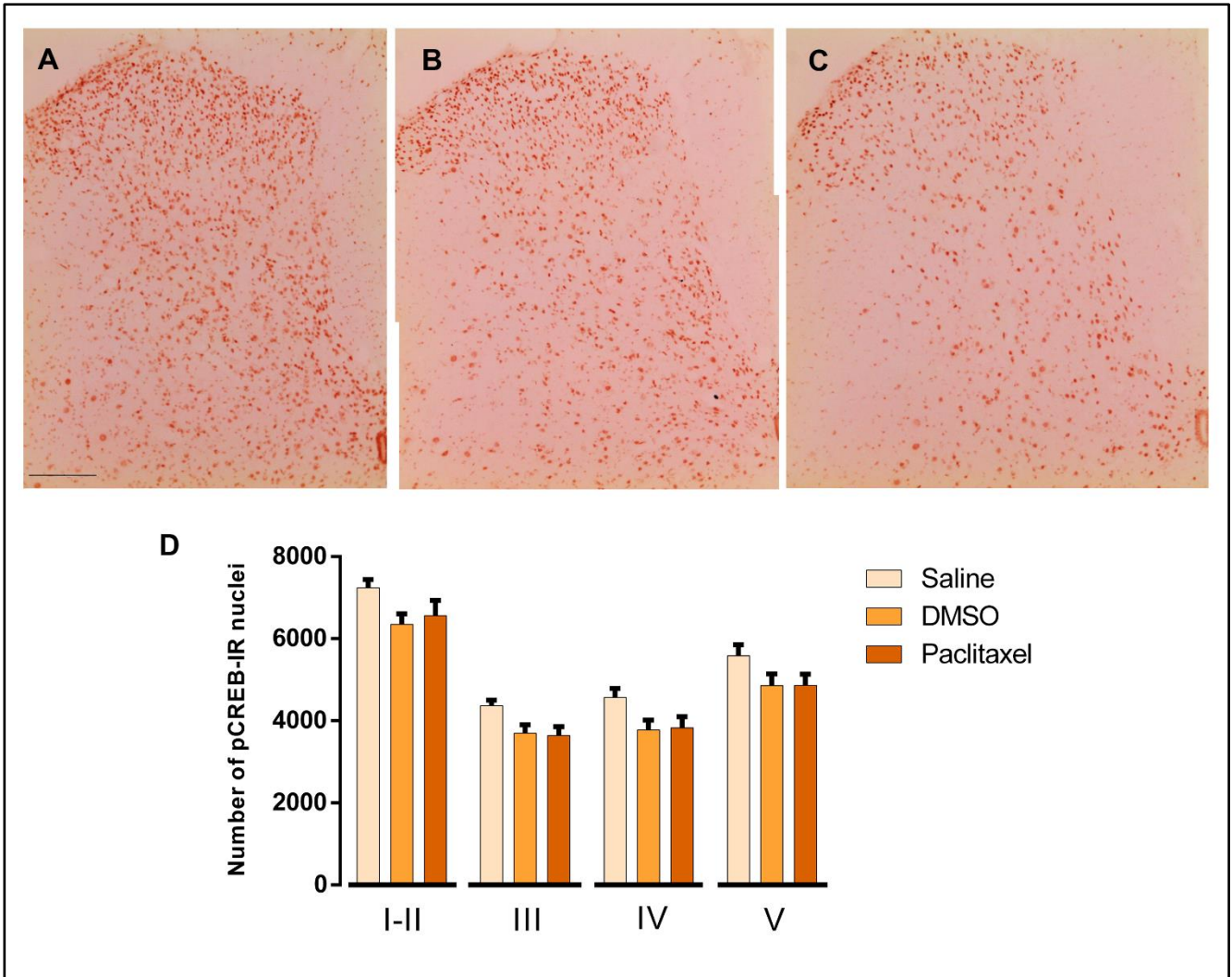


Figure 12. Expression of pCREB in the spinal dorsal horn at one month after CIN induction. Representative photomicrographs show pCREB immunoreactivity in the spinal dorsal horn of saline- (A), DMSO- (B) and paclitaxel-treated (C) animals. Scale bar in A: 200  $\mu$ m. All images were acquired under the same magnification. The number of pCREB-IR nuclei was evaluated in dorsal horn laminae I-II, III, IV and V (D). Data are presented as mean  $\pm$  SEM (paclitaxel, DMSO and saline n = 6 each group).

## 2.2. Cold-induced c-Fos expression

The expression of c-Fos was studied at the spinal lumbar L4 dorsal horn of DMSO- (n = 4; Figure 13-A) and paclitaxel-treated (n = 3; Figure 13-B) animals, at one month after CIN induction. Two hours before vascular perfusion the animals were submitted to noxious-cold stimulation.

Overall, cold stimulation induced a higher number of c-Fos-IR nuclei in paclitaxel-treated animals ( $F_{1,20} = 9.158$ ,  $p = 0.0067$ ). The overall analysis also revealed a main effect of dorsal horn laminae ( $F_{3,20} = 4.955$ ,  $p = 0.0099$ ), but no interaction (treatment x dorsal horn laminae:  $F_{3,20} = 0.8410$ ,  $p = 0.4874$ ). Regardless of the treatment, the

number of c-Fos-IR nuclei was significantly higher in lamina III compared to laminae I-II ( $p = 0.0373$ ; Figure 13-C) and to lamina IV ( $p = 0.0160$ ; Figure 13-C).

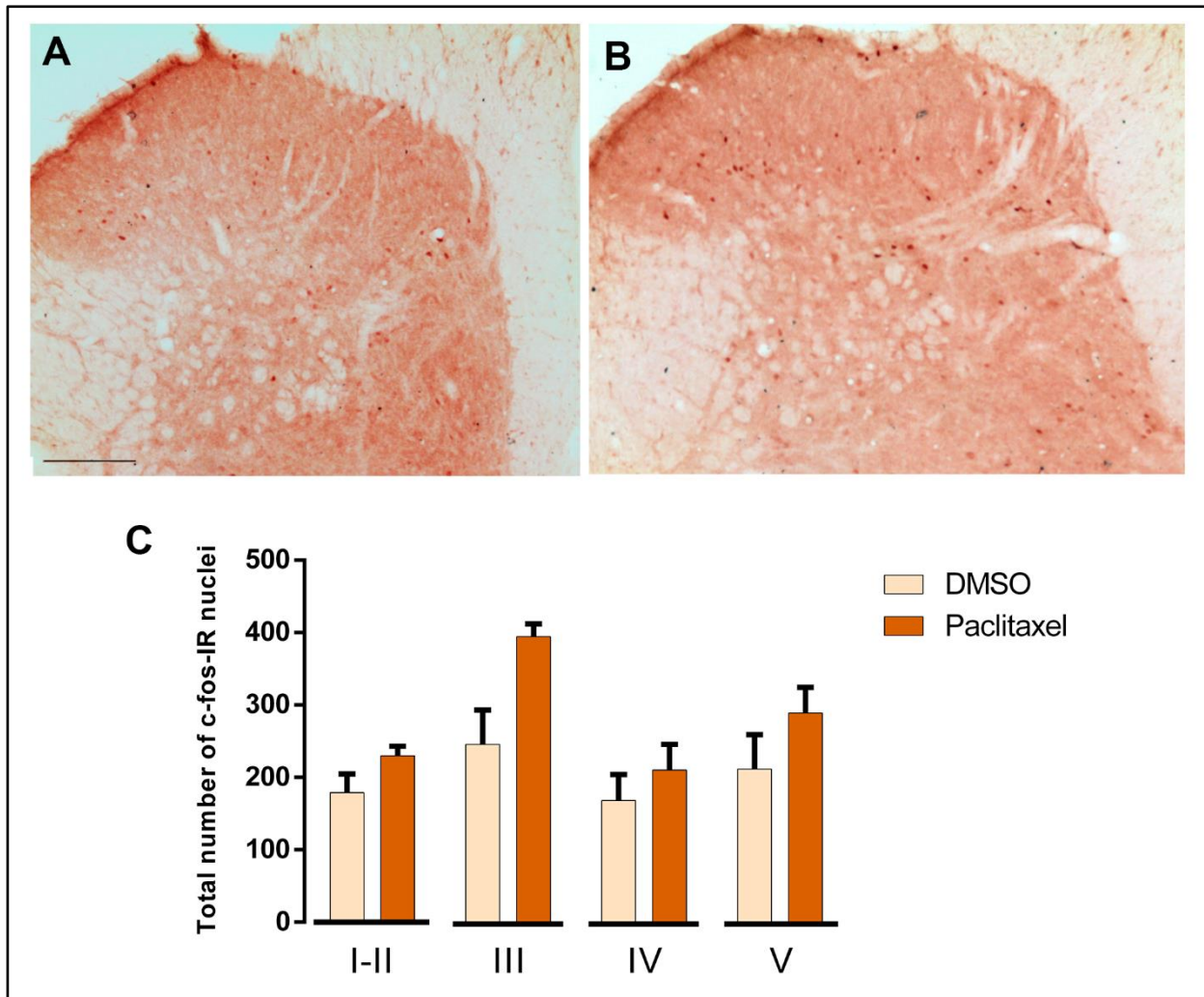


Figure 13. Expression of c-Fos after noxious-cold stimulation in the spinal dorsal horn at one month after CIN induction. Representative photomicrographs of c-Fos immunoreactivity in the spinal dorsal horn of DMSO- (A) and paclitaxel-treated (B) animals. Scale bar in A: 200  $\mu$ m. Both images were acquired under the same magnification. The total number of c-Fos-IR nuclei was evaluated in dorsal horn laminae I-II, III, IV and V (C). Data are presented as mean  $\pm$  SEM (paclitaxel  $n = 3$ ; DMSO  $n = 4$ ).

### **3. Study of descending noradrenergic modulation in the paclitaxel-induced model of neuropathy**

#### **3.1. Analysis of DBH expression**

##### **3.1.1. Optimization of the methodology to analyze DBH expression**

The optimization of the methodology to quantify DBH labelling was conducted on spinal lumbar L4 sections of the two-months experimental group (group 1, scheme 1) treated with paclitaxel (n = 6), DMSO (n = 5) and saline (n = 5).

##### **A. Selection of the method of image analysis**

Densitometric (Figure 14-A, B) and thresholding (Figure 14-C, D) methods of image analysis were compared using the same spinal cord sections and areas (dorsal horn superficial laminae I-II – Figure 14-A, C – and laminae I-VI – Figure 14-B, D). We found the same trend of quantification by both methods of analysis, that is, no differences in DBH labelling between the groups in the superficial dorsal horn laminae (densitometric analysis:  $F_{2, 11} = 2.486$ ,  $p = 0.1286$ ; thresholding analysis:  $F_{2, 11} = 2.120$ ,  $p = 0.1664$ ; Figure 14-A, C) and in the entire dorsal horn area (densitometric analysis:  $F_{2, 11} = 1.052$ ,  $p = 0.3819$ ; thresholding analysis:  $F_{2, 11} = 0.8655$ ,  $p = 0.4476$ ; Figure 14-B, D). The thresholding method yielded the same results as the classic densitometric analysis, which then validated the thresholding method as a reliable tool of analysis for use in the subsequent analysis.

##### **B. Delineation of the region of analysis**

The thresholding method was used for optimization of the delineation of the region/area for DBH labelling analysis in the spinal dorsal horn. We compared the total dorsal horn area (laminae I-VI) delimited manually to a fixed rectangular area (228 x 112  $\mu\text{m}$ ) placed in the center of the dorsal horn as to include laminae I to V. We found the same trend of quantification when analyzing both areas, that is, no differences in DBH labelling between the groups in the manually delimited dorsal horn ( $F_{2, 11} = 0.8655$ ,  $p = 0.4476$ ; Figure 15-A) and when analyzing the fixed area ( $F_{2, 11} = 0.3048$ ,  $p = 0.7433$ ; Figure 15-B).

Since the fixed rectangular area encompassing most of the dorsal horn yielded the same results as the manually delimited area, we selected the fixed area for subsequent analysis.



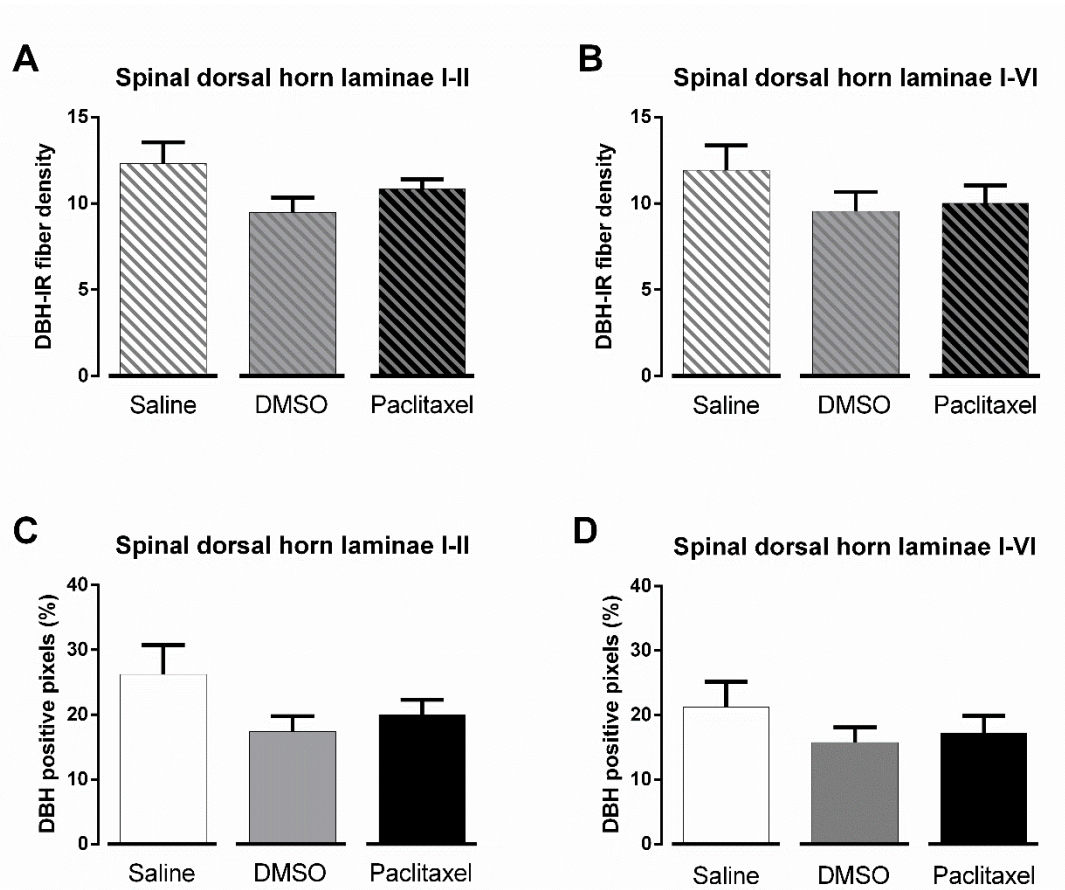


Figure 14. Optimization of the methodology to quantify DBH expression. DBH expression was quantified by a densitometric (A, B) and thresholding (C, D) methods in the superficial laminae I-II (A, C) and in laminae I-VI (B, D) of the spinal dorsal horn. Data are presented as mean  $\pm$  SEM (paclitaxel n = 6; saline and DMSO n = 5 each group).

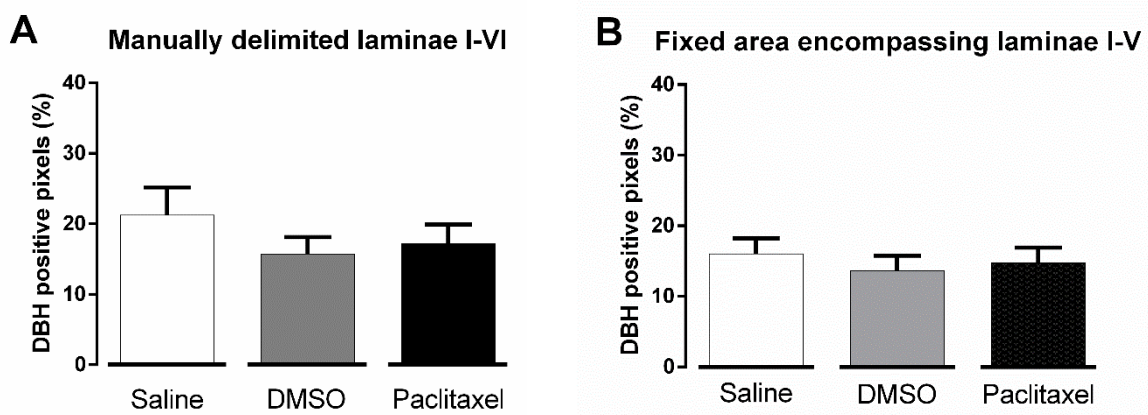


Figure 15. Optimization of the area for analysis of DBH expression. DBH expression was quantified in a manually delimited area (A) and in a fixed area (B) of the spinal dorsal horn. Data are presented as mean  $\pm$  SEM (paclitaxel n = 6; saline and DMSO n = 5 each group).

### 3.1.2. Effects of paclitaxel on DBH expression

The effects of paclitaxel treatment on the expression of DBH in the spinal cord were studied in spinal L4 and L5 sections of the one-month experimental group (group 4: paclitaxel n = 6; DMSO n = 6; saline n = 6; scheme 1) and the two-months experimental group (group 1: paclitaxel n = 6; DMSO n = 5; saline n = 5; scheme 1).

At one month after CIN induction (Figure 16), the overall data analysis showed that there were differences between the three groups analyzed at the spinal L4 segment ( $F_{2, 15} = 3.662$ ,  $p = 0.0500$ ; Figure 16-A-C, G) but not at the L5 segment ( $F_{2, 15} = 3.245$ ,  $p = 0.0674$ ; Figure 16-D-F, H). In L4 sections, paclitaxel-treated animals showed a higher percentage of DBH positive pixels when compared to DMSO-treated ( $p = 0.0495$ ) animals (Figure 16-G). No significant differences were observed between L4 sections of DMSO- and saline-treated animals.

At two months after CIN induction (Figure 17), the data analysis revealed no significant differences between the three groups of animals both at the spinal L4 ( $F_{2, 11} = 0.3048$ ,  $p = 0.7433$ ; Figure 17-A-C, G) and L5 ( $F_{2, 12} = 2.376$ ,  $p = 0.1351$ ; Figure 17-D-F, H) segments.

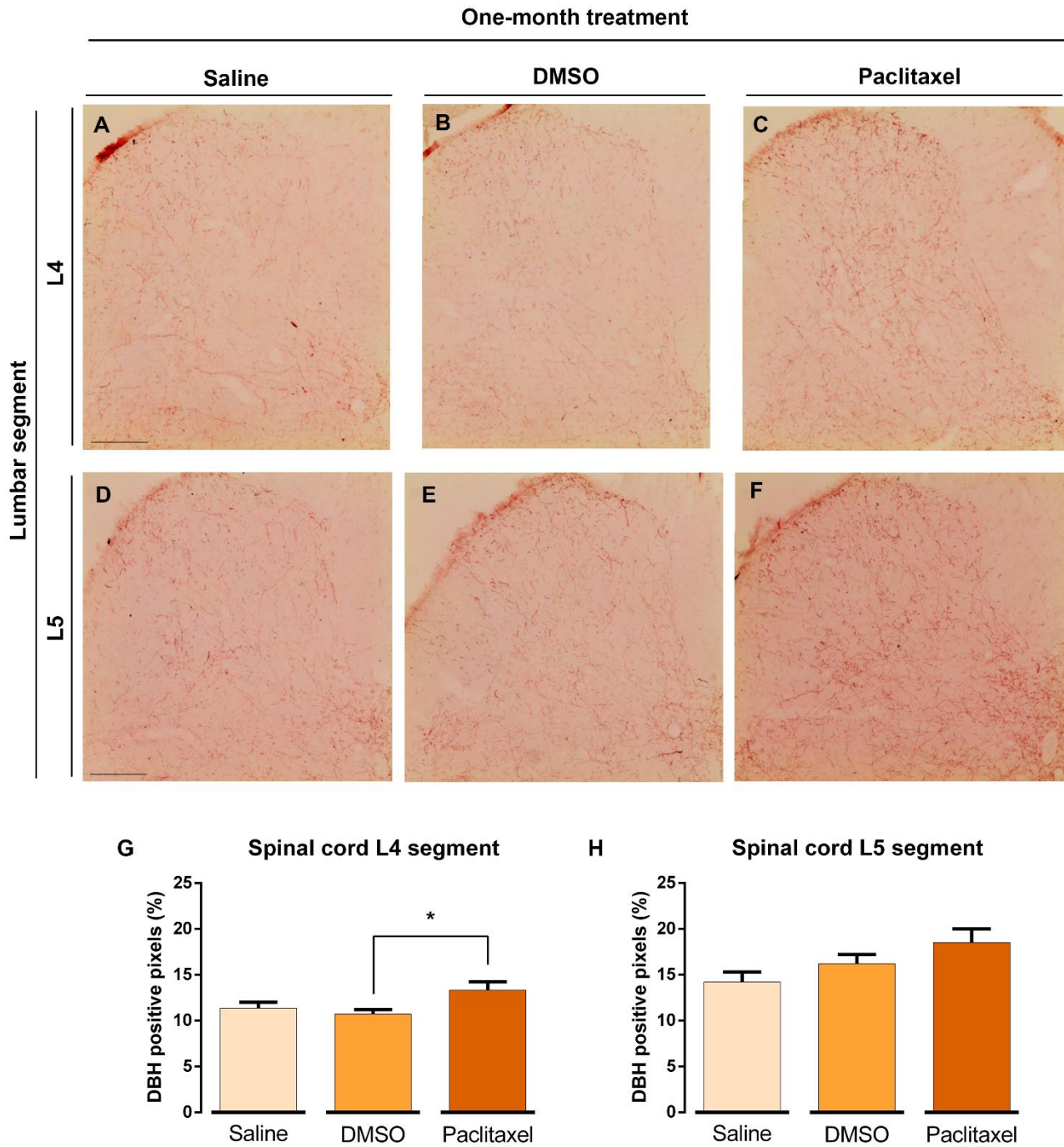


Figure 16. Expression of DBH in the spinal dorsal horn at one month after CIN induction. Representative photomicrographs of DBH immunoreactivity in the spinal L4 (A, B, C) and L5 (D, E, F) segments of saline- (A, D), DMSO- (B, E) and paclitaxel-treated (C, F) animals. Scale bar in A and D: 200  $\mu$ m. All images were acquired under the same magnification. The percentage of DBH positive pixels was determined from a fixed area at the lumbar dorsal horns (G, H). Data are presented as mean  $\pm$  SEM (paclitaxel, DMSO and saline n = 6 for each group). \*p < 0.05 vs DMSO.



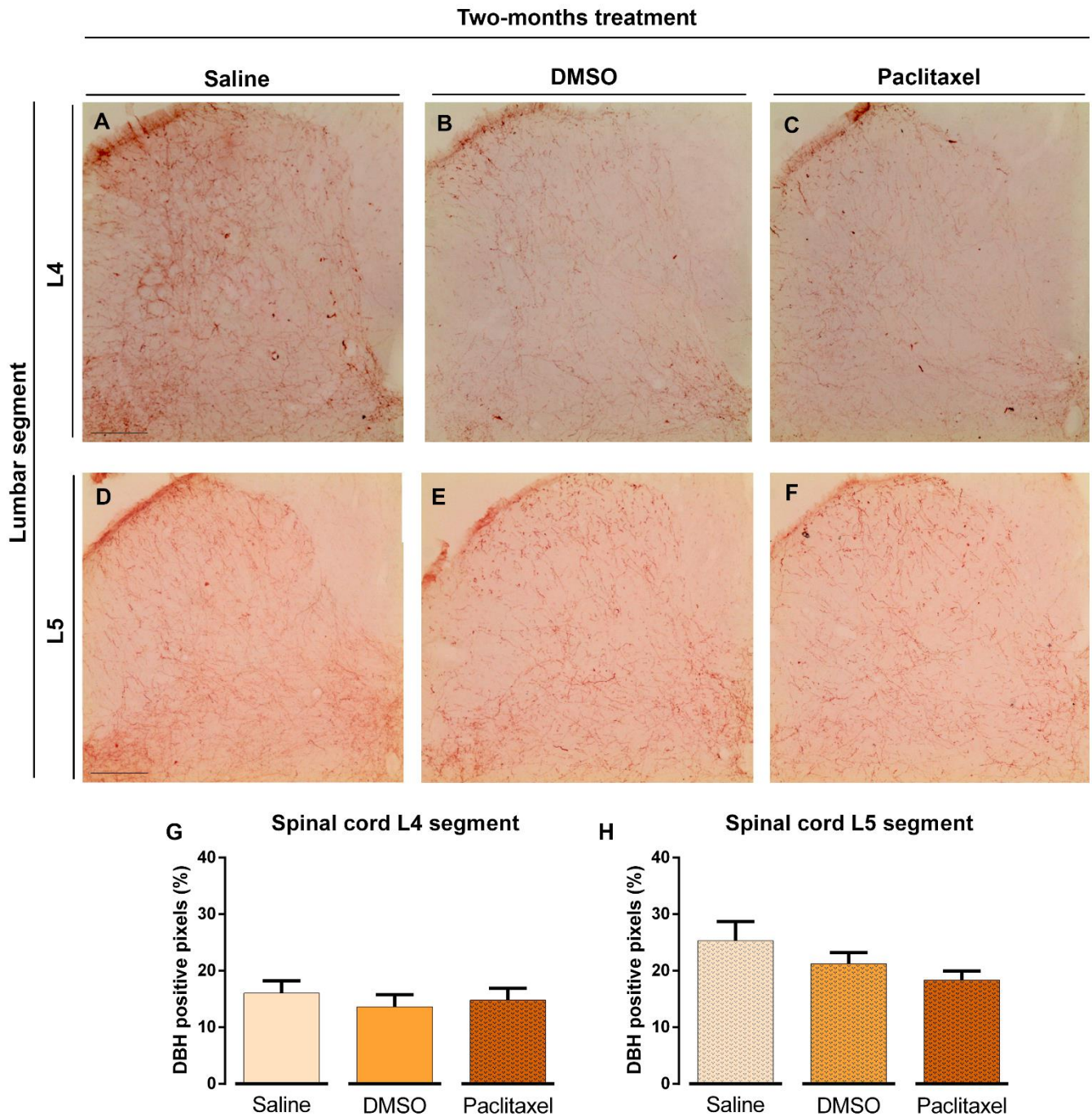


Figure 17. Expression of DBH in the spinal dorsal horn at two months after CIN induction. Representative photomicrographs of DBH immunoreactivity in the spinal L4 (A, B, C) and L5 (D, E, F) segments of saline- (A, D), DMSO- (B, E) and paclitaxel-treated (C, F) animals. Scale bar in A and D: 200  $\mu$ m. All images were acquired under the same magnification. The percentage of DBH positive pixels was determined from a fixed area at the lumbar dorsal horns (G, H). Data are presented as mean  $\pm$  SEM (paclitaxel n = 6; saline and DMSO n = 5 each group).

### 3.2. Analysis of spinal $\alpha_{2A}$ -AR expression

The expression of  $\alpha_{2A}$ -AR at the spinal dorsal horn were analyzed in spinal L4 and L5 sections by immunofluorescence (paclitaxel n = 6; DMSO n = 6; saline n = 6; Figure 18) and western blotting (paclitaxel n = 5; DMSO n = 5; Figure 19) at one month after CIN induction. The immunofluorescence analysis revealed a significant difference between the three groups in the L5 segment ( $F_{2, 13} = 5.727$ ,  $p = 0.0165$ ; Figure 18-D-F, H) but no differences in the L4 segment ( $F_{2, 13} = 1.656$ ,  $p = 0.2287$ ; Figure 18-A-C, G). In the L5 segment, the percentage of  $\alpha_{2A}$ -AR positive pixels was significantly less abundant in paclitaxel- compared to saline-treated animals ( $p = 0.0130$ , Figure 18-D, H). No significant differences were observed between DMSO- and paclitaxel-treated animals ( $p = 0.3351$ ) and between DMSO- and saline-treated animals ( $p = 0.1408$ ; Figure 18-D-F, H).

The western blotting analysis showed that the expression of  $\alpha_{2A}$ -AR remained unaltered between paclitaxel- and DMSO-treated animals ( $F_{4, 4} = 1.214$ ,  $p = 0.8553$ ; Figure 19).

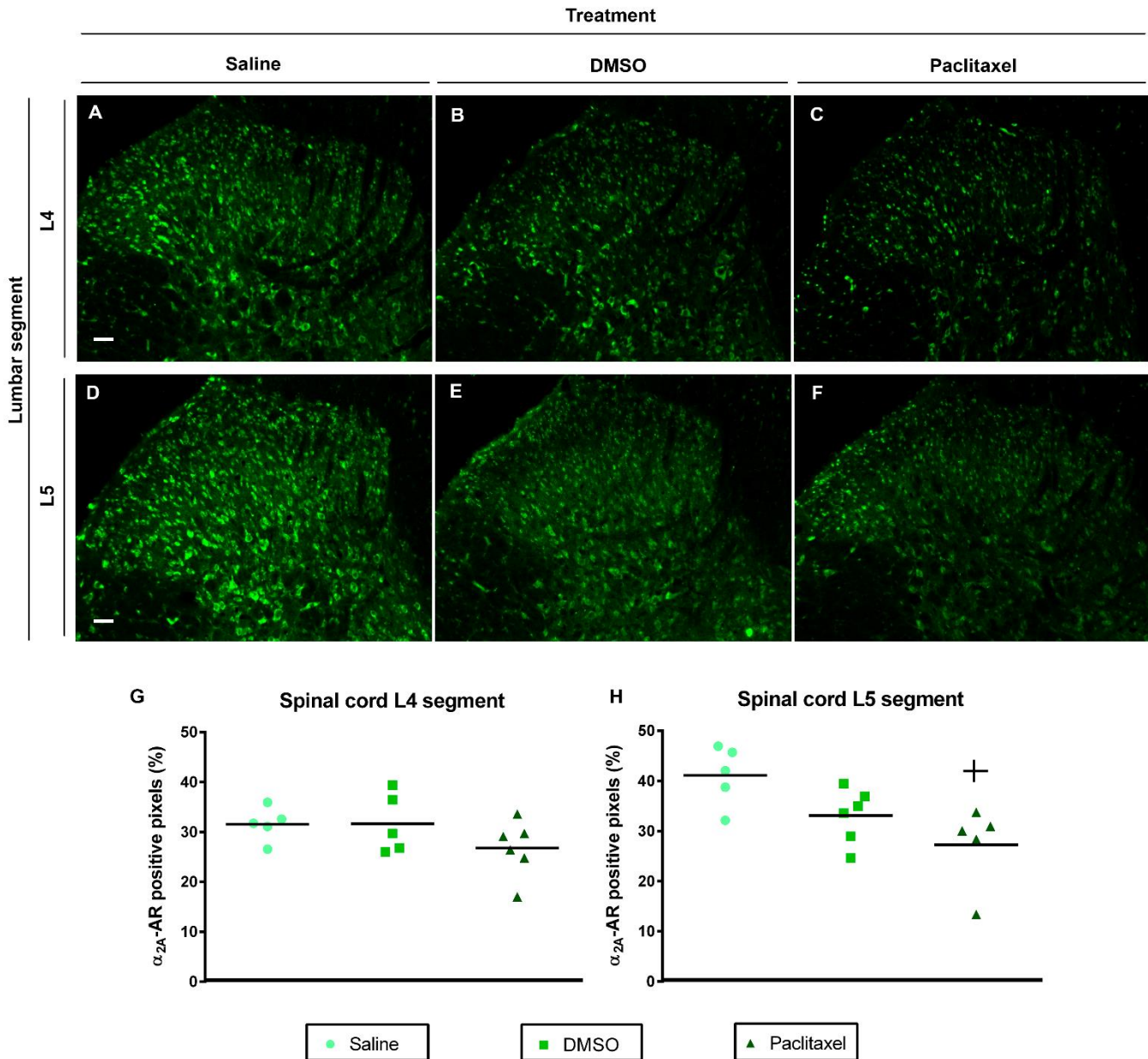


Figure 18. Expression of  $\alpha_{2A}$ -AR at the spinal dorsal horn at one month after CIN induction. Representative fluorescence photomicrographs of  $\alpha_{2A}$ -AR immunoreactivity in the spinal L4 (A, B, C) and L5 (D, E, F) sections of saline- (A, D), DMSO- (B, E) and paclitaxel-treated (C, F) animals. White scale bar in A and D: 50  $\mu$ m. All images were acquired under the same magnification. The percentage of  $\alpha_{2A}$ -AR positive pixels was determined in the laminae I-II. Data are presented as mean  $\pm$  SEM (paclitaxel, DMSO and saline n = 6 each group). +p < 0.05 vs saline.

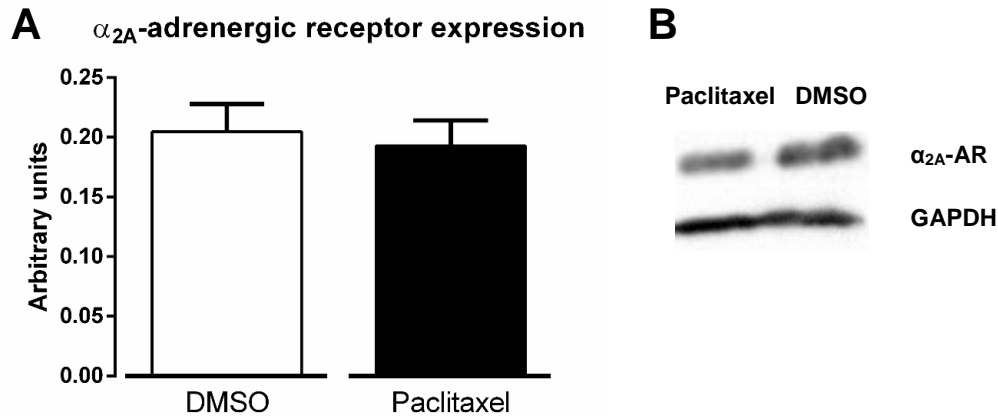


Figure 19. Expression of  $\alpha_{2A}$ -AR in the dorsal portion of the lumbar spinal cord (L4-L5) at one month after CIN induction. Graph A shows the densitometric quantification of  $\alpha_{2A}$ -AR of the blots (B) from DMSO- and paclitaxel-treated animals. GAPDH was used as a control of the western blotting procedure. Data are presented as mean  $\pm$  SEM (paclitaxel and DMSO n = 5 each group).

### 3.3. Analysis of spinal $\alpha_{2A}$ -AR function

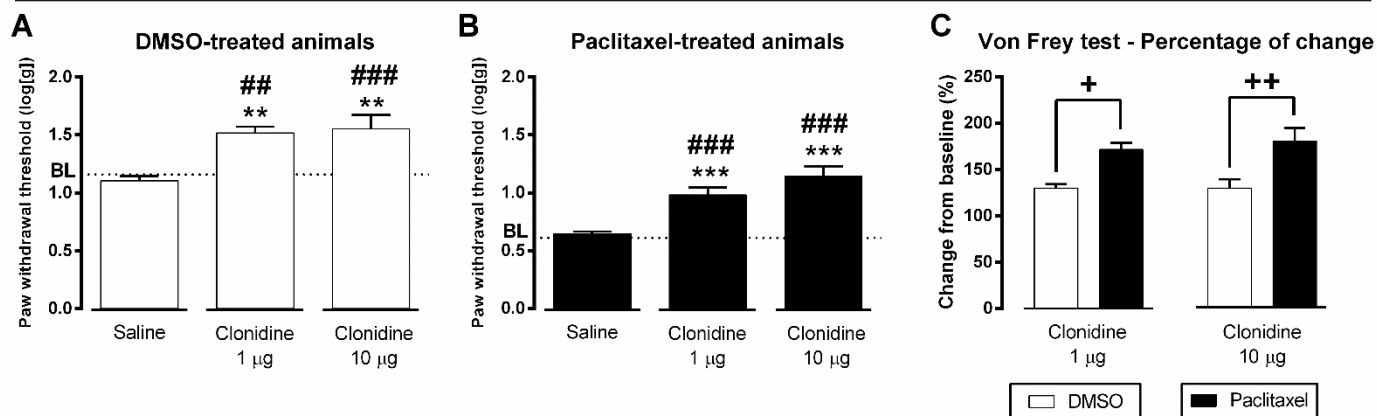
Functional analysis of spinal  $\alpha_{2A}$ -AR was performed upon intrathecal administration of the  $\alpha_{2A}$ -AR agonist clonidine in DMSO- (n = 22) and paclitaxel-treated (n = 19) animals at one month after CIN induction. The behavioral effects of clonidine at 1  $\mu$ g and 10  $\mu$ g were tested on the von Frey (Figure 20-A-C) and cold plate (Figure 20-D-F) tests.

In the von Frey test, the paw withdrawal thresholds were determined from the left hind paw. We determined paw withdrawals only from one paw as the mechanical sensitivity did not differ significantly between left and right paws after CIN induction (section 1.1.). The analysis of the effects of clonidine in paclitaxel-treated animals (Figure 20-B) also revealed a main effect of treatment ( $F_{2, 16} = 8.423$ ,  $p = 0.0032$ ), time ( $F_{1, 16} = 86.15$ ,  $p < 0.0001$ ) and interaction (treatment x time:  $F_{2, 16} = 18.27$ ,  $p < 0.0001$ ). Both doses of clonidine induced a significant increase of paw withdrawal thresholds compared to baseline (clonidine at 1  $\mu$ g:  $p < 0.0001$ ; clonidine at 10  $\mu$ g:  $p < 0.0001$ ) and saline (clonidine at 1  $\mu$ g:  $p = 0.0008$ ; clonidine at 10  $\mu$ g:  $p < 0.0001$ ). There were no differences between clonidine at 1  $\mu$ g and 10  $\mu$ g ( $p = 0.2525$ ). At baseline, paw withdrawal thresholds were not significantly different between the different groups (Figure 20-B). The injection of saline did not induce any significant effects (Figure 20-B). The analysis of the effects of clonidine in DMSO-treated animals (Figure 20-A) revealed a main effect of treatment ( $F_{2, 19} = 7.684$ ,  $p = 0.0036$ ), time ( $F_{1, 19} = 27.96$ ,  $p < 0.0001$ ) and interaction (treatment x time:  $F_{2, 19} = 7.471$ ,  $p = 0.0040$ ). Both doses of clonidine induced a significant increase of paw withdrawal thresholds compared to baseline, i.e. before clonidine injection (clonidine at 1  $\mu$ g:  $p = 0.0070$ ; clonidine at 10  $\mu$ g:  $p = 0.0028$ ), and saline (clonidine at 1

$\mu\text{g}$ :  $p = 0.0010$ ; clonidine at  $10 \mu\text{g}$ :  $p = 0.0002$ ). There were no differences between clonidine at  $1 \mu\text{g}$  and  $10 \mu\text{g}$  ( $p = 0.9985$ ). At baseline, paw withdrawal thresholds were not significantly different between the different groups (Figure 20-A). The injection of saline did not induce any significant effects (Figure 20-A). The analysis of the percentage of change induced by clonidine indicated that paclitaxel induced a higher percentage of change in paw withdrawal thresholds both at clonidine doses of  $1 \mu\text{g}$  ( $p = 0.0177$ ; Figure 20-C) and  $10 \mu\text{g}$  ( $p = 0.0033$ ; Figure 20-C) compared to DMSO.

In the cold plate test, the analysis of the effects of clonidine in paclitaxel-treated animals (Figure 20-E) revealed a main effect of treatment ( $F_{2, 16} = 9.777$ ,  $p = 0.0017$ ), time ( $F_{1, 16} = 50.38$ ,  $p < 0.0001$ ) and interaction (treatment x time:  $F_{2, 16} = 11.41$ ,  $p = 0.0008$ ). Both doses of clonidine induced a significant increase of paw withdrawal latency compared to baseline (clonidine at  $1 \mu\text{g}$ :  $p = 0.0005$ ; clonidine at  $10 \mu\text{g}$ :  $p < 0.0001$ ) and saline (clonidine at  $1 \mu\text{g}$ :  $p = 0.0015$ ; clonidine at  $10 \mu\text{g}$ :  $p < 0.0001$ ). There were no differences between clonidine at  $1 \mu\text{g}$  and  $10 \mu\text{g}$  ( $p = 0.2594$ ). At baseline, paw withdrawal thresholds were not significantly different between the different groups (Figure 20-E). The injection of saline did not induce any significant effects (Figure 20-E). The analysis of the effects of clonidine in DMSO-treated animals (Figure 20-D) revealed a main effect of treatment ( $F_{2, 19} = 14.83$ ,  $p = 0.0001$ ), time ( $F_{1, 19} = 86.54$ ,  $p < 0.0001$ ) and interaction (treatment x time:  $F_{2, 19} = 24.16$ ,  $p < 0.0001$ ). Both doses of clonidine induced a significant increase of paw withdrawal latency compared to baseline (clonidine at  $1 \mu\text{g}$ :  $p = 0.0028$ ; clonidine at  $10 \mu\text{g}$ :  $p < 0.0001$ ) and to saline (clonidine at  $1 \mu\text{g}$ :  $p < 0.0001$ ; clonidine at  $10 \mu\text{g}$ :  $p < 0.0001$ ). There were no differences between clonidine at  $1 \mu\text{g}$  and  $10 \mu\text{g}$  ( $p = 0.9334$ ). At baseline, paw withdrawal latency was not significantly different between the different groups (Figure 20-D). The injection of saline did not induce any significant effects (Figure 20-D). The analysis of the percentage of change induced by clonidine showed that paclitaxel induced only a significant higher percentage of change in paw withdrawal latency at clonidine dose of  $10 \mu\text{g}$  ( $p = 0.0447$ ; Figure 20-F) compared to DMSO.

### Von Frey test



### Cold plate test

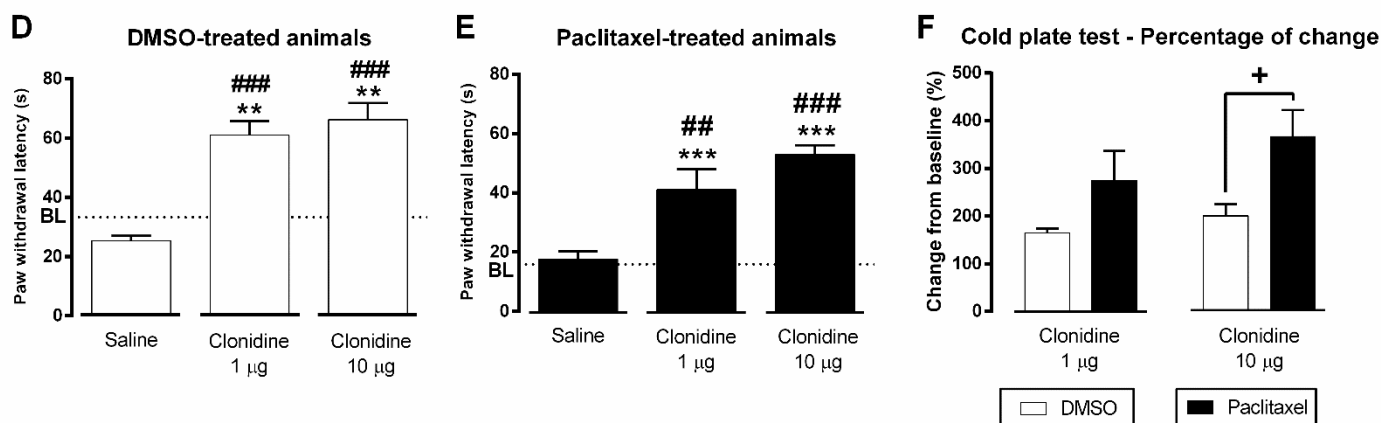


Figure 20. Effects of intrathecal administration of clonidine in the von Frey (A-C) and the cold plate (D-F) tests. Graphs A and B show paw withdrawal thresholds 15-20 minutes after clonidine administration for the von Frey test. Graphs D and E show paw withdrawal latencies 30 minutes after clonidine administration for the cold plate test. Dashed lines represent mean baseline values (BL) for DMSO- and paclitaxel-treated animals. Graphs C and F show the percentage of change from baseline of paw withdrawal thresholds and latencies, respectively, at clonidine doses of 1 and 10 µg. Data are presented as mean ± SEM (clonidine at 1 µg: paclitaxel n = 7; DMSO n = 7; clonidine at 10 µg: paclitaxel n = 6; DMSO n = 8; saline: paclitaxel n = 6; DMSO n = 7). \*\*p < 0.01; \*\*\*p < 0.001 vs baseline; ##p < 0.01; ###p < 0.001 vs saline; +p < 0.05; ++p < 0.01 vs DMSO.

# Discussion

---

The use of a rat model in the current study enabled us to study how systemically administered paclitaxel affects the central nervous system. The main results gathered in this thesis established that paclitaxel-treated animals developed and maintained mechanical sensitivity for at least two months after the beginning of the treatment. Our preliminary behavioral data suggest that paclitaxel also engages the affective component of pain. The alterations in pain behavior are paralleled at the molecular level by an increase in the expression of c-Fos, a marker for the activation of nociceptive neurons, in the spinal dorsal horn after noxious cold stimulation. Finally, paclitaxel treatment also led to increased expression of the noradrenaline biosynthetic enzyme DBH in the spinal cord and a potentiation of the inhibitory function of spinal  $\alpha_2$ -AR. These results suggest a recruitment of descending noradrenergic inhibition probably to remediate increased central sensitization.

## 1. Behavioral alterations during CIN

The nociceptive behavioral testing showed that paclitaxel-treated animals developed significant mechanical sensitivity a few days after initiation of the treatment. The development of mechanical sensitivity has been reported in several other studies which used, as in our study, a low-dose regimen of paclitaxel [71, 74, 95]. In our study, mechanical allodynia was detected from day 5 onwards, however some studies have reported that mechanical sensitivity can appear earlier during a so-called acute painful phase [95]. Indeed, Yan et al. (2015) [96] detected lower paw withdrawal thresholds in response to mechanical stimulation as soon as 2h after a single intravenous injection of paclitaxel at the same dose we used in our study. Dina et al. (2001) [97] reported the same behavior between 1 to 6h after an intraperitoneal injection of paclitaxel at a smaller dose. Our time course study also showed that mechanical allodynia was maintained for at least two months after CIN induction, which confirms the long-lasting chronic effects of paclitaxel treatment previously seen by others [71, 74]. The alterations detected at the level of the sensorial component of pain, either soon after the injection and its perpetuation over time, are due to alterations on sensorial nerves, which have been described by others [66].

Enhanced pain sensitivity is a well-established hallmark of paclitaxel-induced neuropathy, but most of the animal studies on this subject have only focused on how and to what extent paclitaxel alters the sensorial component of pain. It is also likely that paclitaxel treatment impacts on the emotional/affective component of pain since a recent finding showed that under administration of a cumulative dose of paclitaxel similar to our study, the observed mechanical allodynia was paralleled by increased excitability in the anterior cingulate cortex (ACC) [33], which is an area involved in the pain aversiveness circuit [30]. To study whether paclitaxel impacts on the emotional/affective dimension of pain, we started by detecting whether paclitaxel administration was associated to a negative emotion which would be demonstrated by place avoidance or aversion in the CPA test. The CPA paradigm was then used under the assumption that if paclitaxel induces mechanical allodynia soon after i.p. injection, the animals would promptly associate the unpleasantness of the drug to the compartment where they receive the drug, which then would motivate avoidance/escaping from this compartment. Our preliminary results show that paclitaxel induces place aversion. We also wanted to see whether the animals maintained the aversiveness towards the paclitaxel-associated compartment, and for that we placed them again in the CPA box one week later. The animals' behavior remained unchanged from the first post-conditioning session and the fact that they could still associate that compartment to the unpleasant feeling of receiving paclitaxel after one week indicates that paclitaxel induced a strong negative emotion and that memory remained intact. The fact that they did not spend a considerable amount of time in the saline-paired compartment means that they escaped indiscriminately from the paclitaxel-associated compartment to any of the available compartments (both saline-paired and neutral compartments). We must also say that the vehicle DMSO-treated animal also displayed an escape response towards the DMSO-paired compartment. Nonetheless, it was only a single animal and we need to increase the number of vehicle-treated animals as well as the number of paclitaxel-treated animals to validate our initial hypothesis.

## **2. Central sensitization**

Along with the changes in nociceptive behavior, functional changes in the processing of sensory information by spinal cord neurons have been reported following paclitaxel treatment by electrophysiological studies. These studies revealed sensitization mechanisms including spontaneous activity in wide-dynamic-range neurons of the spinal dorsal horn and increased after-discharges to noxious mechanical stimuli, increased neuronal responses to both skin heating and cooling, and windup, which is defined as



increased number of discharges in spinal neurons occurring with repetitive transcutaneous electrical stimulation of C-fibers [98]. Here we aimed to study whether the phenomena of central sensitization could also be monitored by the expression of two classical markers of neuronal activation such as pCREB [79] and c-Fos, the latter being a specific marker of nociceptive activity at the spinal dorsal horn [99].

In our study, under basal conditions (i.e., without nociceptive stimulation), there were no differences in the spinal expression of pCREB between paclitaxel and DMSO treatments. However, saline-treated animals showed a higher expression of the protein in comparison to both paclitaxel- and DMSO-treated animals. These results indicate that the vehicle DMSO impacts on the expression of pCREB. DMSO alone might be acting to reduce spinal neuronal activity as seen by the decreased expression of pCREB. In fact, DMSO was shown to block depolarization through inhibition of potassium channels on C-fibers at low concentrations [100]. It was also shown to cross the blood-brain barrier [101], which would enable an action on spinal dorsal horn neurons and cause inhibition of their activity. The DMSO effect, however, did not significantly impact on spinal nociceptive activation since the expression of the marker, c-Fos, for spinal nociceptive activation was increased after noxious stimulation in paclitaxel-treated animals compared to DMSO-treated animals. Our study also revealed that, although we cannot assume treatment-dependency, labelling of pCREB protein was more intensely observed in the superficial dorsal horn laminae I-II, the spinal laminae receiving noxious peripheral input, which is consistent with previous studies on the expression of spinal pCREB [102].

We assessed c-Fos expression as a marker for neuronal activation in the spinal cord under noxious stimulation. Under normal conditions, c-Fos expression markedly increases in spinal dorsal horn neurons upon noxious stimuli because its protein product, FOS, plays a role in the signaling cascade leading to the production of peptides important for nociceptive neurotransmission [80, 103, 104]. We used a cold stimulation at 0°C, which induced a higher level of c-Fos expression in the spinal dorsal horn of paclitaxel-treated animals compared to DMSO-treated animals. The application of noxious cold to the hind paws of animals, at temperatures below 0°C, has been demonstrated to activate c-Fos expression in the superficial and deep dorsal horn and the expression of c-Fos was shown to be dependent on the intensity and duration of the cold stimulus [12, 99]. Abbadie et al. (1994) [99] reported that the threshold to induce c-Fos expression was -15°C, with little or no expression detected in the lumbar spinal cord when the paws were submitted to temperatures between 15 and -10°C. Compared to Abbadie et al. (1994) [99], our results indicate that paclitaxel treatment decreases the threshold of c-Fos activation, since at 0°C the expression of this marker is significantly increased in

paclitaxel-treated animals. Saline-treated animals were not processed due to previous studies indicating that, under normal conditions, 0°C would not be sufficient to induce c-Fos activation [12, 99]. We, therefore, did not inflict discomfort to an additional group of animals. The DMSO-treated animals showed less c-Fos expression than paclitaxel-treated animals, but the c-Fos immunoreactivity was higher than expected for these animals, probably because the stimulation was prolonged and repeated (3 times for 50 s each). Regarding the distribution of the FOS protein in the dorsal horn, the highest number of c-Fos-IR nuclei was detected in lamina III. This result is surprising and not supported by studies on spinal c-Fos expression which have reported it to be mainly expressed in laminae I-II and V, which is also the location of spinal neurons that receive noxious input from A $\delta$ -fibers and C-fibers, the pain conducting fibers [12, 99, 103]. One possible explanation for our result could be that the central terminals of A $\delta$ - and/or C-fibers sprout into lamina III and activate local spinal neurons. Alternatively, it could be due to a switch in the activity of A $\beta$ -fibers, that project to lamina III, which would make them also conduct noxious stimuli information as a consequence of paclitaxel action in the peripheral sensory nerves. Indeed, A $\beta$  fibers, which normally signal innocuous sensations, reportedly begin to produce pain after neural lesions [105].

Out of the two markers, only c-Fos effectively revealed increased activation of spinal dorsal horn neurons following paclitaxel treatment, which could be indicative of central sensitization. It is noteworthy to mention that the increased activity of spinal nociceptive neurons we detected is likely peripherally-driven since paclitaxel has a limited ability to cross the blood-brain barrier due to the presence of the multidrug transporter P-glycoprotein in the endothelial cells of the blood capillaries that make up the blood-brain barrier. This transporter blocks the transport of paclitaxel. Indeed, the inhibition of this transporter has been shown to promote the entry of paclitaxel to the cerebrospinal fluid [106, 107].

### **3. Engagement of descending noradrenergic modulation**

Plastic changes in the descending modulatory pathways are known to occur during neuropathic pain in rodent models of neuropathic pain and in humans [108]. It is known that these changes result in the disruption of the balance between descending modulatory circuits favoring facilitation, concomitantly with diminished descending inhibition, both alterations contributing to maintaining chronic pain. The descending noradrenergic system exerts inhibitory control of pain by releasing noradrenaline in the spinal cord via projections originating from noradrenergic nuclei in the brain (the locus coeruleus or A6, A5 and A7 nuclei). Noradrenaline in the spinal cord acts on presynaptic

and postsynaptic spinal neurons to inhibit transmission of pain signals [14]. There may be a depressed functionality of this system during neuropathic pain since the administration of noradrenaline reuptake inhibitors in chronic pain patients ameliorates pain [109]. But there is also some evidence suggesting that the activity of the descending noradrenergic system may actually be augmented as to compensate the enhanced nociceptive input in conditions of nerve injury [108]. In our model of chemotherapy-induced neuropathy, whether paclitaxel promotes a loss or an engagement of descending noradrenergic inhibition is not yet known, but our results point to the second hypothesis. Indeed, the expression of DBH, one of the enzymes of the noradrenergic biosynthetic pathway, is increased in the spinal L4 segment of paclitaxel-treated animals in comparison to DMSO-treated animals at one month after CIN induction. This enzyme is primarily synthesized in the cell body of noradrenergic neurons and is then transported to neuronal terminals, including the spinal terminals of noradrenergic neurons [20]. The increase in the density of DBH-IR positive fibers after paclitaxel treatment is indicative of increased DBH expression and possibly an increase of noradrenaline release in the spinal cord. It is possible that the increased DBH labelling originates from local sprouting of terminals of the descending noradrenergic fibers. This process was shown after nerve injury, in a model of chronic constriction injury, where increased density of noradrenergic fibers in the spinal cord was associated to increased brain derived nerve growth factor (BDNF), a neurotrophin known for its role in differentiation of neurons and plasticity processes related to pain [110]. This increase in DBH expression suggests that there might be a recruitment of the descending noradrenergic inhibitory system, probably in response to a depression of local spinal inhibition. Indeed, recently paclitaxel treatment was shown to increase the spinal expression of the gamma-aminobutyric acid (GABA) transporter 1 (GAT-1), which consequently reduces ambient GABA levels and decreases inhibitory tone [111, 112]. On the other hand, the descending noradrenergic inhibitory system may also be recruited in response to increased excitability of spinal nociceptive neurons, as the expression of glutamate transporter proteins in the dorsal horn was shown to be decreased after paclitaxel treatment, which increased glutamate at the synaptic clefts [98]. In our study, increased expression of c-Fos corroborates the thesis of increased neuronal activation. These findings suggest that both increased spinal excitability and reduced spinal inhibitory tone are contributing to amplify excitatory transmission, which may be a signal for the brain to reinforce descending inhibitory modulation. For this part of our study, we investigated the influence of time in the maintenance of paclitaxel-induced plastic changes in the spinal cord. Our results revealed that DBH expression was increased at one month after CIN induction but not at two months. Since our animals were still displaying mechanical allodynia at two

months, we speculate that the absence of alterations compared to control animals at two months was probably due to wear-out of the noradrenergic system resulting from continuous input from the periphery. Although we were not able to confirm whether increased DBH expression results in increased noradrenaline production and release in the spinal cord, previous work showed that increased DBH expression results in increased noradrenaline [110, 113].

Noradrenaline exerts analgesia by acting on spinal presynaptic and postsynaptic  $\alpha_2$ -ARs, which are located on primary afferent terminals and local nociceptive dorsal horn neurons, respectively. Decreased expression or activity of these receptors is sometimes pointed to contribute to the loss of inhibitory tone in the spinal cord during neuropathic pain states [21, 83]. We studied the expression of  $\alpha_{2A}$ -ARs in L4 and L5 spinal lumbar segments by western blotting and by immunofluorescence. For the western blotting analysis, we isolated the entire portion of the dorsal horn while in the immunofluorescence study we were able to spatially isolate the superficial dorsal horn laminae, which receive the terminal fields of the primary sensory neurons. The western blotting study showed no differences in the expression of  $\alpha_{2A}$ -ARs within the whole dorsal horn of the L4-L5 bulk of paclitaxel- and DMSO-treated animals. The analysis of the superficial laminae of L4 and L5 segments, separately, showed that the spinal expression of the  $\alpha_{2A}$ -AR subtype was also not significantly altered by paclitaxel treatment in the superficial laminae of the L4 segment, but it was reduced in the superficial laminae of the L5 segment, although only compared to saline-treated animals only. Although the reduction of  $\alpha_{2A}$ -ARs in the L5 segment was not very strong and was only revealed when comparing paclitaxel-treated animals with saline control animals, we cannot exclude that paclitaxel treatment might have had a higher impact on the peripheral nerves projecting to the L5 segment. Our results suggest that there is not a relationship between density of noradrenergic fibers and expression of  $\alpha_{2A}$ -ARs, i.e., in the spinal L5 segment there is a decreased expression of the receptor but it is not accompanied by a significant increase in the density of those fibers. It seems that, even though they integrate the same system, their expression is not dependent on one another. Whether the expression of this receptor subtype is altered during different neuropathic pain states is not consensual among different studies, but a commonly reported observation in such studies is that there is an augmented efficacy in the antinociceptive activity of the  $\alpha_{2A}$ -AR when its agonist clonidine is administered, which we confirmed. Our study revealed that, even though the expression of the receptor was decreased at some level or remained unchanged, the effects of intrathecally administered clonidine were markedly higher in paclitaxel-treated animals as indicated by the amelioration of mechanical allodynia and cold hyperalgesia. The effect was

greater on mechanical nociception, though. It seems that the dose of 1  $\mu\text{g}$  of clonidine was not sufficient to reduce sensitivity to noxious cold but it was sufficient to reduce sensitivity to mechanical stimulation. This modality-specific effect is a common feature of the noradrenergic system, which seems to be more specifically engaged in the inhibition of mechanical nociception [114, 115]. This means that, clonidine may or may not exert a dose-dependent effect depending on the nature of the stimulus. We cannot completely attribute the increased efficacy of clonidine antinociceptive activity to  $\alpha_{2A}$ -AR subtype because clonidine has been shown to also bind to the  $\alpha_{2C}$ -AR subtype, although with much less affinity [21]. We did not determine the expression of the  $\alpha_{2C}$ -AR subtype, which is also expressed by spinal neurons [20], but it would have been interesting to study whether paclitaxel treatment also changes the expression of the  $\alpha_{2C}$ -AR subtype and how it could contribute to the increased effect of clonidine. The reason for the increased potency of the receptor was viewed in other models of neuropathic pain as the result of increased efficiency of G protein coupling to  $\alpha_2$ -AR [116]. It would be interesting in the future to further study the involvement of G proteins activation in this model of neuropathy.

#### **4. Conclusions and future perspectives**

The studies developed during the present thesis helped to unravel alterations at the level of the central nervous system, namely in what concerns the descending noradrenergic modulatory system. The behavioral studies demonstrated that paclitaxel affects both the sensorial and the emotional dimensions of pain. While the development of mechanical allodynia is commonly reported in other rat studies, the aversiveness of paclitaxel had been, up until now, quite unappreciated. However, to complete our preliminary findings with the CPA test, there is a need to complete the study by increasing the number of animals and it would also be interesting to understand the mechanisms involved in paclitaxel-induced aversion in the brain. The results obtained suggest a recruitment of the descending noradrenergic inhibition pathways based on the spinal increased noradrenergic innervation and the spinal  $\alpha_2$ -AR function potentiation in the paclitaxel-treated animals. It would be interesting to continue the studies and determine whether the increased noradrenergic innervation is paralleled by increased noradrenaline release in the spinal cord. For that, it would be interesting to quantify noradrenaline using high performance liquid chromatography (HPLC). The potentiation of the  $\alpha_2$ -AR might reflect alterations in the intracellular G-protein coupled receptor signaling. It would be interesting to pursue the study to understand the mechanisms

engaged in the potentiation of the receptor as it could open new avenues for the treatment of neuropathic pain during chemotherapy.

## References

---

1. Loeser, J. D. and R. D. Treede, *The Kyoto protocol of IASP Basic Pain Terminology*. Pain, 2008. **137**(3): p. 473-7.
2. Kidd, B. L. and L. A. Urban, *Mechanisms of inflammatory pain*. Br J Anaesth, 2001. **87**(1): p. 3-11.
3. Woolf, C. J., *What is this thing called pain?* J Clin Invest, 2010. **120**(11): p. 3742-4.
4. Dubin, A. E. and Patapoutian, A., *Nociceptors: the sensors of the pain pathway*. J Clin Invest, 2010. **120**(11): p. 3760-72.
5. Chien, G. C. C., Jusino, E. and Deroee, A., *Chronic Pain*, in *Treatment of Chronic Pain Conditions: A Comprehensive Handbook*, S.S.B.M. LLC, Editor. 2017, Springer Nature: New York, NY, USA. p. 3.
6. McGreevy, K., M. M. Bottros, and S. N. Raja, *Preventing Chronic Pain following Acute Pain: Risk Factors, Preventive Strategies, and their Efficacy*. Eur J Pain Suppl, 2011. **5**(2): p. 365-372.
7. Patestas, M. A., L. P. Gartner, *A textbook of neuroanatomy*. 2006, Blackwell Pub.,: Malden, MA. p. ix, 454 p.
8. Marchand, S., *The physiology of pain mechanisms: from the periphery to the brain*. Rheum Dis Clin North Am, 2008. **34**(2): p. 285-309.
9. Guyton, A. C. and Hall, J.E., *Textbook of medical physiology*. 11th ed. 2006, Philadelphia: Elsevier Saunders. xxxv, 1116 p.
10. Kuner, R. and Flor, H., *Structural plasticity and reorganisation in chronic pain*. Nat Rev Neurosci, 2016. **18**(1): p. 20-30.
11. Basbaum, A. I.; Bautista, D. M.; Scherrer, G.; Julius, D., *Cellular and molecular mechanisms of pain*. Cell, 2009. **139**(2): p. 267-84.
12. Khasabov, S. G., Cain, D. M., Thong, D., Mantyh, P. W., Simone, D. A., *Enhanced responses of spinal dorsal horn neurons to heat and cold stimuli following mild freeze injury to the skin*. J Neurophysiol, 2001. **86**(2): p. 986-96.
13. Grace, P. M., Hutchinson, M. R., Maier, S. F., Watkins, L. R., *Pathological pain and the neuroimmune interface*. Nat Rev Immunol, 2014. **14**(4): p. 217-31.
14. Ossipov, M. H., Dussor, G. O., and Porreca, F., *Central modulation of pain*. J Clin Invest, 2010. **120**(11): p. 3779-87.
15. Gebhart, G. F., *Descending modulation of pain*. Neurosci Biobehav Rev, 2004. **27**(8): p. 729-37.
16. Brodin, E., Ernberg, M., and Olgart, L., *Neurobiology: General considerations – from acute to chronic pain*. Nor Tannlegeforen Tid., 2016(126): p. 28–33.

17. Wainger, B. J. and Brenner, G. J., *Mechanisms of Chronic Pain*, in *Anesthesiology*, T.M.-H. Companies, Editor. 2012.
18. Bajic, D. and Proudfit, H. K., *Projections of neurons in the periaqueductal gray to pontine and medullary catecholamine cell groups involved in the modulation of nociception*. *J Comp Neurol*, 1999. **405**(3): p. 359-79.
19. Atzori, M., Cuevas-Olguin, R., Esquivel-Rendon, E., Garcia-Oscos, F., Salgado-Delgado, R. C., Saderi, N., Miranda-Morales, M., Treviño, M., Pineda, J. C., Salgado, H., *Locus Ceruleus Norepinephrine Release: A Central Regulator of CNS Spatio-Temporal Activation?* *Front Synaptic Neurosci*, 2016. **8**: p. 25.
20. Pertovaara, A., *Noradrenergic pain modulation*. *Prog Neurobiol*, 2006. **80**(2): p. 53-83.
21. Fairbanks, C. A., Stone, L. S., and Wilcox, G. L. *Pharmacological profiles of alpha 2 adrenergic receptor agonists identified using genetically altered mice and isobolographic analysis*. *Pharmacol Ther*, 2009. **123**(2): p. 224-38.
22. Nicholson, R., Dixon, A. K., Spanswick, D., Lee, K., *Noradrenergic receptor mRNA expression in adult rat superficial dorsal horn and dorsal root ganglion neurons*. *Neurosci Lett*, 2005. **380**(3): p. 316-21.
23. Stone, L. S., Broberger, C., Vulchanova, L., Wilcox, G. L., Hökfelt, T., Riedl, M. S., Elde, R., *Differential distribution of alpha2A and alpha2C adrenergic receptor immunoreactivity in the rat spinal cord*. *J Neurosci*, 1998. **18**(15): p. 5928-37.
24. Olave, M. J. and Maxwell, D.J., *Axon terminals possessing the alpha 2c-adrenergic receptor in the rat dorsal horn are predominantly excitatory*. *Brain Res*, 2003. **965**(1-2): p. 269-73.
25. Navratilova, E. and Porreca, F., *Reward and motivation in pain and pain relief*. *Nat Neurosci*, 2014. **17**(10): p. 1304-12.
26. Schultz, W., *Updating dopamine reward signals*. *Curr Opin Neurobiol*, 2013. **23**(2): p. 229-38.
27. Noda, K., Akita, H., Ogata, M., Saji, M., *Paclitaxel-induced hyperalgesia modulates negative affective component of pain and NR1 receptor expression in the frontal cortex in rats*. *Neurosci Res*, 2014. **80**: p. 32-7.
28. Li, T. T., Ren, W. H., Xiao, X., Nan, J., Cheng, L. Z., Zhang, X. H., Zhao, Z. Q., Zhang, Y. Q., *NMDA NR2A and NR2B receptors in the rostral anterior cingulate cortex contribute to pain-related aversion in male rats*. *Pain*, 2009. **146**(1-2): p. 183-93.
29. Gao, Y. J., Ren, W. H., Zhang, Y. Q., Zhao, Z. Q., *Contributions of the anterior cingulate cortex and amygdala to pain- and fear-conditioned place avoidance in rats*. *Pain*, 2004. **110**(1-2): p. 343-53.
30. Johansen, J. P., Fields, H. L., and Manning, B. H., *The affective component of pain in rodents: direct evidence for a contribution of the anterior cingulate cortex*. *Proc Natl Acad Sci U S A*, 2001. **98**(14): p. 8077-82.



31. Zhang, Q., Manders, T., Tong, A. P., Yang, R., Garg, A., Martinez, E., Zhou, H., Dale, J., Goyal, A., Urien, L., Yang, G., Chen, Z., Wang, J., *Chronic pain induces generalized enhancement of aversion*. *Elife*, 2017. **6**.
32. Tseng, M. T., Chiang, M. C., Chao, C. C., Tseng, W. Y., Hsieh, S. T., *fMRI evidence of degeneration-induced neuropathic pain in diabetes: enhanced limbic and striatal activations*. *Hum Brain Mapp*, 2013. **34**(10): p. 2733-46.
33. Nashawi, H., Masocha, W., Edafiogho, I. O., Kombian, S. B., *Paclitaxel Causes Electrophysiological Changes in the Anterior Cingulate Cortex via Modulation of the  $\gamma$ -Aminobutyric Acid-ergic System*. *Med Princ Pract*, 2016. **25**(5): p. 423-8.
34. Tavares, I. and Martins, I., *Gene Therapy for Chronic Pain Management*, in *Gene Therapy - Tools and Potential Applications*, F.M. Molina, Editor. 2013, InTech. p. 685-687.
35. Borsook, D., *Neurological diseases and pain*. *Brain*, 2012. **135**(Pt 2): p. 320-44.
36. Ji, R. R., Xu, Z. Z., and Gao, Y. J., *Emerging targets in neuroinflammation-driven chronic pain*. *Nat Rev Drug Discov*, 2014. **13**(7): p. 533-48.
37. Jensen, T. S. and Finnerup, N. B., *Neuropathic pain: Peripheral and central mechanisms*. *European Journal of Pain Supplements*, 2009(3): p. 33-36.
38. Neumann, S., Doubell, T. P., Leslie, T., Woolf, C. J., *Inflammatory pain hypersensitivity mediated by phenotypic switch in myelinated primary sensory neurons*. *Nature*, 1996. **384**(6607): p. 360-4.
39. Feizerfan, A. and Sheh, G., *Transition from acute to chronic pain*. *Continuing Education in Anaesthesia Critical Care & Pain*, 2015. **15**(2): p98-102.
40. Campbell, J. N. and Meyer, R.A., *Mechanisms of neuropathic pain*. *Neuron*, 2006. **52**(1): p. 77-92.
41. National Institute of Neurological Disorders and Stroke. *Peripheral Neuropathy Fact Sheet*. 2014 [cited 2016 October]; Available from: [http://www.ninds.nih.gov/disorders/peripheralneuropathy/detail\\_peripheralneuropathy.htm](http://www.ninds.nih.gov/disorders/peripheralneuropathy/detail_peripheralneuropathy.htm).
42. Callaghan, B. C., Cheng, H. T., Stables, C. L., Smith, A. L., Feldman, E. L., *Diabetic neuropathy: clinical manifestations and current treatments*. *Lancet Neurol*, 2012. **11**(6): p. 521-34.
43. Dobretsov, M., Romanovsky, D., and Stimers, J. R., *Early diabetic neuropathy: triggers and mechanisms*. *World J Gastroenterol*, 2007. **13**(2): p. 175-91.
44. Russell, J. W. and Zilliox, L. A., *Diabetic neuropathies*. *Continuum (Minneapolis)*, 2014. **20**(5 Peripheral Nervous System Disorders): p. 1226-40.
45. Lai, J., Hunter, J. C., and Porreca, F., *The role of voltage-gated sodium channels in neuropathic pain*. *Curr Opin Neurobiol*, 2003. **13**(3): p. 291-7.
46. Hong, S. and Wiley, J. W., *Early painful diabetic neuropathy is associated with differential changes in the expression and function of vanilloid receptor 1*. *J Biol Chem*, 2005. **280**(1): p. 618-27.

47. Baron, R., *Mechanisms of disease: neuropathic pain--a clinical perspective*. Nat Clin Pract Neurol, 2006. **2**(2): p. 95-106.
48. Latremoliere, A. and Woolf, C. J., *Central sensitization: a generator of pain hypersensitivity by central neural plasticity*. J Pain, 2009. **10**(9): p. 895-926.
49. Garcia, J. B. S., Neto, J. O. B., Amancio, E. J., Andrade, E. T. F., *Central neuropathic pain*. Rev. dor, 2016. **17**: p. 67-71.
50. Watson, J. C. and Sandroni, P., *Central Neuropathic Pain Syndromes*. Mayo Clin Proc, 2016. **91**(3): p. 372-85.
51. Kumar, G. and Soni, C. R., *Central post-stroke pain: current evidence*. J Neurol Sci, 2009. **284**(1-2): p. 10-7.
52. Vestergaard, K., Nielsen, J., Andersen, G., Ingeman-Nielsen, M., Arendt-Nielsen, L., Jensen, T. S., *Sensory abnormalities in consecutive, unselected patients with central post-stroke pain*. Pain, 1995. **61**(2): p. 177-86.
53. Wasner, G., Lee, B. B., Engel, S., McLachlan, E., *Residual spinothalamic tract pathways predict development of central pain after spinal cord injury*. Brain, 2008. **131**(Pt 9): p. 2387-400.
54. Raffa, R. B., *Chemotherapy-induced neuropathic pain*. 2013, Boca Raton: CRC Press. xii, 221 p.
55. Park, S. B., Goldstein, D., Krishnan, A. V., Lin, C. S., Friedlander, M. L., Cassidy, J., Koltzenburg, M., Kiernan, M. C., *Chemotherapy-induced peripheral neurotoxicity: a critical analysis*. CA Cancer J Clin, 2013. **63**(6): p. 419-37.
56. Addington, J. and Freimer, M., *Chemotherapy-induced peripheral neuropathy: an update on the current understanding*. F1000Res, 2016. **5**.
57. Kiernan, J. A., *Vascular permeability in the peripheral autonomic and somatic nervous systems: controversial aspects and comparisons with the blood-brain barrier*. Microsc Res Tech, 1996. **35**(2): p. 122-36.
58. Windebank, A. J. and Grisold, W., *Chemotherapy-induced neuropathy*. J Peripher Nerv Syst, 2008. **13**(1): p. 27-46.
59. Brewer, J. R., Morrison, G., Dolan, M. E., Fleming, G. F., *Chemotherapy-induced peripheral neuropathy: Current status and progress*. Gynecol Oncol, 2016. **140**(1): p. 176-83.
60. Farquhar-Smith, P., *Chemotherapy-induced neuropathic pain*. Curr Opin Support Palliat Care, 2011. **5**(1): p. 1-7.
61. Xiao, W. H., Zheng, H., Zheng, F. Y., Nuydens, R., Meert, T. F., Bennett, G. J., *Mitochondrial abnormality in sensory, but not motor, axons in paclitaxel-evoked painful peripheral neuropathy in the rat*. Neuroscience, 2011. **199**: p. 461-9.
62. Iżycki, D., Niezgoda, A. A., Kaźmierczak, M., Piorunek, T., Iżycka, N., Karaszewska, B., Nowak-Markwitz, E., *Chemotherapy-induced peripheral neuropathy - diagnosis, evolution and treatment*. Ginekol Pol, 2016. **87**(7): p. 516-21.

63. Cavaletti, G. and Marmiroli, P., *Chemotherapy-induced peripheral neurotoxicity*. Nat Rev Neurol, 2010. **6**(12): p. 657-66.
64. Chemocare. *How Do Doctors Decide Which Chemotherapy Drugs To Give?* 2016 [cited 2016 1 December]; Available from: <http://chemocare.com/chemotherapy/what-is-chemotherapy/how-do-doctors-decide-which-chemotherapy-drugs-to-give.aspx>.
65. Katsumata, N., Yasuda, M., Takahashi, F., Isonishi, S., Jobo, T., Aoki, D., Tsuda, H., Sugiyama, T., Kodama, S., Kimura, E., Ochiai, K., Noda, K., *Dose-dense paclitaxel once a week in combination with carboplatin every 3 weeks for advanced ovarian cancer: a phase 3, open-label, randomised controlled trial*. Lancet, 2009. **374**(9698): p. 1331-8.
66. Scripture, C. D., Figg, W. D., and Sparreboom, A., *Peripheral neuropathy induced by paclitaxel: recent insights and future perspectives*. Curr Neuropharmacol, 2006. **4**(2): p. 165-72.
67. Fidanboyulu, M., Griffiths, L. A., and Flatters, S. J., *Global inhibition of reactive oxygen species (ROS) inhibits paclitaxel-induced painful peripheral neuropathy*. PLoS One, 2011. **6**(9): p. e25212.
68. Sisignano, M., Baron, R., Scholich, K., Geisslinger, G., *Mechanism-based treatment for chemotherapy-induced peripheral neuropathic pain*. Nat Rev Neurol, 2014. **10**(12): p. 694-707.
69. Shemesh, O. A. and Spira, M. E., *Paclitaxel induces axonal microtubules polar reconfiguration and impaired organelle transport: implications for the pathogenesis of paclitaxel-induced polyneuropathy*. Acta Neuropathol, 2010. **119**(2): p. 235-48.
70. Siau, C., Xiao, W., and Bennett, G. J., *Paclitaxel- and vincristine-evoked painful peripheral neuropathies: loss of epidermal innervation and activation of Langerhans cells*. Exp Neurol, 2006. **201**(2): p. 507-14.
71. Flatters, S. J. and Bennett, G. J., *Studies of peripheral sensory nerves in paclitaxel-induced painful peripheral neuropathy: evidence for mitochondrial dysfunction*. Pain, 2006. **122**(3): p. 245-57.
72. Li, Y., Kosturakis, A. K., Cassidy, R. M., Harrison, D. S., Cata, J. P., Sapire, K., Kennamer-Chapman, R. M., Jawad, A. B., Ghetti, A., Yan, J., Palecek, J., Dougherty, P. M., *The Cancer Chemotherapeutic Paclitaxel Increases Human and Rodent Sensory Neuron Responses to TRPV1 by Activation of TLR4*. J Neurosci, 2015. **35**(39): p. 13487-500.
73. Cliffer, K. D., Siuciak, J. A., Carson, S. R., Radley, H. E., Park, J. S., Lewis, D. R., Zlotchenko, E., Nguyen, T., Garcia, K., Tonra, J. R., Stambler, N., Cedarbaum, J. M., Bodine, S. C., Lindsay, R. M., DiStefano, P. S., *Physiological characterization of Taxol-induced large-fiber sensory neuropathy in the rat*. Ann Neurol, 1998. **43**(1): p. 46-55.
74. Polomano, R. C., Mannes, A. J., Clark, U. S., Bennett, G. J., *A painful peripheral neuropathy in the rat produced by the chemotherapeutic drug, paclitaxel*. Pain, 2001. **94**(3): p. 293-304.

75. Höke, A., *Animal models of peripheral neuropathies*. Neurotherapeutics, 2012. **9**(2): p. 262-9.
76. Lu, J., Luo, C., Bali, K. K., Xie, R. G., Mains, R. E., Eipper, B. A., Kuner, R., *A role for Kalirin-7 in nociceptive sensitization via activity-dependent modulation of spinal synapses*. Nat Commun, 2015. **6**: p. 6820.
77. Raghavendra, V., Tanga, F., and DeLeo, J. A., *Inhibition of microglial activation attenuates the development but not existing hypersensitivity in a rat model of neuropathy*. J Pharmacol Exp Ther, 2003. **306**(2): p. 624-30.
78. Boyette-Davis, J. A., Walters, E. T., and Dougherty, P. M., *Mechanisms involved in the development of chemotherapy-induced neuropathy*. Pain Manag, 2015. **5**(4): p. 285-96.
79. Pancaro, C., Ma, W., Vincler, M., Duflo, F., Eisenach, J. C., *Clonidine-induced neuronal activation in the spinal cord is altered after peripheral nerve injury*. Anesthesiology, 2003. **98**(3): p. 748-53.
80. Bullitt, E., *Expression of c-fos-like protein as a marker for neuronal activity following noxious stimulation in the rat*. J Comp Neurol, 1990. **296**(4): p. 517-30.
81. Gao, Y. J. and Ji, R. R., *c-Fos and pERK, which is a better marker for neuronal activation and central sensitization after noxious stimulation and tissue injury?* Open Pain J, 2009. **2**: p. 11-17.
82. Bannister, K. and Dickenson, A. H., *What the brain tells the spinal cord*. Pain, 2016. **157**(10): p. 2148-51.
83. Hughes, S. W., Hickey, L., Hulse, R. P., Lumb, B. M., Pickering, A. E., *Endogenous analgesic action of the pontospinal noradrenergic system spatially restricts and temporally delays the progression of neuropathic pain following tibial nerve injury*. Pain, 2013. **154**(9): p. 1680-90.
84. Hickey, L., Li, Y., Fyson, S. J., Watson, T. C., Perrins, R., Hewinson, J., Teschemacher, A. G., Furue, H., Lumb, B. M., Pickering, A. E., *Optoactivation of locus ceruleus neurons evokes bidirectional changes in thermal nociception in rats*. J Neurosci, 2014. **34**(12): p. 4148-60.
85. Zimmermann, M., *Ethical guidelines for investigations of experimental pain in conscious animals*. Pain, 1983. **16**(2): p. 109-10.
86. Jasmin, L., Kohan, L., Franssen, M., Janni, G., Goff, J. R., *The cold plate as a test of nociceptive behaviors: description and application to the study of chronic neuropathic and inflammatory pain models*. Pain, 1998. **75**(2-3): p. 367-82.
87. Pertovaara, A. and Kalmari, J., *Comparison of the visceral antinociceptive effects of spinally administered MPV-2426 (fadolmidine) and clonidine in the rat*. Anesthesiology, 2003. **98**(1): p. 189-94.
88. Allchorne, A. J., Broom, D. C., and Woolf, C. J., *Detection of cold pain, cold allodynia and cold hyperalgesia in freely behaving rats*. Mol Pain, 2005. **1**: p. 36.
89. Navratilova, E., Xie, J. Y., King, T., Porreca, F., *Evaluation of reward from pain relief*. Ann N Y Acad Sci, 2013. **1282**: p. 1-11.

90. Dai, Y., Iwata, K., Kondo, E., Morimoto, T., Noguchi, K., *A selective increase in Fos expression in spinal dorsal horn neurons following graded thermal stimulation in rats with experimental mononeuropathy*. Pain, 2001. **90**(3): p. 287-96.
91. Hunt, S. P., Pini, A., and Evan, G., *Induction of c-fos-like protein in spinal cord neurons following sensory stimulation*. Nature, 1987. **328**(6131): p. 632-4.
92. Martins, I., Carvalho, P., de Vries, M. G., Teixeira-Pinto, A., Wilson, S. P., Westerink, B. H., Tavares, I., *Increased noradrenergic neurotransmission to a pain facilitatory area of the brain is implicated in facilitation of chronic pain*. Anesthesiology, 2015. **123**(3): p. 642-53.
93. Paxinos, G. and Watson, C., *The rat brain in stereotaxic coordinates*. 6th ed. 2007, Amsterdam ; Boston: Elsevier.
94. Zhu, Y. F., Ungard, R., Zacal, N., Huizinga, J.D., Henry, J.L., Singh, G., *Rat model of cancer-induced bone pain: changes in nonnociceptive sensory neurons in vivo*. PAIN reports, 2017. **2**(4): p. 1-10.
95. Rigo, F. K., Dalmolin, G. D., Trevisan, G., Tonello, R., Silva, M. A., Rossato, M. F., Klafke, J. Z., Cordeiro, M. N., Castro Junior, C. J., Montijo, D., Gomez, M. V., Ferreira, J., *Effect of  $\omega$ -conotoxin MVIIA and  $Pha1\beta$  on paclitaxel-induced acute and chronic pain*. Pharmacol Biochem Behav, 2013. **114-115**: p. 16-22.
96. Yan, X., Maixner, D. W., Yadav, R., Gao, M., Li, P., Bartlett, M. G., Weng, H. R., *Paclitaxel induces acute pain via directly activating toll like receptor 4*. Mol Pain, 2015. **11**: p. 10.
97. Dina, O. A., Chen, X., Reichling, D., Levine, J. D., *Role of protein kinase Cepsilon and protein kinase A in a model of paclitaxel-induced painful peripheral neuropathy in the rat*. Neuroscience, 2001. **108**(3): p. 507-15.
98. Cata, J. P., Weng, H. R., Chen, J. H., Dougherty, P. M., *Altered discharges of spinal wide dynamic range neurons and down-regulation of glutamate transporter expression in rats with paclitaxel-induced hyperalgesia*. Neuroscience, 2006. **138**(1): p. 329-38.
99. Abbadie, C., Honoré, P., and Besson, J. M., *Intense cold noxious stimulation of the rat hindpaw induces c-fos expression in lumbar spinal cord neurons*. Neuroscience, 1994. **59**(2): p. 457-68.
100. Evans, M. S., Reid, K. H., and Sharp, J. B., *Dimethylsulfoxide (DMSO) blocks conduction in peripheral nerve C fibers: a possible mechanism of analgesia*. Neurosci Lett, 1993. **150**(2): p. 145-8.
101. Broadwell, R. D., Salcman, M., and Kaplan, R. S., *Morphologic effect of dimethyl sulfoxide on the blood-brain barrier*. Science, 1982. **217**(4555): p. 164-6.
102. Ji, R. R. and Rupp, F., *Phosphorylation of transcription factor CREB in rat spinal cord after formalin-induced hyperalgesia: relationship to c-fos induction*. J Neurosci, 1997. **17**(5): p. 1776-85.
103. Lee, W. T., Sohn, M. K., Park, S. H., Ahn, S. K., Lee, J. E., Park, K. A., *Studies on the changes of c-fos protein in spinal cord and neurotransmitter in dorsal root*

- ganglion of the rat with an experimental peripheral neuropathy*. Yonsei Med J, 2001. **42**(1): p. 30-40.
104. Harris, J. A., *Using c-fos as a neural marker of pain*. Brain Res Bull, 1998. **45**(1): p. 1-8.
  105. Costigan, M., Scholz, J., and Woolf, C. J., *Neuropathic pain: a maladaptive response of the nervous system to damage*. Annu Rev Neurosci, 2009. **32**: p. 1-32.
  106. Fellner, S., Bauer, B., Miller, D. S., Schaffrik, M., Fankhänel, M., Spruss, T., Bernhardt, G., Graeff, C., Färber, L., Gschaidmeier, H., Buschauer, A., Fricker, G., *Transport of paclitaxel (Taxol) across the blood-brain barrier in vitro and in vivo*. J Clin Invest, 2002. **110**(9): p. 1309-18.
  107. Kemper, E. M., van Zandbergen, A. E., Cleypool, C., Mos, H. A., Boogerd, W., Beijnen, J. H., van Tellingen, O., *Increased penetration of paclitaxel into the brain by inhibition of P-Glycoprotein*. Clin Cancer Res, 2003. **9**(7): p. 2849-55.
  108. Ossipov, M. H., Morimura, K., and Porreca, F., *Descending pain modulation and chronification of pain*. Curr Opin Support Palliat Care, 2014. **8**(2): p. 143-51.
  109. Marks, D. M., Shah, M. J., Patkar, A. A., Masand, P. S., Park, G. Y., Pae, C. U., *Serotonin-norepinephrine reuptake inhibitors for pain control: premise and promise*. Curr Neuropharmacol, 2009. **7**(4): p. 331-6.
  110. Hayashida, K., Clayton, B. A., Johnson, J. E., Eisenach, J. C., *Brain derived nerve growth factor induces spinal noradrenergic fiber sprouting and enhances clonidine analgesia following nerve injury in rats*. Pain, 2008. **136**(3): p. 348-55.
  111. Yadav, R., Yan, X., Maixner, D. W., Gao, M., Weng, H. R., *Blocking the GABA transporter GAT-1 ameliorates spinal GABAergic disinhibition and neuropathic pain induced by paclitaxel*. J Neurochem, 2015. **133**(6): p. 857-69.
  112. Masocha, W. and Parvathy, S. S., *Preventative and therapeutic effects of a GABA transporter 1 inhibitor administered systemically in a mouse model of paclitaxel-induced neuropathic pain*. PeerJ, 2016. **4**: p. e2798.
  113. Kinoshita, J., Takahashi, Y., atabe, A. M., Utsunomiya, K., Kato, F., *Impaired noradrenaline homeostasis in rats with painful diabetic neuropathy as a target of duloxetine analgesia*. Mol Pain, 2013. **9**: p. 59.
  114. Tanabe, M., Tokuda, Y., Takasu, K., Ono, K., Honda, M., Ono, H., *The synthetic TRH analogue taltirelin exerts modality-specific antinociceptive effects via distinct descending monoaminergic systems*. Br J Pharmacol, 2007. **150**(4): p. 403-14.
  115. Chen, S. R., Pan, H. M., Richardson, T. E., Pan, H. L., *Potentiation of spinal alpha(2)-adrenoceptor analgesia in rats deficient in TRPV1-expressing afferent neurons*. Neuropharmacology, 2007. **52**(8): p. 1624-30.
  116. Bantel, C., Eisenach, J. C., Duflo, F., Tobin, J. R., Childers, S. R., *Spinal nerve ligation increases alpha2-adrenergic receptor G-protein coupling in the spinal cord*. Brain Res, 2005. **1038**(1): p. 76-82.

## Appendix A: Composition of solutions

### 1. PHOSPHATE BUFFER SALINE (PBS) (1 L)

Phosphate buffer (PB) 0.1 M pH = 7.2:

$\text{Na}_2\text{H}_2\text{PO}_4\text{H}_2\text{O}$  – 15.60 g

$\text{K}_2\text{HPO}_4$  – 17.4 g

$\text{H}_2\text{O}$  up to 1L

PBS:

PB 250 ml

$\text{H}_2\text{O}$  up to 1 L

$\text{NaCl}$  – 9 g

### 2. PHOSPHATE BUFFER SALINE WITH TRITON X-100 (PBS-T)

PBS – 996 ml

Triton X-100 – 4 ml

### 3. TYRODE'S SOLUTION (1 L)

$\text{NaCl}$  – 6.8 g

$\text{KCl}$  – 0.40 g

$\text{MgCl}_2 \cdot 6\text{H}_2\text{O}$  – 0.32 g

$\text{MgSO}_4 \cdot 7\text{H}_2\text{O}$  – 0.1 g

$\text{NaH}_2(\text{PO}_4) \cdot \text{H}_2\text{O}$  – 0.17 g

Glucose 1 g

$\text{NaHCO}_3$  – 2.2 g

$\text{H}_2\text{O}$  up to 1 L

### 4. CRYOPROTECTOR SOLUTION (1 L)

PB 0.1 M pH = 7.2 – 125 ml

$\text{H}_2\text{O}$  – 375 ml


Sucrose – 300 g

Ethylene glycol – 300 ml


PB 0.1 M pH = 7.2 up to 1 L

## Appendix B: Publication and oral communication

1. Abstract publication on “Porto Biomedical Journal” entitled “Paclitaxel-induced neuropathic pain: Unravelling the underlying mechanisms at the central nervous system”.



**Porto Biomedical Journal**  
Volume 2, Issue 5, September–October 2017, Page 192  
[open access](#)



---

PS141

**Paclitaxel-induced neuropathic pain: Unravelling the underlying mechanisms at the central nervous system**

J. Ribeiro <sup>1, 2, 3, 4, 5</sup>, J.T. Costa-Pereira <sup>1, 2, 3</sup>, I. Tavares <sup>1, 2, 3</sup>, I. Martins <sup>1, 2, 3</sup>

[Show more](#)

<https://doi.org/10.1016/j.pbj.2017.07.040> [Get rights and content](#)

Open Access funded by PBJ-Associação Porto Biomedical/Porto Biomedical Society  
Under a [Creative Commons license](#)

---

**Aim:** Here we studied the effects of the cytostatic paclitaxel on: (i) the development of nociceptive and aversive behaviors; (ii) noxious-evoked-activation of spinal dorsal horn neurons and (iii) on descending noradrenergic modulation, which is the main spinal nociceptive inhibitory system.

**Introduction:** Chemotherapeutic drugs are widely used for cancer treatment but they also cause numerous deleterious side effects. Chemotherapy-induced neuropathy (CIN) is one of the most common side effects. The mechanisms underlying CIN are starting to be uncovered namely the alterations induced by cytostatics at the peripheral nervous system but the effects of these drugs at the central nervous system are still poorly studied.

**Methods:** Male Wistar rats were injected with paclitaxel (Taxol, 2.0 mg/kg) or the vehicle solution dimethyl sulfoxide on four alternate days. Nociceptive and aversive behaviors were assessed by the von Frey and conditioned place aversion (CPA) tests, respectively. Noxious-evoked-activation of spinal dorsal neurons was achieved at one month after CIN by evaluating the expression of c-fos expression upon cold stimulation. To study the descending noradrenergic pain modulation we assessed the effects of the  $\alpha$ 2-adrenoreceptor agonist clonidine at 1 and 10  $\mu$ g administered intrathecally, on the von Frey test. We further assessed the expression of the  $\alpha$ 2-adrenoreceptor and dopamine- $\beta$ -hydroxylase (DBH), a noradrenaline biosynthetic enzyme expressed in noradrenergic fibers, at the spinal dorsal horn.

**Results:** Paclitaxel induced mechanical allodynia and aversive behaviors. c-fos and DBH expression were increased in paclitaxel-treated animals while  $\alpha$ 2-adrenoreceptor expression remained unaltered. Clonidine induced antinociception at both doses with more pronounced effects in paclitaxel-treated animals.

**Conclusion:** Paclitaxel-treated animals showed neuropathic like-behaviors and increased spinal neuronal activation. It remains to ascertain if DHB upregulation results in increased spinal noradrenaline levels, but the increase of  $\alpha$ 2-AR antinociceptive potency in paclitaxel-treated animals indicates the recruitment of descending inhibition probably as a buffer to increased spinal sensitization.

**Acknowledgements:** Funding: Norte 2020 refs: NORTE-01-0145-FEDER-000008.

Copyright © 2017 Published by Elsevier España S.L.

2. Oral presentation in the Plenary session (“Neurosciences” field) at the 12<sup>th</sup> Young European Scientist Meeting (14<sup>th</sup> September-17<sup>th</sup> September 2017), at Faculty of Medicine of the University of Porto.